

SHALE OIL RESOURCE PLAY POTENTIAL OF THE GREEN RIVER FORMATION, UINTA BASIN, UTAH

by Steven Schamel



OPEN-FILE REPORT 639
UTAH GEOLOGICAL SURVEY
a division of
UTAH DEPARTMENT OF NATURAL RESOURCES
2015

Shale Oil Resource Play Potential of the Green River Formation, Uinta Basin, Utah

by Steven Schamel

Cover photo: Outcrop of the middle Green River Formation, Willow Creek Canyon. Photo by Michael Vanden Berg.



OPEN-FILE REPORT 639
UTAH GEOLOGICAL SURVEY
a division of
UTAH DEPARTMENT OF NATURAL RESOURCES
2015

STATE OF UTAH

Gary R. Herbert, Governor

DEPARTMENT OF NATURAL RESOURCES

Michael Styler, Executive Director

UTAH GEOLOGICAL SURVEY

Richard G. Allis, Director

PUBLICATIONS

contact

Natural Resources Map & Bookstore

1594 W. North Temple

Salt Lake City, UT 84114

telephone: 801-537-3320

toll-free: 1-888-UTAH MAP

website: mapstore.utah.gov

email: geostore@utah.gov

UTAH GEOLOGICAL SURVEY

contact

1594 W. North Temple, Suite 3110

Salt Lake City, UT 84114

telephone: 801-537-3300

website: geology.utah.gov

This open-file release makes information available to the public that may not conform to UGS technical, editorial, or policy standards; this should be considered by an individual or group planning to take action based on the contents of this report. The Utah Department of Natural Resources, Utah Geological Survey, makes no warranty, expressed or implied, regarding its suitability for a particular use. The Utah Department of Natural Resources, Utah Geological Survey, shall not be liable under any circumstances for any direct, indirect, special, incidental, or consequential damages with respect to claims by users of this product.

CONTENTS

ABSTRACT	1
1. INTRODUCTION	2
2. STRATIGRAPHY	4
Green River Formation	4
Post-Green River Overburden	10
3. ORGANIC GEOCHEMISTRY	18
Programmed Pyrolysis Source Rock Characterization	18
Organic Maturity and Anomalous Formation Pressure	27
4. NUMERICAL SIMULATIONS OF ORGANIC MATURATION	31
Model Input Parameters	32
Numerical Simulation Output Parameters	41
5. DISCUSSION	52
ACKNOWLEDGMENTS	61
REFERENCES	61
APPENDICES	on CD
Appendix A—Stratigraphy	on CD
Appendix B—Organic Geochemistry	on CD
Appendix C—Thermal Modeling	on CD
Appendix D—Discussion	on CD

SHALE OIL RESOURCE PLAY POTENTIAL OF THE GREEN RIVER FORMATION, UINTA BASIN, UTAH

by Steven Schamel

ABSTRACT

The Green River Formation in the Uinta Basin has many characteristics typical of an ideal shale oil resource play. It is a world-class oil-prone source rock. In nearly all parts of the basin there are many thousands of net feet of Type-I and Type-II kerogen-rich calcareous mudstones, many intervals of which have average total organic carbon (TOC) of 5–10% or greater. In the north-central and western parts of the basin a substantial part of the formation is in the oil-generative window. A large volume of the formation has reached “peak oil”. Furthermore, organic maturation simulations done in this study using PRA BasinView-3D™ indicates early entry into the oil-generative window. In the northwest parts of the basin the lower Green River Formation was generating oil even before the end of the Eocene and slowing of sediment accumulation in the basin. Anomalous formation pressures are observed in the lower Green River Formation across much of the basin. In the area of the greater Altamont-Bluebell field in the northwest of the basin, the abnormal pressures are nearly lithostatic (0.6 to 0.8 psi/ft). The Green River Formation is unquestionably a superb petroleum system responsible for very large cumulative production of oil and associated natural gas, and an even larger potential oil sand resource.

This assessment of the shale oil resource play potential of the Green River Formation is based on the integration of:

- basin-wide stratigraphy and facies distributions;
- programmed pyrolysis and other geochemical data from organic-rich calcareous mudstone in fourteen wells, most of which are in the northern and western quadrants of the basin;
- new basin-wide BasinView 3D™ numerical modeling of thermal maturation at a 1.0 kilometer resolution;
- the known distribution of oil and oil sand accumulations in Green River Formation and age-equivalent reservoirs; and
- the current revitalization of oil production from Green River–Wasatch reservoirs.

Typical shale oil resource plays are self-contained petroleum systems having ineffective carrier systems that severely restrict migration of oil generated in the source rocks from mi-

grating outward or upward into traps in reservoirs marginal to the oil kitchens. Consequently, the oil backs up into any and all pore space in the source rock succession, even creating fracture storage space where anomalous pressures occur. Relatively tight rocks that would normally never be considered reservoirs can have very high oil saturations and oil-in-place. In a shale oil resource play these are what are exploited by horizontal wells and hydraulic fracture stimulation.

As more of the shale oil plays receive close scrutiny, it is becoming clear that no two are the same with regards to character of source rock or reservoir. What they all have in common, however, is (1) an organic-rich source rock capable of generating large volumes of oil, (2) interbedded or proximal reservoir intervals that, although tight, have sufficient porosity and/or natural fractures to be capable of hosting commercially significant volumes of the producible oil, and (3) inefficient carrier systems resulting in the oil generated remaining in proximity to the oil-generative source rock. The presence of anomalous formation pressures appears necessary to drive the oil from reservoir to well bore, even when fracture stimulated. These are “self-sourcing” petroleum systems only when viewed on a scale that encompasses the entire source rock formation and its immediately adjacent strata, or a significant portion thereof. And so it is with the Green River Formation, which has both an internal “self-sourcing” continuous oil play within the oil generative window and conventional oil accumulations on its periphery. Due to the lenticular character of the sandstone and carbonate beds in the Green River Formation and the underlying Wasatch Formation, some beds trap oil locally, while others carry the oil up-dip into traps at a distance from the oil generative window.

Only a few years after the discovery of the Altamont field, it was described as an “oil accumulation near the center of a deep basin”, an example of a then newly-recognized “group of deep-basin, organic-shale-related, overpressured accumulations” having significant hydrocarbon potential. Altamont-Bluebell field characteristics subsequently have come to identify a basin-centered, continuous resource play. These characteristics include:

- difficulty in defining field limits laterally and vertically because the trap is stratigraphic with no simple down-dip water levels or facies boundaries to the productive horizons,

- multiple thin productive zones with abnormally high fluid pressures, and
- very low matrix porosities enhanced by post-lithification fractures.

The companies now using fracture stimulation and horizontal wells to produce oil from Green River–Wasatch sandstone and carbonate reservoirs have merely *rediscovered* this basin-centered, continuous shale oil resource play.

1. INTRODUCTION

The Uinta Basin (Fig. 1-1) is a mature oil and gas province (USGS, 2003). Through the beginning of 2015, the two counties producing nearly all of the hydrocarbons from the basin, Duchesne and Uintah, had cumulative life-time production of 712 million barrels of oil and 5438 billion cubic feet of natural gas (Utah Division of Oil, Gas, and Mining [DOGMI]). All, or virtually all, of the oil, constituting 45% of the state’s total, is sourced from the Green River Formation and extracted from what have been considered to be conventional reservoirs in this or immediately adjacent formations (Fouch and others, 1994). The principal oil fields in the Uinta Basin are shown with green overprint in Figure 1-2. Their cumulative production and recent annual production are presented in Table 1-1. Production rates of oil and associated gas have been increasing recently through the adoption of various enhanced recovery strategies. With the increasing interest in finding and developing unconventional shale oil and shale gas resources in North America and elsewhere, it is natural to inquire into the possibility for a shale oil resource play in the Green River Formation in the Uinta Basin. An earlier study (Schamel, 2005) supported by the Utah Geological Survey UGS) had concluded that the possibility of a successful shale gas play was small due to low thermal maturity for gas, but a potential shale oil resource play was not considered, nor was it investigated.

A shale oil resource has all of the characteristics of a viable petroleum system except one: the presence of an efficient network of carrier beds linking the source rock with reservoir traps. In a petroleum system with conventional oil plays, hydrocarbons generated in a source rock migrate out of the source rock (primary migration; Mann, 1994) through an interacting combination of molecular diffusion through the source rock’s kerogen network and Darcy flow within the micro-pore network. On encountering more porous and permeable laminae, distinct beds and/or fracture networks, the oil can enter a carrier system (secondary migration; England, 1994) that leads either to discrete traps or eventually to the surface. In situations where the carrier system does not exist or is ineffective relative to the rate of hydrocarbon generation, the oil backs up within the source rock formation filling all available pore space. When organic-rich rock layers are intercalated with organic-lean, but more porous, layers, the

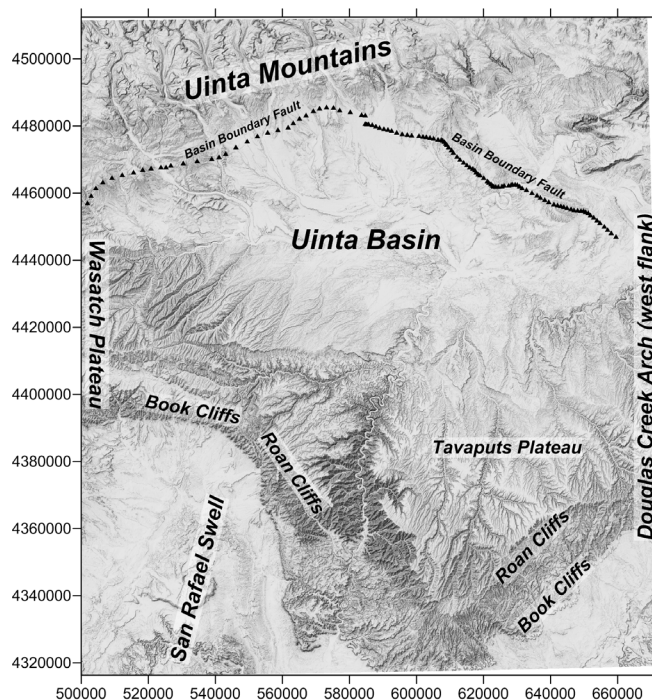


Figure 1-1: Shaded relief map of the Uinta Basin and bounding structural uplifts: Uinta Mountains, Douglas Creek Arch, San Rafael Swell, and Wasatch Plateau. The Tavaputs Plateau is a southern extension of the basin, which is bounded on the south by its erosional limits in the Roan Cliffs (lower Tertiary) and Book Cliffs (Upper Cretaceous). The geographic coordinates are meters in UTM NAD83, Zone 12.

oil tends to concentrate in the more porous strata. This is true even when the “reservoir” is a micropore or a sub-micropore system. If sufficiently thick, porous and permeable, these are the targets (“sweet spots”) on which the shale oil play is based. In contrast to a shale gas reservoir, which normally is the source rock, the shale oil reservoirs are strata immediately adjacent to and/or interbedded with the primary source rock. In the Williston Basin it is the silty, but organic carbon-lean, Middle Bakken Member and silty beds of the Sanish and Three Forks Formations below the organic carbon-rich Lower Bakken Member. In the Niobrara Formation shale oil play throughout the eastern Rockies, it is chinks intercalated within and totally enclosed by the source rock that is the micropore reservoir. The Bakken Shale and the Niobrara Formation are actually hybrid, dual-reservoir, systems.

The general characteristics of a successful shale oil reservoir drawn from Sonnenberg (2010) for the Bakken Shale and from general knowledge of other shale oil plays include:

- a “world-class” source rock containing abundant oil-prone kerogen,
- within the oil-generative window such that oil has been generated and retained,
- oil saturations high enough to permit expulsion from the rock matrix into a system of fractures and microfractures,

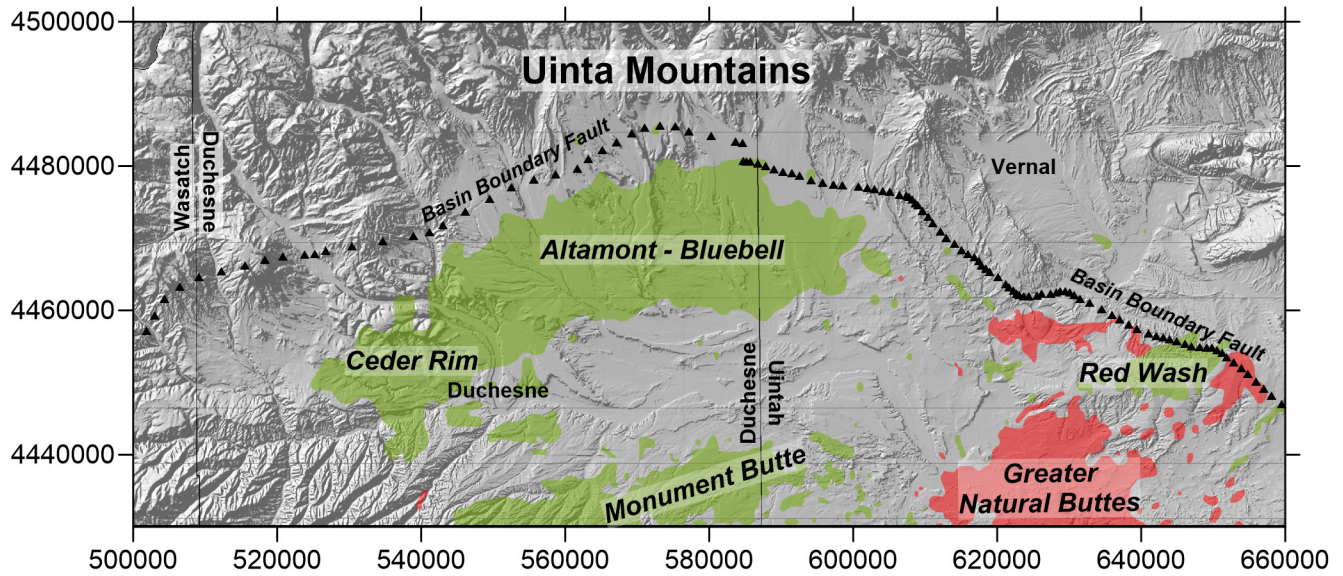


Figure 1-2: The principal oil fields (green, natural gas fields in red) in the Uinta Basin that produce Green River-sourced oil from Green River Formation and stratigraphically proximal conventional reservoirs. County lines and two of the major towns in the basin are indicated for geographic reference. The geographic coordinates are meters in UTM NAD83, Zone 12.

Table 1-1: Cumulative and annual production of oil and natural gas from significant fields in the Uinta Basin producing hydrocarbons sourced dominantly from the Green River Formation. Cumulative production includes January 2014. Data from Utah DOGM.

Fields	Cumulative Oil	Cumulative Natural Gas	Oil annual production (barrels)				Natural gas annual production (mcf)			
			2013	2012	2011	2010	2013	2012	2011	2010
ALTAMONT	137,197,157	299,180,399	4,297,355	3,343,734	2,627,584	2,265,728	12,376,431	10,266,582	8,298,294	5,860,603
ANTELOPE CREEK	7,878,325	16,648,174	682,449	490,980	319,155	278,107	843,854	623,143	390,761	314,392
BLUEBELL	177,233,246	249,065,474	3,038,817	2,677,485	2,312,062	2,005,642	4,663,075	4,138,947	3,614,384	3,226,331
BRENNAN BOTTOM	3,409,391	3,337,841	434,477	289,115	208,361	256,352	266,595	151,809	147,176	182,540
BRUNDAGE CANYON	19,583,962	118,277,192	1,501,765	1,147,654	1,222,258	1,247,192	10,477,530	9,535,775	12,051,108	12,475,577
CEDAR RIM	15,403,691	36,258,555	419,331	681,205	494,921	356,076	1,385,808	1,656,282	1,196,972	794,471
DUCHESNE	1,693,012	3,619,765	71,444	67,055	56,088	72,003	178,403	129,852	121,035	161,608
EIGHT-MILE FLAT	614,380	7,262,708	118,897	104,831	74,165	12,067	542,337	550,433	596,459	759,264
HORSESHOE BEND	2,232,303	28,912,625	51,119	42,426	43,285	40,907	305,869	321,919	320,740	405,694
LAKE CANYON	1,422,988	7,061,515	482,574	453,427	131,183	77,528	1,805,405	1,331,572	634,750	728,883
MONUMENT BUTTE	63,337,441	137,818,755	5,078,350	5,313,430	4,946,775	5,043,418	7,920,771	10,106,427	9,467,740	10,013,766
N MYTON BENCH	4,416,549	5,076,251	2,101,854	1,369,038	364,100	77,274	2,615,199	1,403,846	330,287	107,084
PARIETTE BENCH	1,885,842	46,660,646	72,407	98,840	119,449	129,748	4,218,894	4,773,217	5,331,734	5,555,566
RED WASH	87,145,167	385,941,002	375,336	343,832	392,406	379,295	12,714,842	9,246,892	4,185,771	2,603,713
SOUTH MYTON BENCH	2,256,216	18,907,657	185,825	287,825	662,916	845,493	3,340,534	4,522,616	5,671,716	3,782,840
UTELAND BUTTE	1,963,845	9,378,239	150,771	119,361	83,398	63,331	933,906	927,861	998,520	1,058,743
WALKER HOLLOW	19,901,521	34,490,387	144,685	156,592	160,937	166,319	217,471	245,535	255,606	259,869
WEST WILLOW CREEK	1,127,578	11,995,905	7,261	8,535	9,918	12,936	118,430	156,089	210,000	273,768
WHITE RIVER	3,068,967	14,886,277	27,344	27,275	27,971	38,314	378,441	404,951	499,536	652,153
WINDY RIDGE	4,581,345	7,179,336	1,000,293	841,247	914,013	348,822	1,963,165	1,617,790	1,129,994	368,959
WONSITS VALLEY	52,103,370	132,341,530	253,939	231,116	258,088	276,685	3,609,907	4,032,357	4,471,751	5,370,324
	608,456,296	1,574,300,233	20,496,293	18,095,003	15,429,033	13,993,237	70,876,867	66,143,895	59,924,334	54,956,148

- commonly associated with abnormally high fluid pressure gradients; as high as 0.73 psi/ft in the Bakken Shale, but just greater than 0.50 psi/ft is more normal, and
- a mudstone or siltstone reservoir host rock that is naturally fractured or capable of fracture stimulation.

It is clear from the large volume of oil and associated natural gas trapped in conventional elastic and porous limestone reservoirs within and rimming the Uinta Basin, that the Green River Formation has, or has had, a very efficient carrier system that guided the hydrocarbons from the source kitchen in the basin center to the productive reservoirs.

This study has sought evidence for conditions that could support a shale oil play in the stratigraphy, organic geochemistry, and simulated history of organic maturation of the Green River Formation.

2. STRATIGRAPHY

The Uinta Basin is a strongly asymmetric intracratonic depression formed by crustal loading beneath the rising Uinta Mountains anticlinorium (Fig. 1-1). Pre- and synorogenic strata within the basin dip uniformly northward towards the Uinta Basin Boundary Fault, which borders the deepest part of the basin. The south flank of the basin is elevated by two Laramide uplifts, the San Rafael Swell on the southwest and the reactivated Uncompaghre Uplift (Stone, 1977) on the southeast. Douglas Creek Arch, a north-south trending Laramide uplift, forms the eastern flank of the basin immediately east of the Utah-Colorado state line. The south rim of the basin is formed by the Book (Cretaceous) and Roan (Paleocene) Cliffs capped by a high plateau rising to elevations of 8000 to 10,000 feet.

The stratigraphy of the Uinta Basin records an evolution from a passive margin basin through the Paleozoic and most of the Mesozoic to a foreland basin east of the Sevier Thrust Belt in the Late Cretaceous, to finally a Laramide intracratonic depression in the latest Cretaceous through late Eocene. It was during this last phase that large lakes formed throughout the region that previously was an extensive foreland basin, the Western Interior Seaway (Franczyk and others, 1992). In northeast Utah, in the general area of the Uinta Basin, there were two major lakes (Fig. 2-1), Lake Flagstaff of Paleocene age and Lake Uinta of Eocene age (Ryder and others, 1976; Fouch and others, 1992). Light gray and varicolored biomicrites of the Flagstaff Limestone are the record of Lake Flagstaff and organic-rich lacustrine shales of the Green River Formation were deposited in Lake Uinta (Fouch and others, 1994). During the dry period between Lake Flagstaff and Lake Uinta time, 800 to 1200 ft of continental red mudstone and sandstones were deposited in a fluvial-flood plain setting. This is the Wasatch Formation, which in part interfingers with both the underlying Flagstaff Limestone and the overlying Green River Formation. As Lake Uinta expanded during

Green River time, the fluvial-flood plain setting was replaced by periodic sandy delta systems that emptied northward across marginal lacustrine carbonate muds and limestones (Ryder and others, 1976; Castle, 1990). These deltaic and shoreline sandstones are the reservoirs for the heavy oil and bitumen on the south flank of the Uinta Basin (Schamel, 2013).

In the Uinta Basin, conventional oil and associated natural gas are produced principally from sandstones and bioclastic limestones in the Green River Formation and the upper Wasatch Formation (Morgan, 2003; Morgan and others, 2003; Kelso and Eherenzeller, 2008; Morgan, 2008). Natural gas is produced from a variety of Paleocene through Jurassic sandstone reservoirs. In a few fields, biogenic methane is extracted from the upper Eocene Uinta Formation. The immobile oil and bitumen are reservoirized in many of these same units (Fig. 2-2). The Uinta Basin oil is sourced from the Green River Formation (Fouch and others, 1994; Ruble and others, 2001; Lillis and others, 2003) and the natural gas is sourced from the organic-rich Mancos Shale and/or Mowry Shale, as well as coals within the Frontier Formation and Mesaverde Group (Rice and others, 1992).

Green River Formation

The basal Green River Formation represents the initiation of Lake Uinta as a single, large lake. For much of the Eocene, the lake occupied only a small part of the basin along the northern margin of the structural depression (Fig. 2-1). The lake was ringed by a 'marginal lacustrine' mudflat that was periodically inundated by lake waters. Beyond the shoreline were alluvial fans and delta complexes that sometimes encroached on the lake and at other times were flooded. The consequence was a broad region in which reservoir and carrier-bed sandstones and shoreline bioclastic carbonates are intimately intercalated with organic-rich lacustrine source rocks (Keighley and others, 2002; Keighley and Flint, 2008). The basin continued to receive sediments as long as the basin subsided, driven by the Laramide orogeny and uplift of the Uinta Mountains. However, in the middle Eocene to earliest Oligocene, the basin filled in with red fluvial mudstone, sandstones, and conglomerates of the Uinta and Duchesne River Formations. There must have been a climatic factor to the end of Lake Uinta. The main lacustrine period coincided with the Early Eocene Climatic Optimum (Smith and others, 2008a), a period of a historically hot global climate. This was followed by a long period of increasing aridity.

The most important Tertiary source rocks in the Uinta Basin are the kerogen-rich calcareous claystones and marlstones deposited as the open-lacustrine facies of the Green River Formation (Katz, 1995; Ruble and Philp, 1998). A distinction is drawn between those open-lacustrine facies assemblages that are *offshore* and continuously subaqueous and those that are *nearshore* and subjected to shoreline influences, including periodic subaerial exposure. The offshore open-lacustrine facies

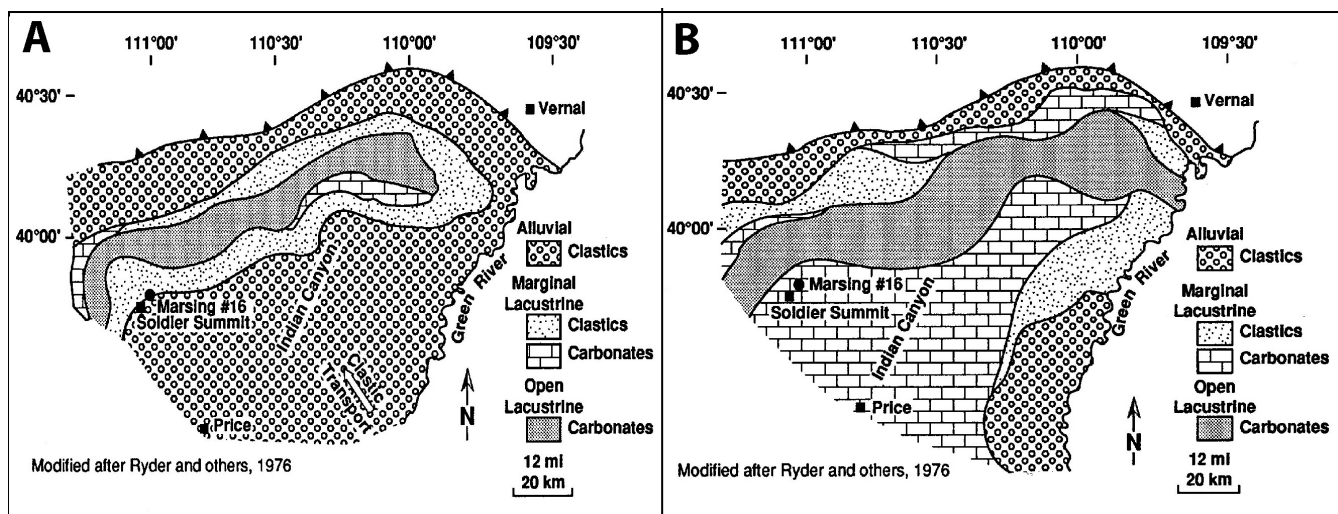


Figure 2-1: Green River Formation facies distributions in western Lake Uinta, the part of the Uinta Basin west of the Green River (Schamel, 2005, after Wiggins and Harris, 1994). A. Late Paleocene – at this time the lacustrine facies had relatively limited extent in the foredeep immediately to the south of the Uinta thrust. B. Early Eocene – time of expanded open and marginal lacustrine deposition.

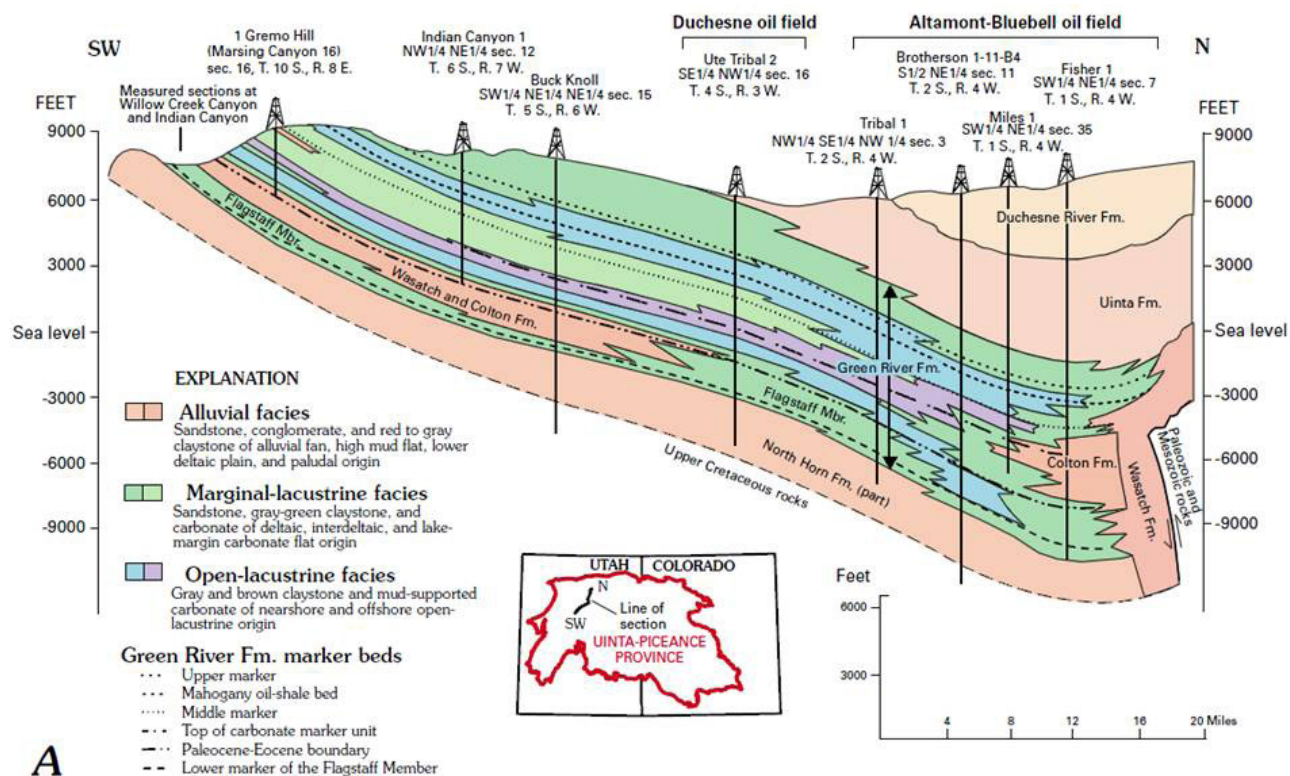


Figure 2-2: Structural cross section from Soldier Summit (Marsing 16 well) northeast to the Altamont-Bluebell field and South Uinta thrust near the structural and depositional axis of the Uinta Basin (Wiggins and Harris, 1994). The open lacustrine facies, blue in the cross section, constitute the main body of 'black shales' in the Green River Formation.

is characterized by black to beige, laminated or very thinly bedded calcareous claystone and shaly carbonate. The kerogen in these high-grade "oil shales" is Type I. They formed in relatively deep, quiet anoxic lake waters as alternating laminae of bacterial/algal ooze (Ruble and others, 1994) and algae-derived low-Mg calcite. The clay content is minor. The nearshore open-lacustrine facies is lithologically diverse and includes weakly laminated, organic-rich, mud-supported car-

bonate containing large Unionid pelecypods with black laminated mudstone and coal beds, and scattered thin sandstone-siltstone beds. Present also are beds of wackestone/packstone rich in ostracods and gastropod fragments (Wiggins and Harris, 1994). The siliciclastics accumulated mainly in offshore bars related spatially to deltas (Castle, 1990; Remy, 1992) entering the lake. In the interdeltic portions of the shoreline (marginal lacustrine facies) were carbonate mudflats, ephem-

eral ponds, and small peat mires that may or may not have preserved organic matter (Ryder and others, 1976).

The open-lacustrine (black shale) facies rocks are distributed in two principal zones (Figs. 2-3 and 2-4) representing extended periods of lake flooding. The lower interval, the Black Shale facies (Thompson, 1971; Picard and others, 1973) is at or near the base of the Green River Formation (Fig. 2-3). The upper black shale is the Parachute Creek Member, which contains the exceptionally organic-rich Mahogany Zone. Near the paleo-axis of the lake, the two black shale intervals merge (Ryder and others, 1976; Fig. 2-3, Duchesne section).

With deltas and fan deltas entering the basin from the basin margins, broad mudflats that rapidly cycle between subaerial and subaqueous, and a relatively limited perennial lake that with a longer cyclicity flooded nearly the entire basin, it is understandable that the stratigraphic nomenclature of the Green River Formation is complex and, in part, contradictory. Fortunately, there were several episodes of maximum lake flooding that deposited stratigraphic markers that can be followed in wells and outcrop across large portions of the basin (Fig. 2-2). These markers serve to permit the formation to be divided into three members. The ages of several of the markers can be

dated by intercalated tuffs (Smith and others, 2008b; Birgenheier and Vanden Berg, 2011).

The base of a persistent ostracod-rich limestone (55.3 Ma) marking the earliest widespread flooding of Lake Uinta, the Uteland Butte Limestone, is the base of the Green River Formation and the Lower Member. The top of the Lower Member is another distinctive limestone, the “Carbonate Marker” (53.9 Ma). The Long Point Bed (54.0 Ma) is a marker within the Lower Member. The Lower Member encompasses the Black Shale facies unit. The Middle Member extends from the top of the Carbonate Marker to the Mahogany Zone (49.3 – 48.9 Ma), an exceptionally organic-rich shale marker representing a wide-spread persistent flooding event. In some nomenclatures the Middle Member is equivalent in its entirety to the Douglas Creek Member, but Johnson and Roberts (2003) place the base of the younger Parachute Creek Member (Fig. 2-2) at the base of the organic-rich R-4 interval (51.6 Ma), well below the Mahogany Zone (R-7). The Upper Member begins at the top of the Mahogany Zone and extends to the top of the formation. The uppermost parts of the lacustrine succession, the organic-carbon-lean “saline facies” and the “limestone and sandstone facies”, are placed in the Upper Member.

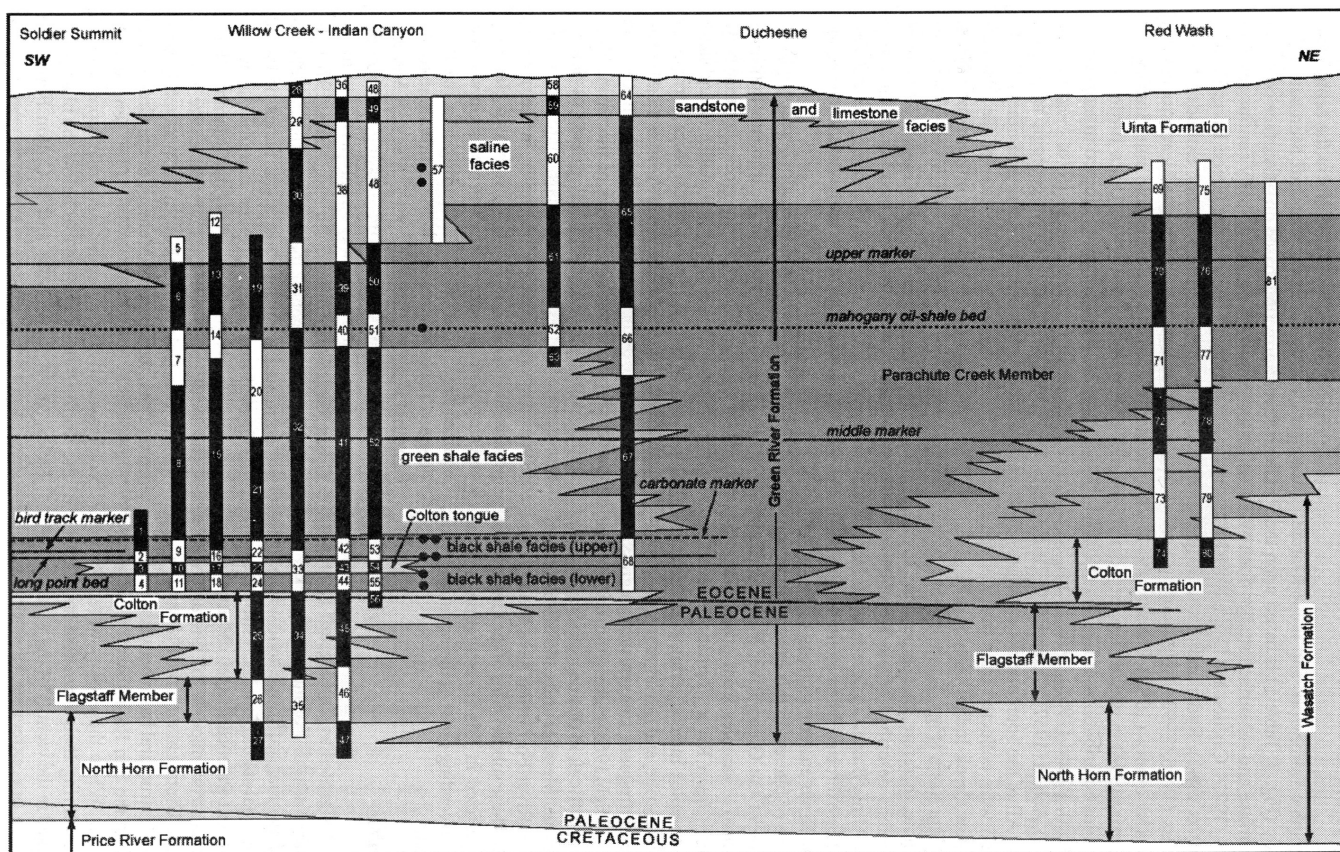


Figure 2-3: Stratigraphic cross section from Soldier Summit northeast across the Uinta Basin to the Red Wash field, just east of the Green River south of Vernal (Ruble and Philp, 1998, redrawn after Ryder and others, 1976). The section illustrates temporal expansions and contractions of the open lacustrine (dark gray) and marginal lacustrine (medium gray) facies associations. In the basin depocenter (Duchesne) the open lacustrine facies merge into a continuous organic-rich mudstone succession.

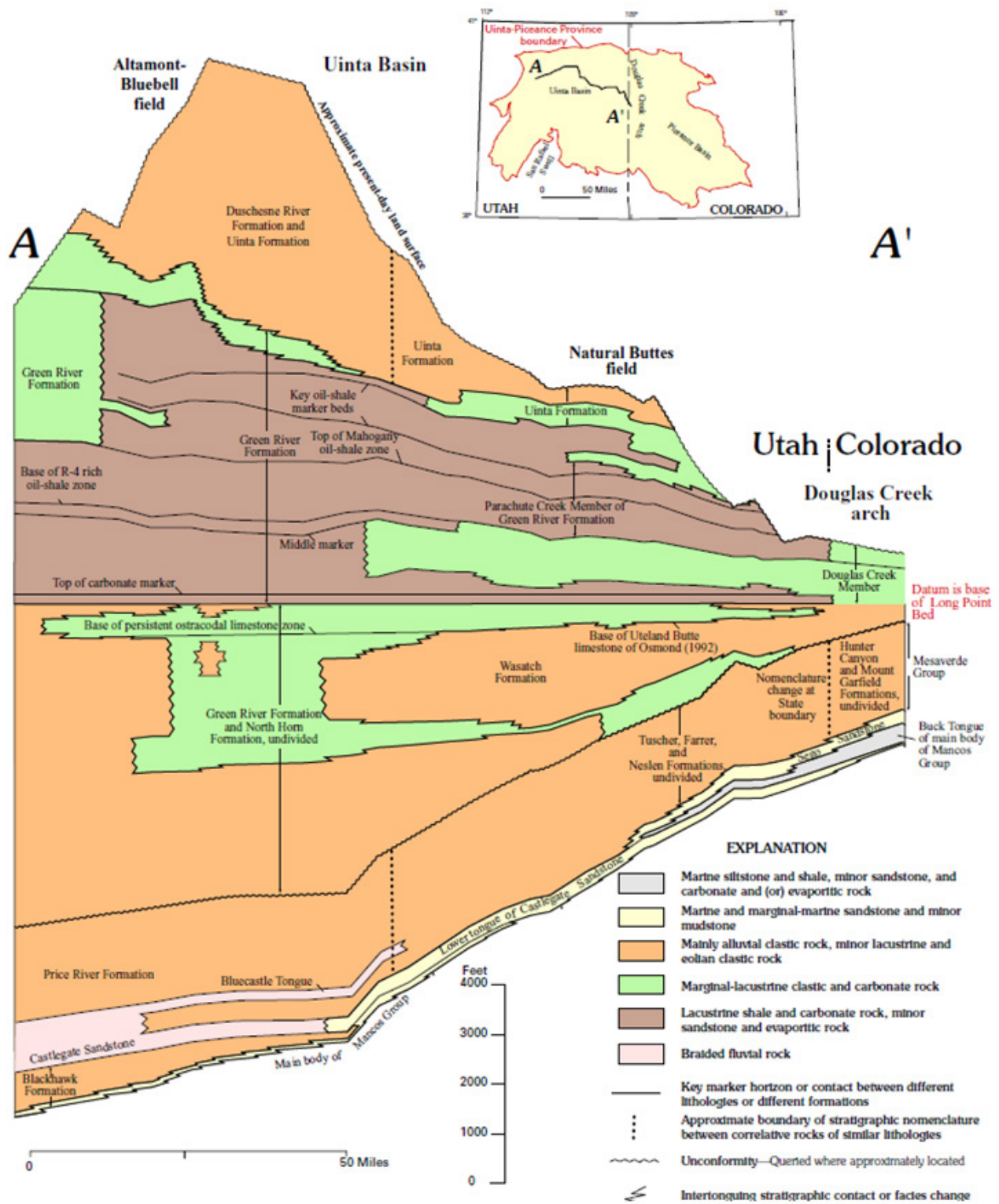


Figure 2-4: Stratigraphic correlations and marker beds of the Green River Formation and adjacent dominantly siliciclastic formations (modified after Johnson and Roberts, 2003). Key to lithologies: orange, mainly alluvial siliciclastic rock; green, marginal-lacustrine siliciclastic and carbonate rock; brown, lacustrine mudstone and carbonate rock.

An alternative, and perhaps more useful, division of the formation in the parts of the basin where open and marginal lacustrine facies dominate is to divide it based on the degree of organic richness (Ryder and others, 1976; Fig. 2-3), separating organic-rich and organic-lean intervals based on bulk density or sonic log signatures or direct measurement of organic content (Vanden Berg, 2008; Fig. 2-5).

The Marsing 16 core (Fig. 2-6; Wiggins and Harris, 1994) samples the cyclic marginal lacustrine facies of the Green Shale facies (Middle Green River Formation), open and marginal lacustrine rocks of the Black Shale facies (Lower Green River Formation), and a short interval of the underlying Wasatch (Colton) deltaic sandstones. The core hole twins the Gremo Hill Fee 1 well (16-10S-8E; API 435130002). A set of core photographs

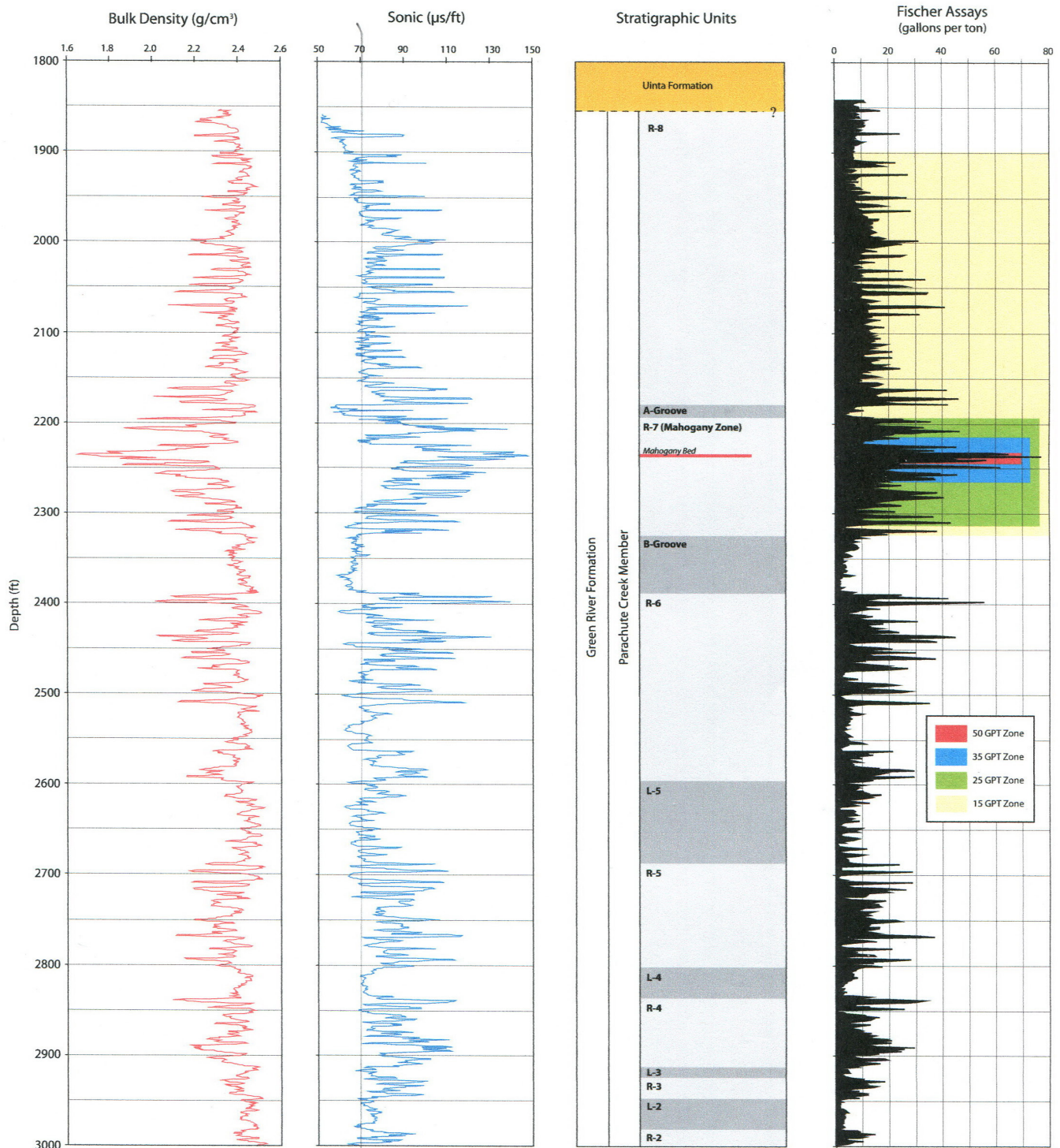


Figure 2-5: Stratigraphy of the Middle and Upper Green River Formation showing organic-rich (R-) and organic-lean (L-) alternations (Vanden Berg, 2008).

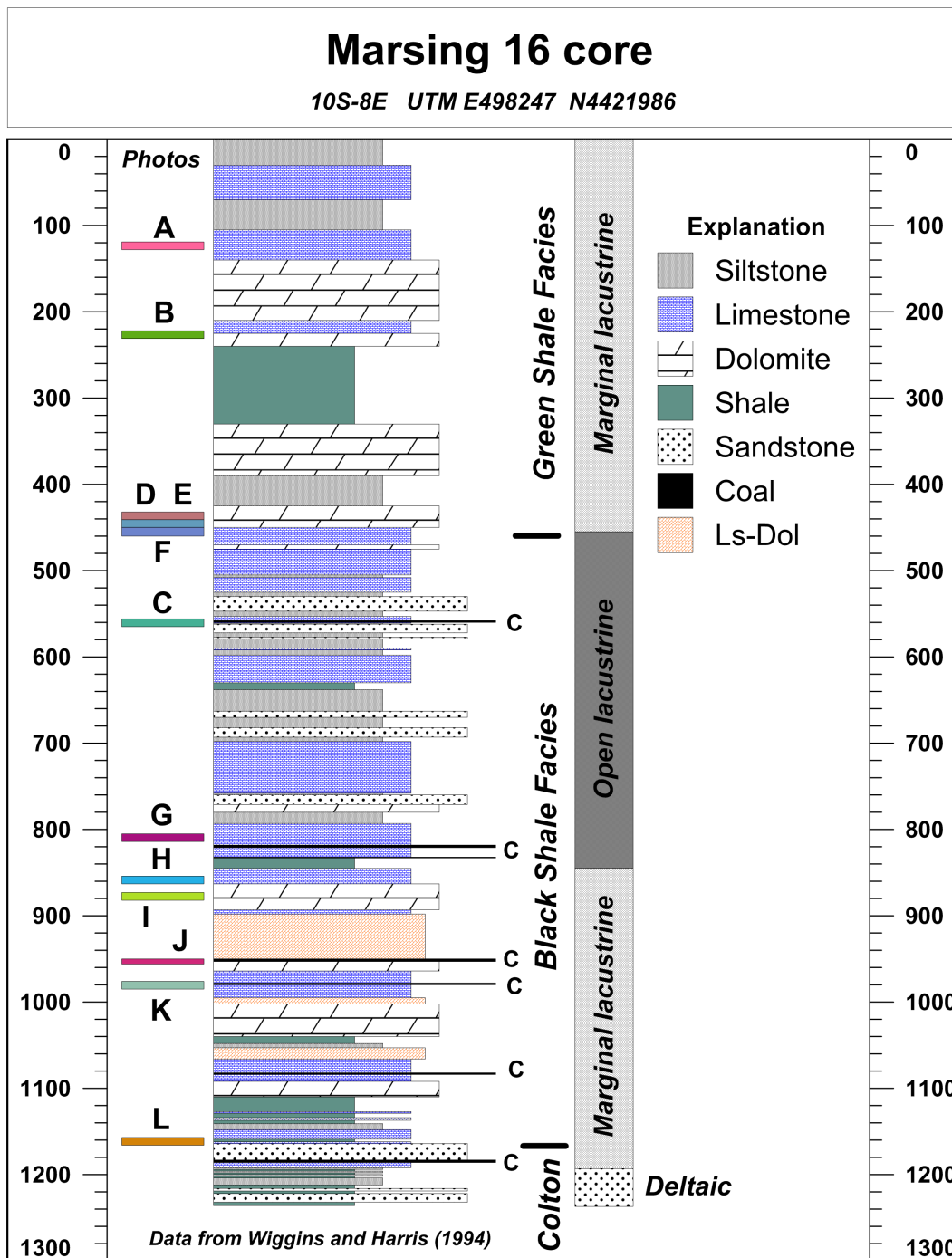


Figure 2-6: Marginal and open lacustrine lithologies in the Marsing 16 core (Wiggins and Harris, 1994). The letter “C” indicates coal beds observed in core. Core depths in feet. See text for description of the core.

of selected segments are in Figures 2-7 and 2-8. Near the top of the core is a thick, uniform limestone, the “Middle Marker” (Fig. 2-7, A). The remainder of the section is thinly laminated alternations of gray-green claystone and carbonates deposited on a carbonate flat (Fig. 2-7, B, D-F). The open lacustrine rocks of the Black Shale facies are cyclically alternating siliciclastics and carbonates (Figure 2-7, C; note algal coal at 563 ft). The silt and sand is thought to have been transported into the deep lake from shoreline deltaic deposits by wind-generated currents. The carbonate intervals are black, laminated limy

mudstone commonly with abundant pelecypods, ostracods, and coals (Figs. 2-8, G-K). Fractured oil-saturated sandstone beds are observed (Fig. 2-8, L), as are numerous subvertical open and partially-open fractures (Fig. 2-8, J).

In stratigraphically equivalent strata to the east of Marsing 16, fine-grained, cross-bedded sandstone fills fluvial channels incised into cyclically laminated claystone and carbonates (Figs. 2-9 and 2-10). These channels provide carrier systems from the organic-rich basin center to thicker alluvial sand-

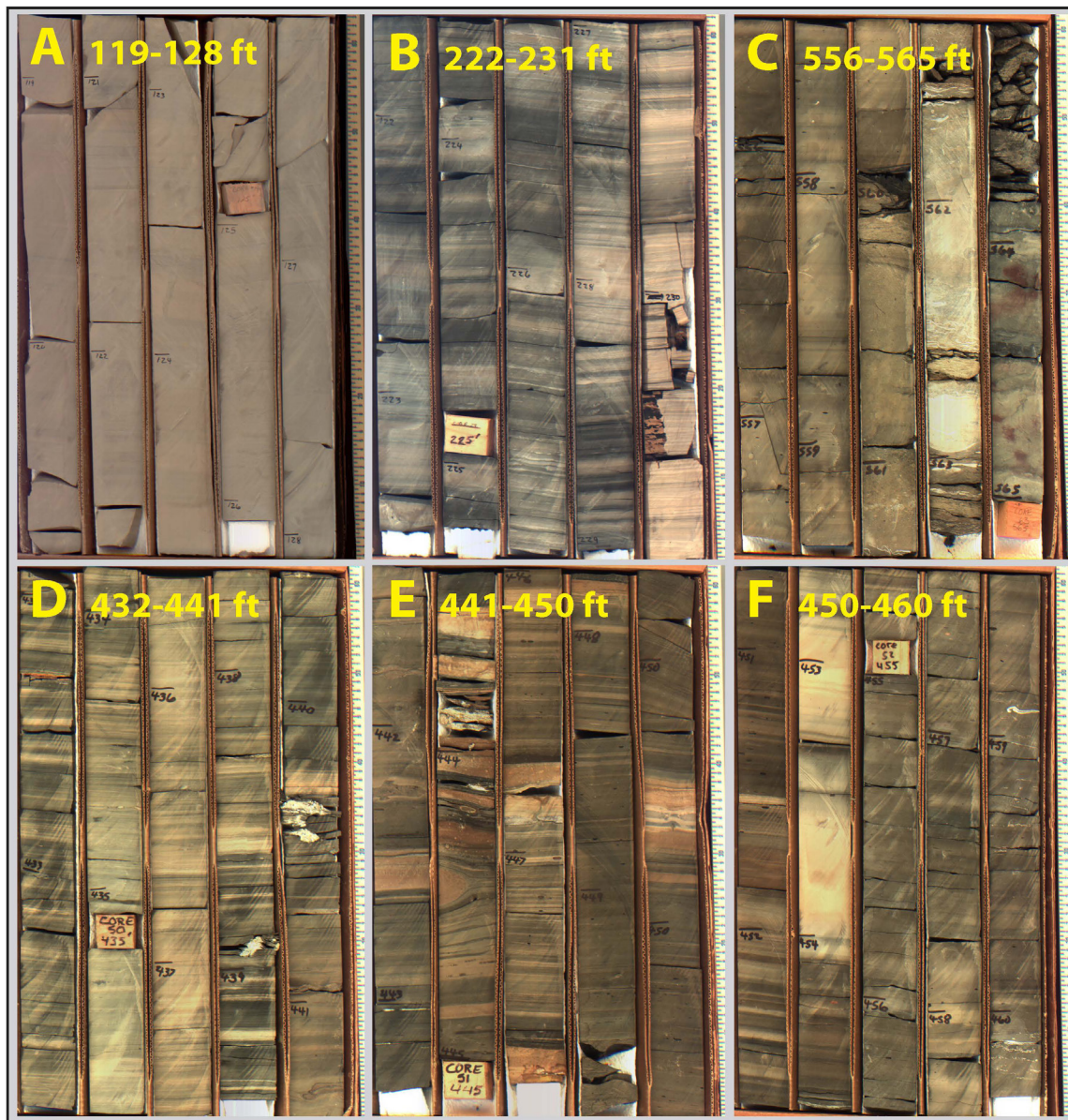


Figure 2-7: Photographs of segments of the Marsing 16 core showing the variety of lithotypes and bedding characteristics in the Green Shale facies. The locations of each panel are indicated in Figure 2-6. See text for description.

stone bodies on the basin margins. In the basin center, however, there appear to be relatively thick intervals of monotonous laminated gray to black claystone lacking siliciclastics (Figs. 2-11 and 2-12) that are not connected to carrier systems supporting secondary migration of hydrocarbons. The Virgil Mecham 1-11A2 well tested (DSTs) over 125 barrels of “highly gas-cut oil” from the interval depicted in Figure 2-11.

The total thickness of the Green River Formation varies from less than 2000 feet in the southeast against the Douglas Creek Arch to over 7500 feet thick in the west near Duchesne (Fig. 2-13). The isopach thick delineates the basin depocenter paralleling the Basin Boundary Fault. The isopachs for each of the portions of the Green River Formation and structure maps for selected markers are shown in Figures 2-14 through 2-24. Figure captions describe the content of the individual maps.

Post-Green River Overburden

In the Uinta Basin south of the Basin Boundary Fault, the Green River Formation is presently overlain by just two formations, the Uinta Formation of late middle Eocene age and the later Eocene-earliest Oligocene Duchesne River Formation. Due to erosional beveling of the post-Green River overburden, just the Uinta Formation is present in the central part of the basin (Fig. 2-25), but both formations are found to the north up to and even beneath the Basin Boundary Fault. The total thickness of the post-Green River overburden exceeds 7000 ft in the extreme northwest (Fig. 2-25), adjacent to the fault, and thins southward to the present outcrop edge of the Uinta Formation. Due to late Neogene erosion, the full original thickness of the Duchesne River Formation is nowhere preserved south of the fault. The original thickness of the Uin-



Figure 2-8: Photographs of segments of the Marsing 16 core showing the variety of lithotypes and bedding characteristics in the Black Shale facies. The locations of each panel are indicated in Figure 2-6. See text for description.



Figure 2-9: Twenty-foot wide fluvial sandstone channel incised into cyclic marginal lacustrine sediments at Indian Canyon (11S-10E) on Rt. 191 southwest of Duchesne and close to the Marsing 16 well (10S-8E).



Figure 2-10: Twenty-foot thick fluvial sandstone channel incised into marginal lacustrine Black Shale facies at Indian Canyon (11S-10E) southwest of Duchesne.

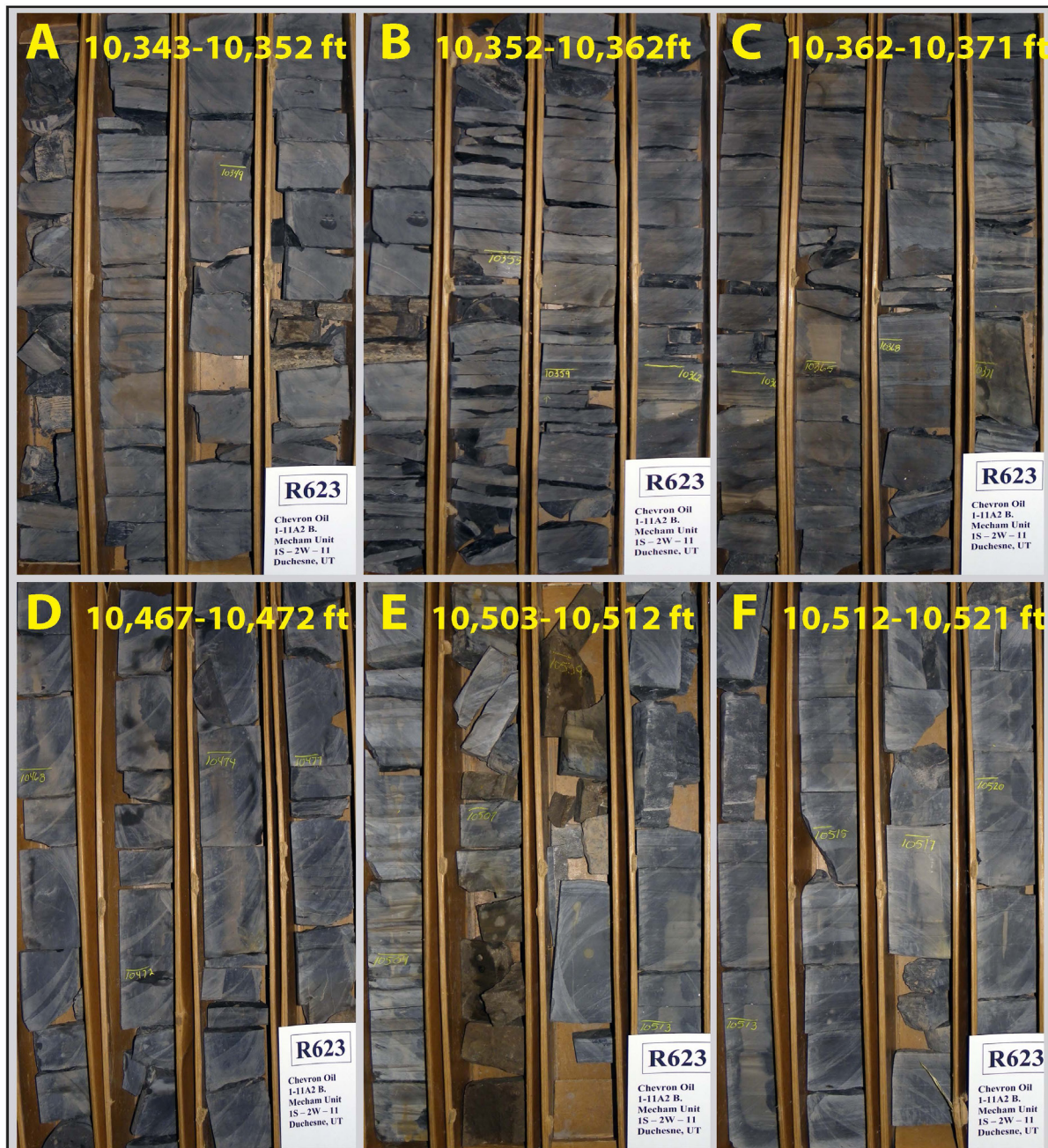


Figure 2-11: Photographs of lower Green River Formation (Black Shale facies) open lacustrine organic-rich sediments in core from the Virgil Mecham 1-11A2 well (API 4301330009; 1S-2W). See text for description.

ta Formation is preserved only north of the Duchesne River outcrop edge (blue line in Figure 2-25).

In order to assess the degree of thermal maturation of the Green River Formation source rocks, the spatial variation in maturity levels, and the times at which these levels are reached in different parts of the basin, it is essential to reconstruct, as best as possible, the full original thickness of the overburden, the times of deposition of the various units, and the history of exhumation. The procedures for doing this are presented in Chapter 4. However, this section discusses what is firmly known about the overburden succession.

Perhaps driven by the onset of glaciations in the Antarctic (Berggren and Prothero, 1992), global cooling and increased aridity began in the late middle Eocene, ending the Early Eocene Climatic Optimum, and continued into the earliest Oligocene. In middle Eocene time, Lake Uinta experienced a gradual transition from wet to increasingly arid climates. This was observed in the Upper Green River Formation by the progression from oil shales of the R-8 interval (humid) to the “saline facies” and the “limestone and sandstone facies” (arid playa and alluvial). The Uinta Formation (late middle Eocene) records the encroachment of alluvial sedimentation on the remaining playas in the basin depocenter. Based on magneto-

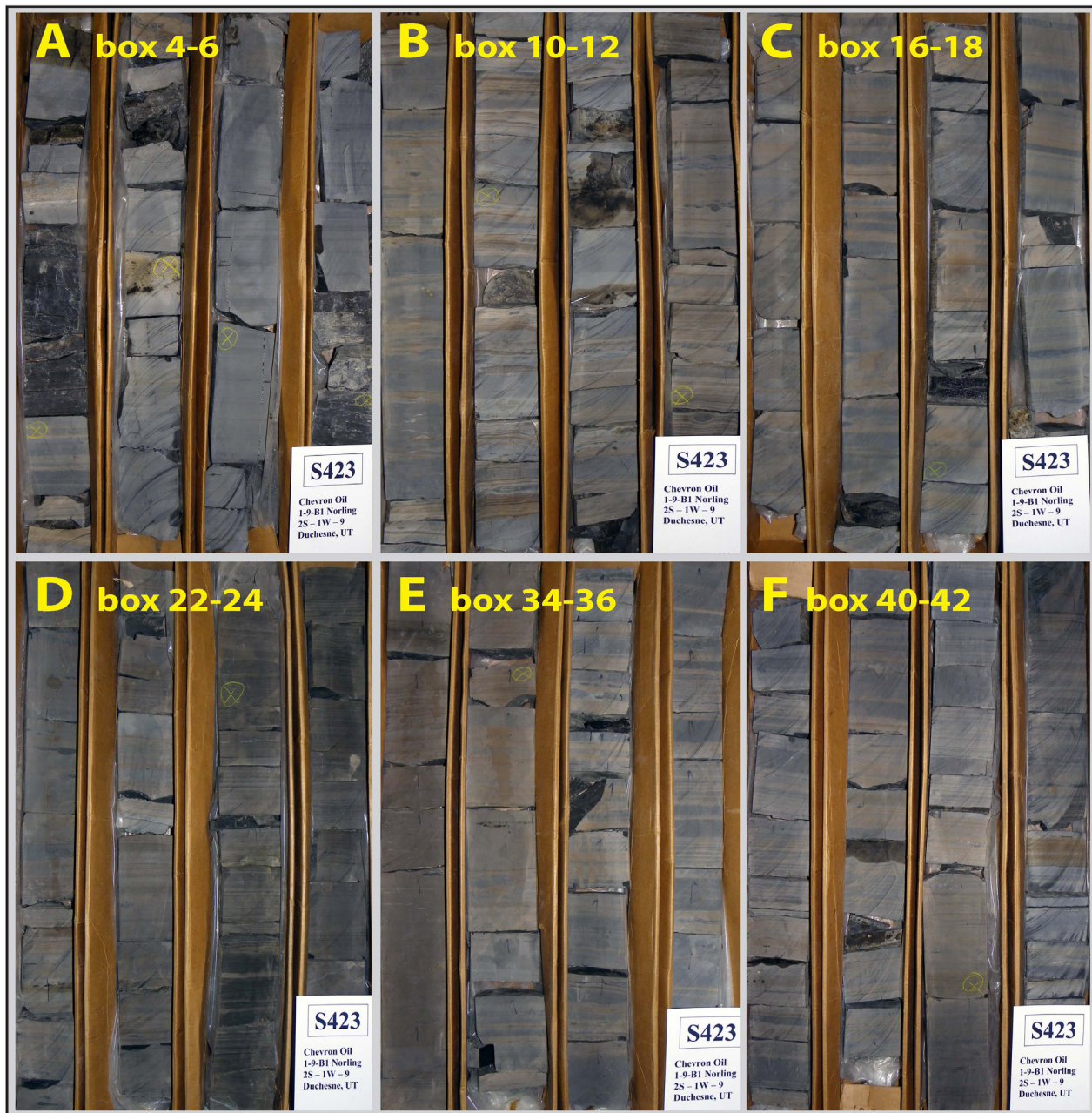


Figure 2-12: Photographs of lower Green River Formation (Black Shale facies) open lacustrine organic-rich sediments in core from the Norling 1-9B1 well (API 4301330315; 2S-1W). See text for description.

stratigraphy, Prothero (1996) dates the base of the Uinta Formation as 47.0 Ma, but more convincingly Smith and others (2008a, 2008b) consider the contact to be time-transgressive, ranging in age from 47 Ma in the east to 44 Ma in the western basin depocenter where the playas lingered longest. The Uinta Formation is fluvial variegated mudstone and fine-grained sandstone with minor conglomerate and volcanic tuffs. In the extreme north of the basin, the formation is reported to be 3100 to 3200 feet thick, but in the southeast it is just 1300 to 1400 feet thick (Sprinkel, 2007, Plate 3).

The Duchesne River Formation has been divided into four members, the first three of which are distinguished by dif-

fering proportions of varicolored sandstone and mudstone with minor conglomerate. The depositional setting is fluvial with minor interfluvial lakes (Murphey and others, 2011). The highest unit, the Starr Flat Member, stands apart for its abundance of conglomerate with minor sandstone and mudstone (Sprinkel, 2006). In the northern Uinta Basin, the Duchesne River Formation is reported to be about 3650 feet thick (Sprinkel, 2007, Plate 3). The Lapoint ash bed at the base of the third highest member (Lapoint Member) has been dated as 39.74 ± 0.07 Ma (Prothero and Swisher, 1992). The Duchesne River Formation is the stratotype for the Duchesnean North American Land Mammal Age (NALMA) which records a major faunal replacement in North America during which there

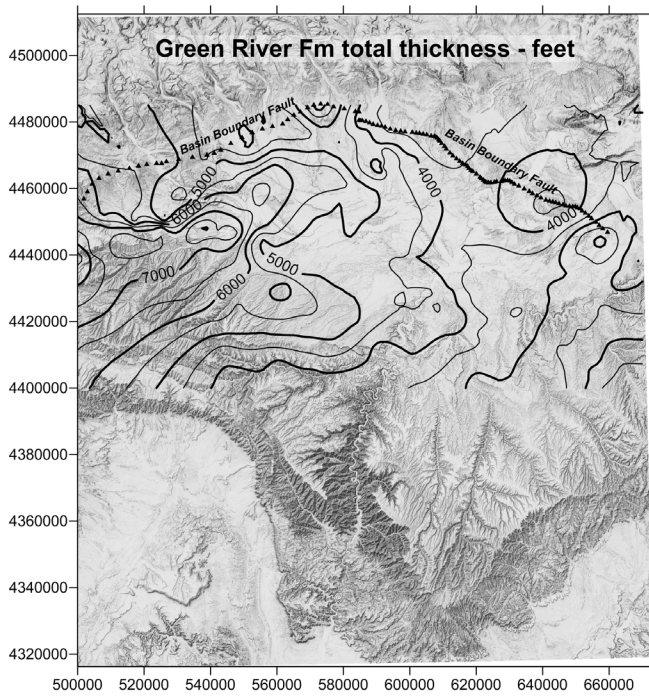


Figure 2-13: Isopach for the entire Green River Formation from the base of the Uteland Butte member to the top of the formation. For the areas of the basin where the formation is not erosionally truncated, thickness varies from less than 3000 feet in the southeast against the Douglas Creek Arch to over 7500 feet in the northeast-trending basin depocenter in the western part of the basin. There is a secondary thick trending eastward from the depocenter. These large differences in formation thickness will influence the spatial distribution of thermal maturity of the Green River source rocks. The geographic coordinates are meters in UTM NAD83, Zone 12. Contour interval: 500 feet.

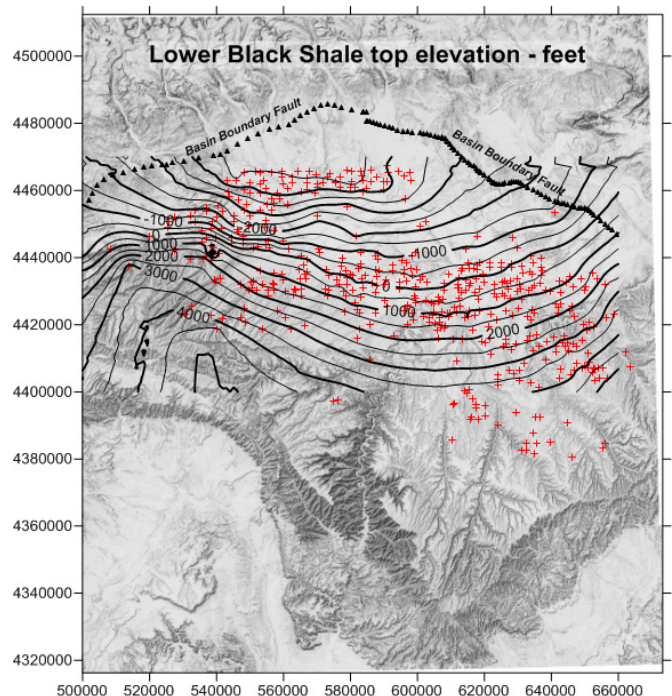


Figure 2-15: Elevation of the top of the Carbonate Marker or the top of the Lower Green River Formation and the lower Black Shale facies. Red crosses indicate wells with elevation control. Contour interval: 500 feet

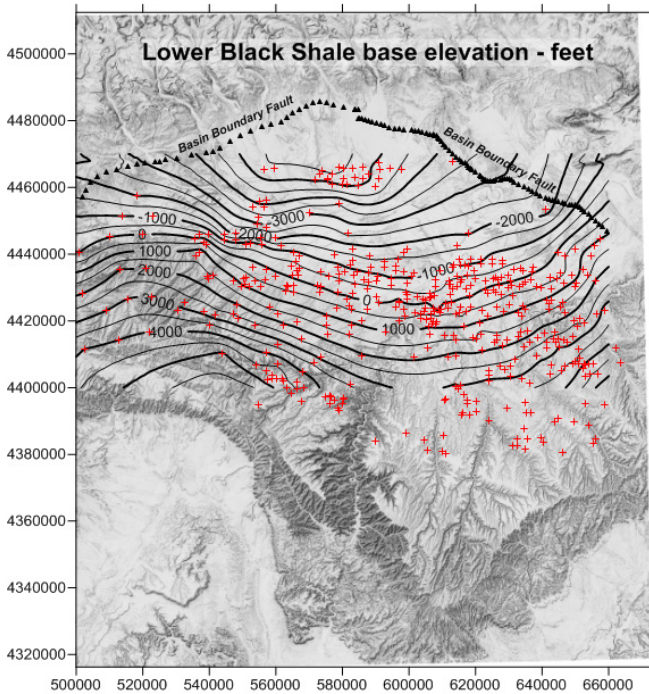


Figure 2-14: Elevation (msl) of the base of the Uteland Butte Limestone and Lower Black Shale. This is the base of the Green River Formation. Red crosses indicate wells with elevation control; gridding of well tops was limited to the central and northern basin. Contour interval: 500 feet.

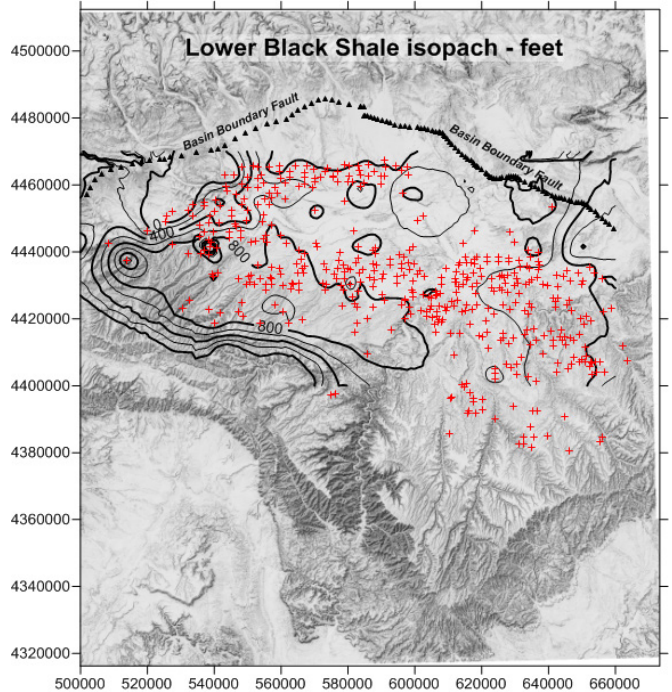


Figure 2-16: Isopach of the lower Black Shale unit, the Lower Green River Formation. The 800+ foot thick trends east-west along the present south erosional edge of the southwest part of the basin. The rapid thinning to the south is an artifact of erosional thinning in the Roan Cliffs. The isopach thick coincides with the known distribution of the Wasatch (Colton) tongue within the Black Shale unit as mapped. Red crosses indicate wells with interval thickness control. Contour interval: 200 feet.

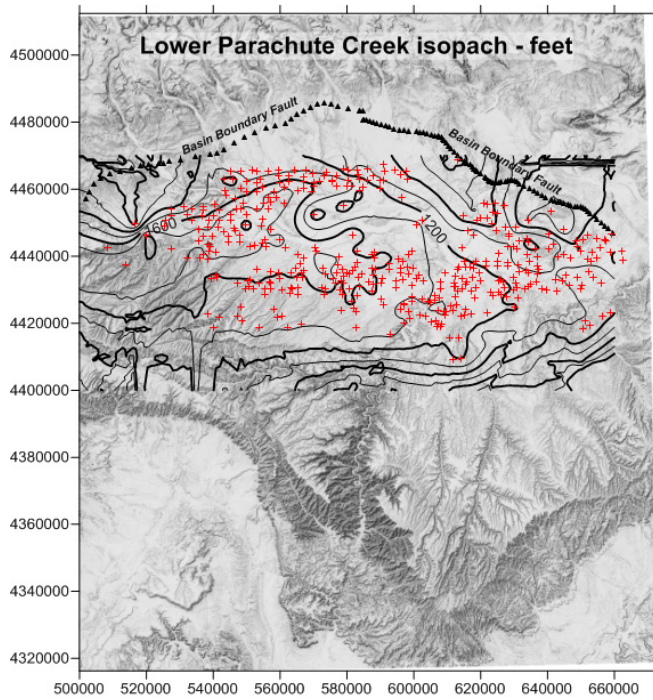


Figure 2-17: Isopach of the lower Parachute Creek Member; the interval from the top of the Carbonate Marker to the base of the R-4 interval. This is the lower part of the Middle Green River Formation, commonly correlated with the Douglas Creek Member. Thickness exceeds 1800 feet in the northeast-trending basin depocenter and is between 1200 to 1600 feet over a broad east-west trending area in the southern part of the basin. Red crosses indicate wells with interval thickness control. Contour interval: 200 feet.

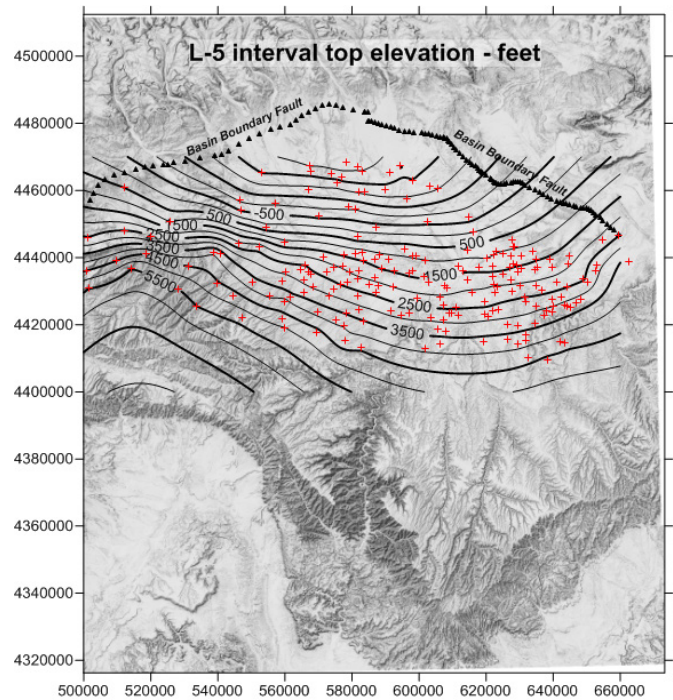


Figure 2-19: Elevation (msl) of the top of the L-5 interval (refer to Figure 2-5; Vanden Berg, 2008). Red crosses indicate wells with elevation control. Contour interval: 250 feet.

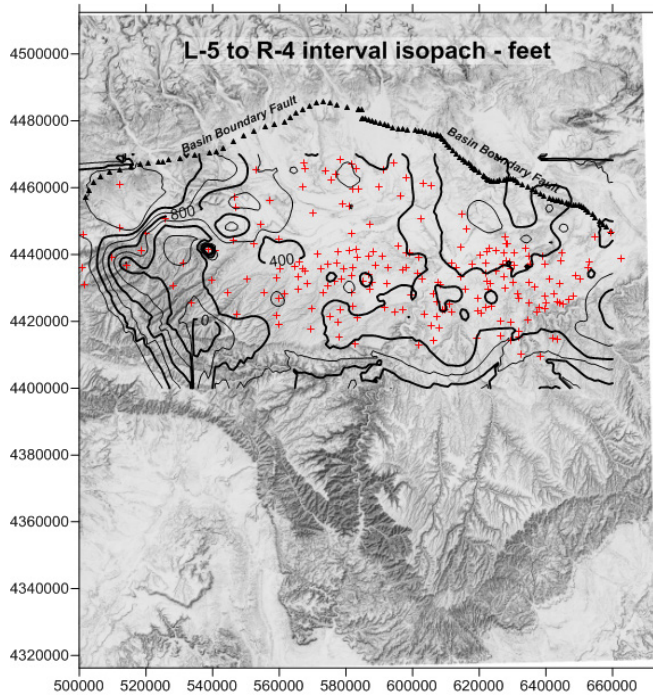


Figure 2-18: Isopach of the portion of the Parachute Creek Member between the base of the R-4 interval to the top of the L-5 interval (refer to Figure 2-5; Vanden Berg, 2008). Thickness is relatively uniform across the basin. Red crosses indicate wells with interval thickness control. Contour interval: 200 feet.

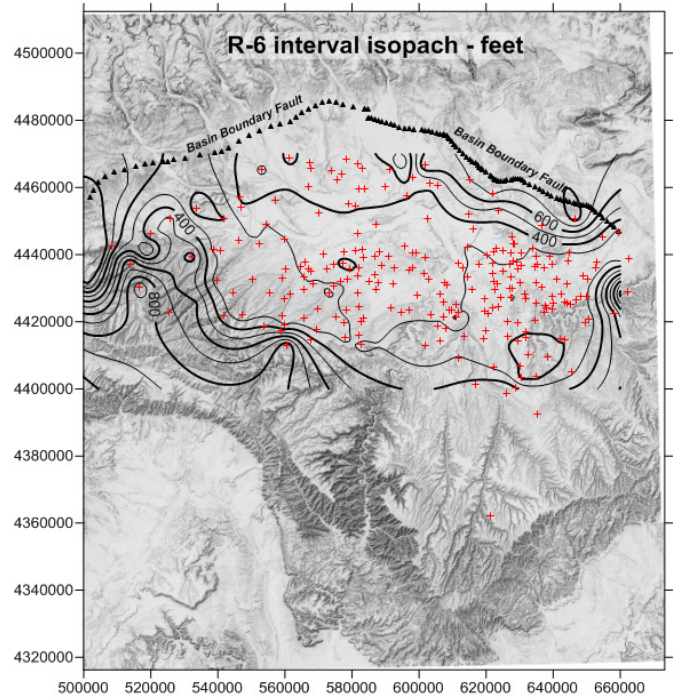


Figure 2-20: Isopach of the R-6 and B-groove intervals (refer to Figure 2-5; Vanden Berg, 2008) between the top of the L-5 interval and the base of the Mahogany Zone (top of B-groove). Across most of the basin this interval is less than 400 feet thick. Red crosses indicate wells with interval thickness control. Contour interval: 100 feet.

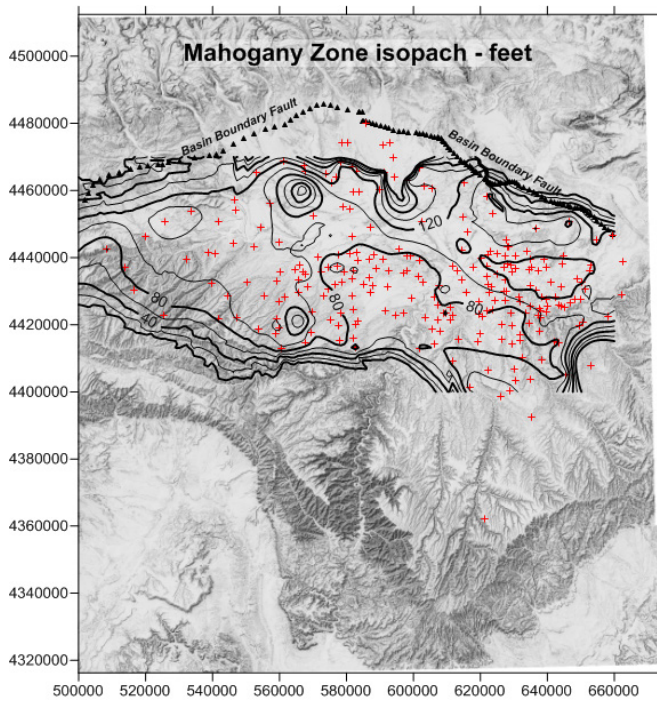


Figure 2-21: Isopach for the Mahogany Zone, the R-7 interval (refer to Figure 2-5; Vanden Berg, 2008). Across the greater part of the basin, this exceptionally organic-rich zone is 80 to 120 feet thick. However, it is observed to be thickening towards the Basin Boundary Fault. Red crosses indicate wells with interval thickness control. Contour interval: 20 feet.

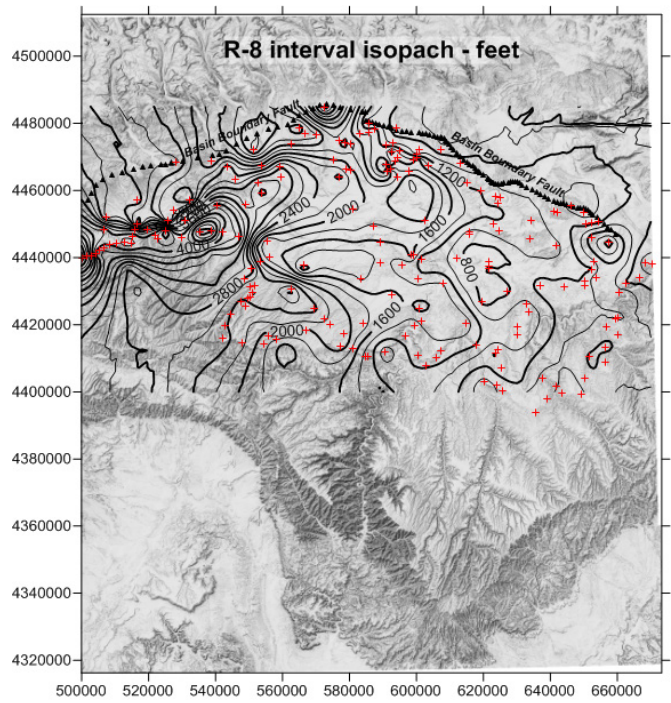


Figure 2-23: Isopach of the Upper Green River Formation above the Mahogany Zone. Thickness increases dramatically from east to west, from less than 400 feet in the southeast to more than 4000 feet in the basin depocenter in the west. Some portion of the irregularities in this isopach may relate to the difficulty in accurately determining the top of the Green River Formation. Red crosses indicate wells with interval thickness control. Contour interval: 200 feet.

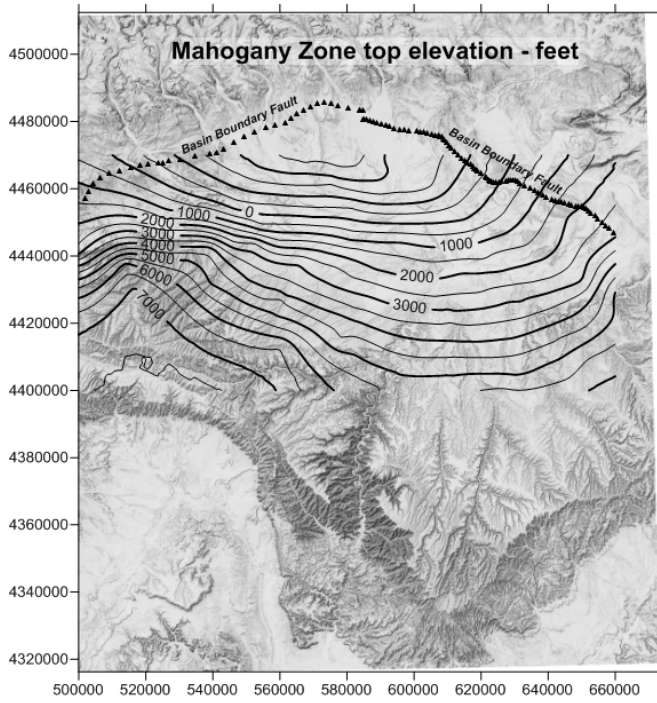


Figure 2-22: Elevation (msl) of the top of the Mahogany Zone, R-7, the base of the Upper Green River Formation (refer to Figure 2-5; Vanden Berg, 2008). The control wells are the same as those shown in Figure 2-21. Contour interval: 500 feet.

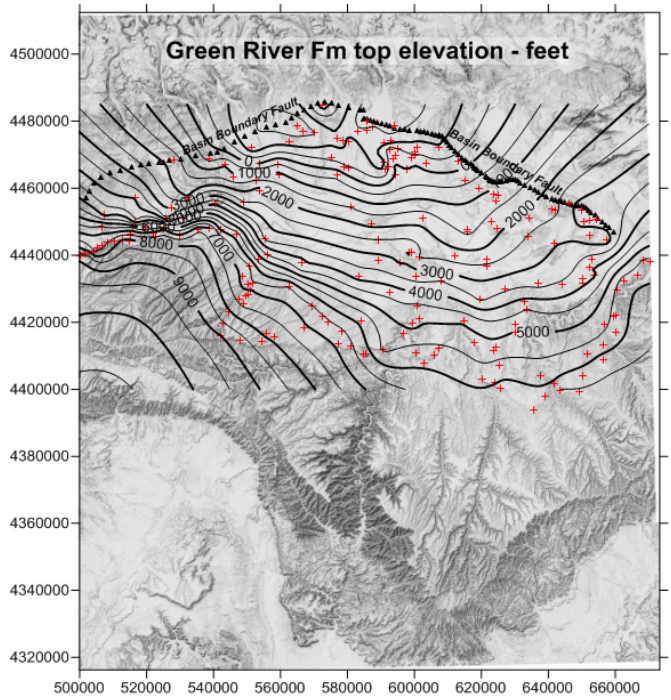


Figure 2-24: Elevation (msl) of the top of the Green River Formation. Red crosses indicate wells with elevation control. Contour interval: 500 feet.

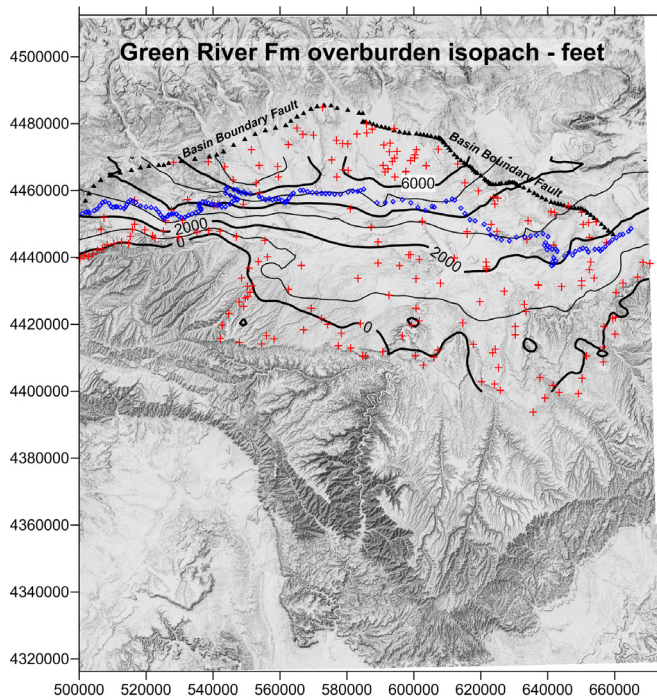


Figure 2-25: Isopach of the post-Green River Formation overburden, the combined Uinta and Duchesne River Formations. The thickness ranges from zero at the southern erosion edge of the base of the Uinta Formation to over 7000 feet along the Basin Boundary Fault in the extreme northwest of the basin. This isopach was constructed by subtracting the top of the Green River Formation (Fig. 2-24) from the present ground surface at each of the wells indicated by the red cross. The zero isopleth is the outcrop edge of the Uinta Formation on geologic maps (Bryant, 2010; Weiss and others, 2003; Sprinkel, 2007; Sprinkel, 2009). The blue dotted line indicates the present south outcrop edge of the Duchesne River Formation. Contour interval: 1000 feet.

were large numbers of last and first occurrences of land mammal genera (Murphey and others, 2011).

Along the south flank of the Uinta Mountains, and capping the Diamond Mountain and the Blue Mountain plateaus, there are erosional remnants of a poorly-sorted boulder to pebble conglomerate (Rowley and others, 1985; Sprinkel, 2006; Bryant, 2010), the Bishop Conglomerate. In nearly all instances the mapped Bishop Conglomerate rests conformably on the conglomeratic Starr Flat Member of the Duchesne River Formation. Kowallis and others (2005) have dated tuffs in the Bishop Conglomerate on the Diamond Mountain Plateau as 30.54 ± 0.22 Ma using $^{40}\text{Ar}/^{39}\text{Ar}$ laser fusion methods. Furthermore, they argue that the Bishop Conglomerate and Starr Flat Member are the same stratigraphic unit and propose dropping the name Starr Flat.

The end of the Eocene was apparently the time in which the Laramide orogeny was ending, thus permitting regionally extensive pedimentation of the mountains flanking the Uinta Basin. The Gilbert Peak erosion surface was formed by this episode of pedimentation (Hansen, 1986). This surface forms the top (depositional and/or erosional) of the Duchesne River Formation. The Bishop Conglomerate-Starr Flat Member was

deposited on top of and basinward of the Gilbert Peak surface (Pedersen and Hadder, 2005).

Until the mid-Tertiary, the modern Green River existed in two segments separated by the Uinta Mountains–White River Uplift. The upper Green River drained eastward well north of the mountain range and the lower Green River was just a minor tributary to the Colorado River south of the mountains. In the early Miocene, extension on the north flank of the Uinta Mountains was instrumental in capturing the upper Green River and diverting it along the graben into northwest Colorado (Hansen, 1986). The river deposited the Miocene Browns Park Formation in this newly-formed, structurally-controlled basin. At the time of early Miocene (20.3 Ma) crustal extension, the Gilbert Peak erosion surface tilted northward, thus ending deposition of the Bishop Conglomerate (Hansen, 1986). Due perhaps to infilling of the Browns Park basin or headward erosion of the lower Green River, in the late Neogene the two segments of the Green River eventually connected, either through the Gates of Lodore (Hansen, 1986) or the Canyons of Lodore (Pedersen and Hadder, 2005). The incision of entrenched meander canyons into plateaus capped and rimmed by the Gilbert Peak surface suggests that the connection occurred in the Pleistocene (Hansen, 1986). The widespread occurrence of gravels dated as middle Pleistocene resting with minor erosion on the Bishop Conglomerate strongly implies that little erosion occurred in the Uinta Basin before about 0.5 Ma (Sprinkel and others, 2013).

Based on the discussion above and in consultation with Douglas Sprinkel, Utah Geological Survey, the following scenario is proposed for the post-Green River Formation stratigraphy and geomorphic development of the Uinta Basin.

- Accompanying a period of global cooling and increasing aridity from the late middle Eocene through the earliest Oligocene, deposition in the Uinta Basin laid down a very thick succession of fluvial sediments, up to 3200 feet of Uinta Formation and 3600 feet of the three lower members of the Duchesne River Formation.
- An interval of tectonic quiescence near the Eocene-Oligocene boundary accompanied by extensive pedimentation creating the Gilbert Peak erosion surface that in the Uinta Basin forms the top of the Duchesne River Formation.
- Beginning in early Oligocene time (30.5 Ma), deposition on the Gilbert Peak surface of coarse proximal alluvium of the Bishop Conglomerate and age-equivalent Starr Flat Member. Alluvium continues to accumulate into the earliest Miocene.
- Early Miocene (20.3 Ma) crustal extension leading to grabens on the north flank of the Uinta Mountains is accompanied by northward tilting of the Gilbert Peak erosion surface and its sedimentary cover, effectively turning off sediment accumulation on the high arid plateau across the structural Uinta Basin.

- Starting in the late Miocene, approximately 10 Ma, low-energy streams in the headwaters of the lower Green River drainage begin cutting into the high plateau. Erosion rates are very slow.
- In the middle Quaternary (0.5 Ma), the upper Green and Yampa Rivers join with the lower Green River resulting in very rapid incision of the high plateau and lowering of Green River tributary base levels in the Uinta Basin. It was in this half million year period that the major part of the present landscape was carved, exhuming many thousands of feet of post-Green River overburden.

3. ORGANIC GEOCHEMISTRY

Lacustrine basins are ideal settings for the accumulation and preservation of organic matter, especially large volumes of hydrogen-rich kerogens (Fleet and others, 1988; Carroll and Bohacs, 2001; Katz, 1990; Carroll and Wartes, 2003; Bohacs and others, 2003). The Eocene Green River Formation is widely recognized as a world-class source-rock succession for conventional oil resources and for having the potential for unconventional oil (Fouch and others, 1994; Katz, 1995; Dubiel, 2003; Lillis and others, 2003; among many others). The purpose of this study is not to re-establish the quality of the Green River source rocks, but rather to determine if they have characteristics common to known shale oil resource plays, such as the marine Niobrara Formation and Bakken Shale.

All lacustrine basins have a diversity of depositional settings that shift back and forth with the climatically-driven rise and fall of the lake system. Lake Uinta was not exceptional. As discussed in the previous chapter, fluvial delta and alluvial plains rimmed the outer parts of the lake basin. Broad and ever-changing mudflats formed the ever-migrating lake shoreline, and the near-perennial lake itself was subject to cyclic sedimentation that was influenced by internal and external drivers. Therefore, it is not surprising that the kerogen types found in the Green River Formation (Fig. 3-1) are wide-ranging from humic and algal coals to exceptionally hydrogen-rich sapropel, each characteristic of a different part of the total lake system (Fig. 3-2).

The wells for which organic geochemical analyses are presented in this chapter are identified in Table 3-1 and located on a map (Fig. 3-3). The data reported in Anders and Gerrild (1984) are from cuttings; all other analyses are from core material. With the exception of the analyses tabulated in Dean and Anders (1991), all of the analyses are new to the public domain and are being presented herein perhaps for the first time. Data from the recently drilled Bill Barrett Corporation 16X-23D-36 and 14X-22-46 cores were donated to the UGS in March 2012. In early 2010, Dan Jarvie (Texas Christian University) graciously donated a large set of analyses for the Marsing 16 core. In addition, El Paso E & P contributed anal-

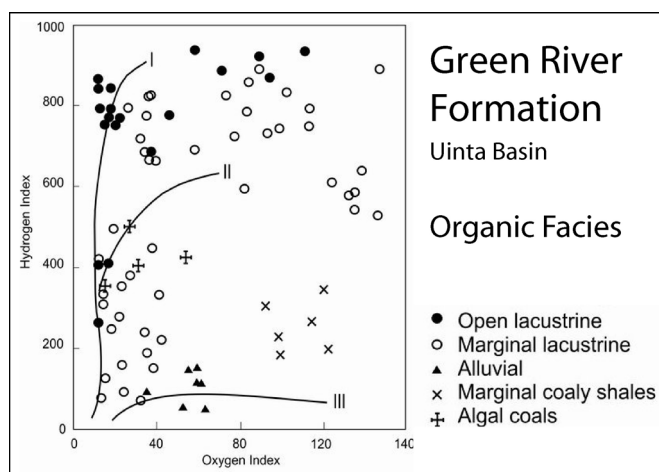


Figure 3-1: Organic facies of the Green River Formation as indicated by fields on a van Krevelen plot. Kerogens range from high-HI algal-rich organics in the open lacustrine sediments to algal and humic coals and carbonaceous sediments in an alluvial setting on the extreme margins of the lacustrine basin. Data from Anders and Gerrild (1984).

yses from six deep Green River Formation cores drilled in the Altamont-Bluebell field. The cores, housed at the U.S. Geological Survey Core Research Center (USGS CRC) in Denver, date from the late 1960s to early 1980s, but the analyses are very recent.

Programmed Pyrolysis Source Rock Characterization

Programmed pyrolysis (Peters and Cassa, 1994, Appendix D) refers to an analytical technique by which a known weight of dry source rock is heated in a specially designed micro-oven at a programmed rate, such as 15°C/min to drive off and measure with a gas detector initially the free hydrocarbons in the rock that can be volatilized without cracking the kerogen (S1 peak), then at higher temperatures the hydrocarbons pyrolyses generated by kerogen cracking (S2 peak), and finally at the highest temperature the CO₂ generated by the burning of carbon with the oxygen within the remaining kerogen or char (S3 peak). The S1 peak is a measure of the residual liquid hydrocarbons already in the rock in units of mg HC/g dry rock. The S2 peak is a measure of the rock's capacity for generating new hydrocarbons by thermal cracking, also in units of mg HC/g rock. The sum of these two peaks (S1+S2) indicates the total oil generating capacity, the *genetic potential* (GP). The oven temperature at which the maximum generation of S2 pyrolysate is measured is the *T_{max}* parameter, which can be related to the thermal maturity of the source rock. The higher the *T_{max}*, the larger the quantity of hydrocarbons that had been generated already in the rock (higher transformation ratio), therefore, the greater the thermal maturity. The parameters also can be used to calculate pseudo-values of hydrogen index (HI) and oxygen index (OI). The formulas are: HI = (S2/TOC) x 100, in units of mg HC/ g TOC and OI = (S3/TOC) x 100, in units of mg CO₂/g TOC. RockEval™ is just

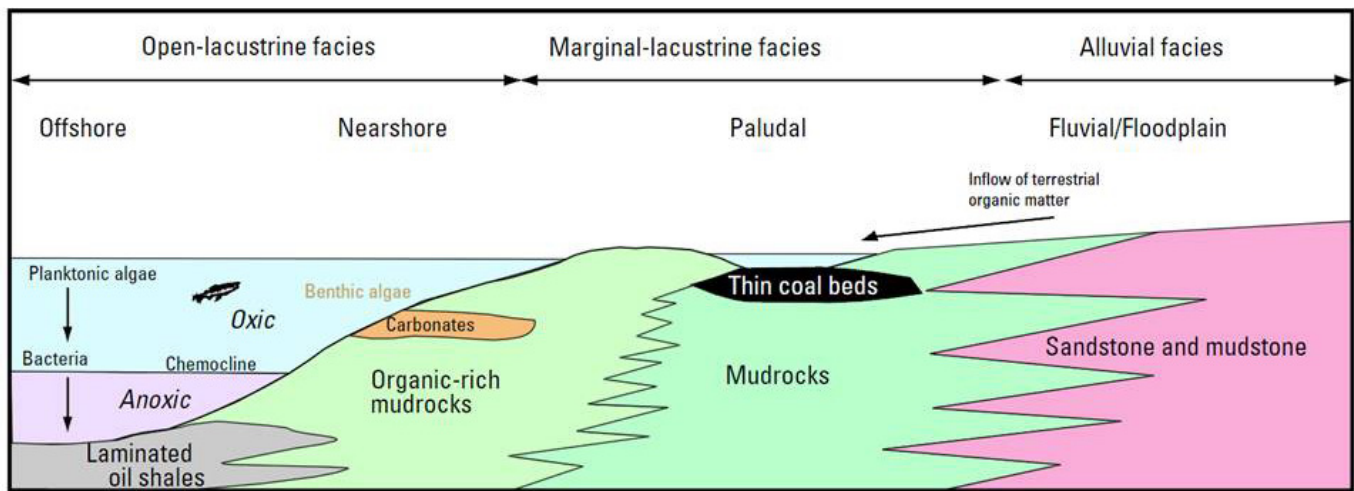


Figure 3-2: Generalized depositional settings for the several organic facies of Lake Uinta. Dubiel (2003), modified from Ruble and others (2001).

Table 3-1: Wells for which programmed pyrolysis analyses were available to and used in this study.

Well API	Well name	T-R	UTM E	UTM N	Depth range, ft	Data source
4301350623	16X-23D-36BTR	3S-6W	540518	4450034	3887-5150	UGS file
4301350351	14X-22-46DLB	4S-6W	537941	4440231	5480-5625	UGS file
4305130002	Marsing 16	10S-8E	498247	4421986	57-1223	UGS file
4301330030	Chasel 1-81A1	1S-1W	581901	4472569	10639-10705	USGS CRC file
4301330031	Olsen U1-12A2	1S-2W	580308	4773988	10495-10603	USGS CRC file
4304731470	DR Long 2-19A1E	1S-1W	591251	4470045	9163-9716	USGS CRC file
4301330036	Lamiq-Urrity 1-8A2	1S-2W	573084	4473208	10833-10951	USGS CRC file
4301330009	Virgil Mecham 1-11A2	1S-2W	578696	4474035	10348-10634	USGS CRC file
4301330315	Norling 1-9B1	2S-1W	535097	4464443	7497-7618	USGS CRC file
na	WOSCO EX-1	9S-20E	619749	4426824	2181-2963	Dean and Anders (1991)
na	Coyote Wash 1	9S-23E	644159	4431387	571-1043	Dean and Anders (1991)
4301330114	Ute Tribal 1-16	4S-7W	527471	4442295	7030-8110	Anders and Gerrild (1984)
4301330040	Cedar Rim 3	3S-6W	533730	4450740	4600-7400	Anders and Gerrild (1984)
4301330122	Dustin 1	2S-3W	567013	4460465	8500-14080	Anders and Gerrild (1984)
4301330113	Daniel Uresk Fee 1	4S-1W	581626	4446093	5030-11080	Anders and Gerrild (1984)

one of several patented analytical devices for conducting programmed pyrolysis of source rocks. All others work on the same basic principles as the original RockEval™.

Cross plots of programmed pyrolysis derived HI vs. TOC and HI vs. OI taken together are standard measures of both source rock organic richness and kerogen types. The HI vs. OI is a version of the industry-standard van Krevelen plot. A cross plot of genetic potential (GP) vs. TOC is a standard tool for evaluating overall source rock quality. Commonly used threshold values for all of these parameters are tabulated in Peters and Cassa (1994).

Noble and others (1997) introduced a technique developed at ARCO for rapid assessment of the effectiveness of shale seals, those with sufficiently high capillary pore pressures to inhibit

the penetration of oil upward out of a “shale-sealed” oil pool. The method used programmed pyrolysis data, which at the time was widely available to industry. The parameter introduced as a measure of oil saturation in the shale is (S1/TOC) x 100, in units of mg HC/g TOC. The logic was that a highly effective shale seal would have low values of oil saturation, whereas a “leaky” shale would have high values. Shales with values of 120 mg HC/g TOC or greater clearly would contain non-indigenous hydrocarbons that leaked in from the underlying oil pool.

This same parameter, referred to as the “oil saturation index” (OSI) is now gaining popularity in the search for shale oil resource plays. Most of the geochemical service companies include this parameter in their standard programmed pyrolysis reports. Jarvie (2012) has identified any shale with an index

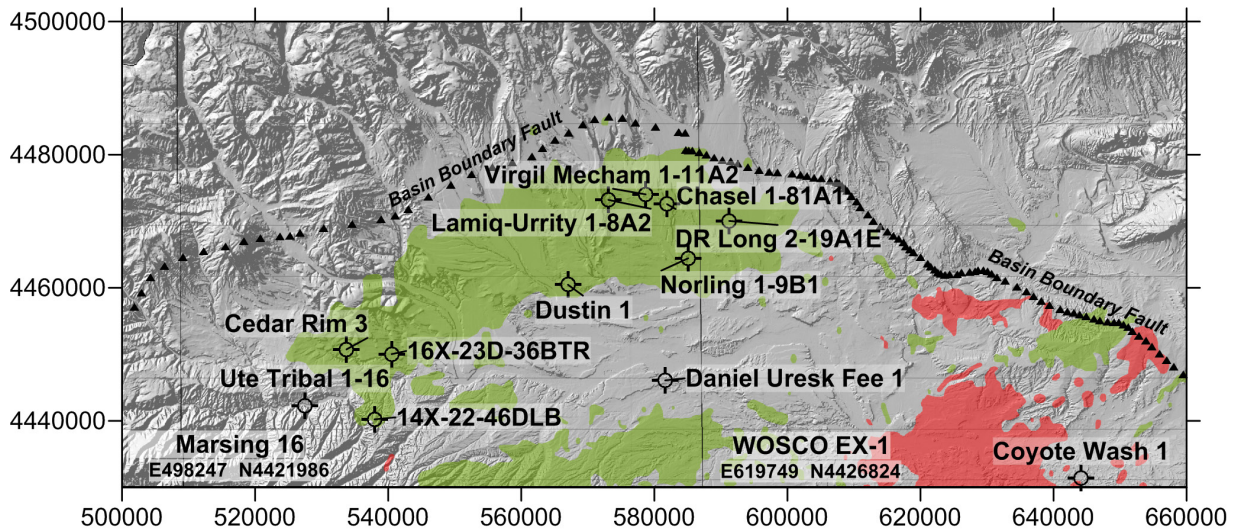


Figure 3-3: Location of cored wells having programmed pyrolysis data used in this study. Refer to Table 3-1 for the well coordinates, API numbers and data sources. Marsing 16 and WOSCO EX-1 lie immediately to the southwest and south, respectively, of the map. The geographic coordinates are meters in UTM NAD83, Zone 12.

greater than 80 to 100 mg HC/g TOC as having the potential to be a commercial shale oil resource. In the absence of natural fractures, organic-rich mudstones retain as much as 70–80 mg of hydrocarbons per gram of TOC. Oil at these levels of concentration is bound by the organic-matter by adsorption and solvation (absorption) and is not mobile (Jarvie, 2012). Potentially productive source-rock intervals are either those with very high values of OSI, such as the Eagle Ford Formation in southeast Texas (Figure 3-4), or intercalated or proximal low-TOC strata that have been charged with oil from adjacent productive beds, as in the Bakken (Figure 3-5) and Niobrara Formations.

The OSI is an effective predictor of potential shale oil reservoirs only for rocks within the oil-generative window. As the gas-generative window is reached, the residual oil is cracked,

reducing the value of S1. This is what is observed in organic-rich mudstone of the Paradox Formation in the Paradox Basin. In the oil-generative window in the Paradox Formation in Utah, both the GP and OSI values are high relative to TOC, but both parameters are lower in southwest Colorado which is in the gas-generative window (Figs. 3-6 and 3-7). The Paradox Formation organic-rich mudstones produce oil in Utah and gas with minor gas-liquids in Colorado (Schamel, 2009).

For each group of Green River Formation core samples, this chapter presents four cross plots of programmed pyrolysis data: TOC vs. HI, HI vs. OI, GP vs. TOC, and finally S1 vs. TOC, an x-y representation of the OSI that displays more information than just the index itself. Where a large amount of data is available for a single core, these key parameters are also displayed in a geochemical log.

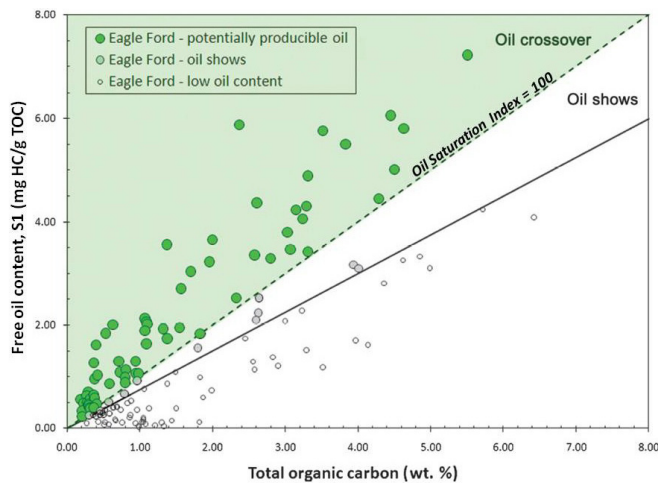


Figure 3-4: Total organic carbon (TOC) plotted against S1 for Eagle Ford Formation mudstones with a range of oil contents as evidenced in well tests. Figure is modified from Jarvie (2012). AAPG©2012, reprinted by permission of the AAPG whose permission is required for further use.

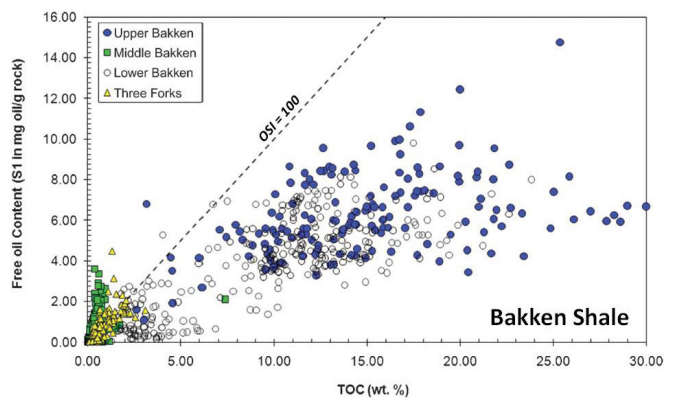


Figure 3-5: TOC plotted against S1, a measure of residual oil in the rock, for the Bakken Shale. The values with low TOC and very high S1 are Middle Bakken “reservoir” samples in an oil-impregnated, but non-source rock portion of the Bakken Shale. The Three Forks Formation commonly plays a similar role as a non-source oil reservoir. Figure modified after Jarvie (2012). AAPG©2012, reprinted by permission of the AAPG whose permission is required for further use.

The 1237-foot-long Marsing 16 core samples a large segment of the Green River Formation immediately southwest of its depocenter in the western part of the basin. The upper part contains the “Middle Marker” and the Green Shale facies of the lower Middle Green River Formation (refer to Figure 2-6). The lower part samples the entire Lower Green River Black Shale facies and the uppermost deltaic sandstones of the un-

derlying Wasatch (Colton) Formation. The full range of kerogen types known in the Green River Formation are present in this core (Figs. 3-8 and 3-9). Note that there are both algal and humic coals. Source-rock quality ranges from poor to excellent (Fig. 3-10), with the majority of the samples being very good and excellent. It is interesting that the Green Shale facies is a consistently better source rock than the Black Shale

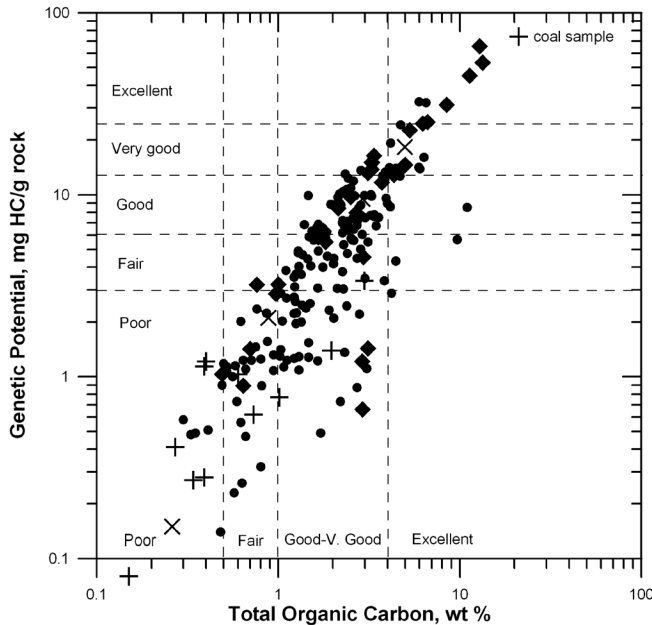


Figure 3-6: TOC plotted against genetic potential (S1+S2) for various Paradox Formation shales in the Paradox Basin of Utah. This plot serves to indicate general source rock quality, as indicated in the figure. Data reported in Schamel (2009).

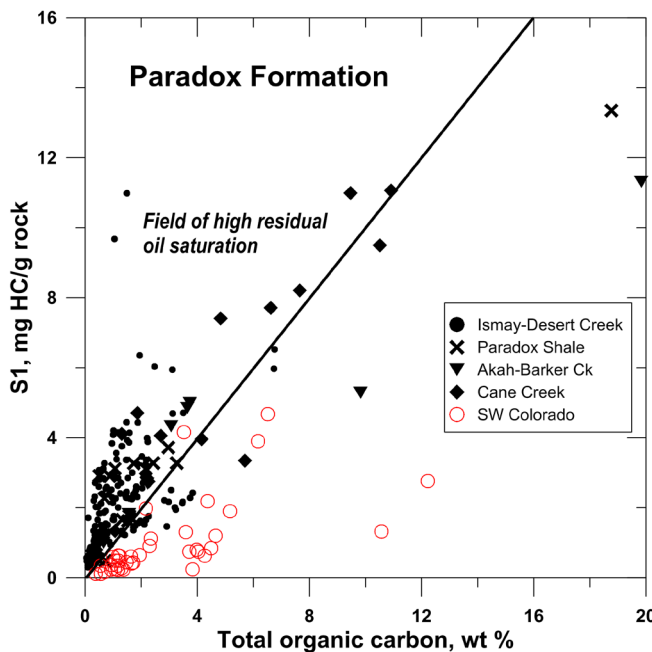


Figure 3-7: TOC plotted against S1 from programmed pyrolysis for Paradox Formation shales in oil-producing Utah (black symbols) and natural gas-producing southwest Colorado (red circles). Data from Schamel (2009) and GeoX Consulting Inc internal files.

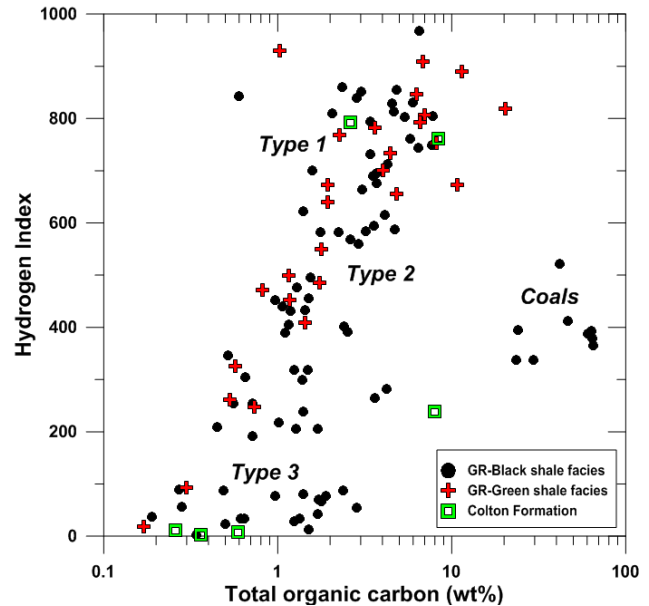


Figure 3-8: For Marsing 16 core samples, TOC plotted against hydrogen index (HI) showing that except for the coals, hydrogen content of the kerogen increases with increased organic richness. The most oil prone source rocks are also the richest. This 1237 ft core sampled the lower Green River Formation in the southwest Uinta Basin. Data from UGS CRC files.

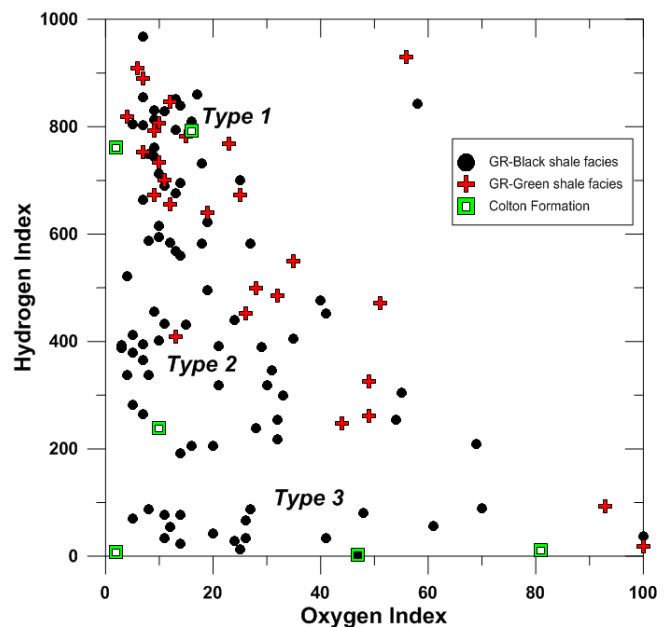


Figure 3-9: A van Krevelen plot showing the wide range of kerogen types found in the lower Green River Formation sampled in the Marsing 16 core. The diversity of kerogen types exists in each of the three stratigraphic units cored. Data from UGS CRC files.

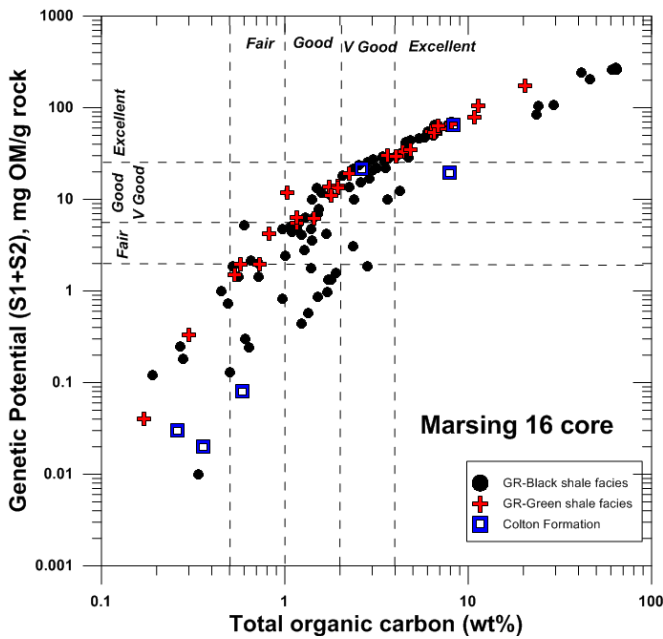


Figure 3-10: TOC vs. genetic potential plot for Marsing 16 core samples indicating the high quality of source rocks in the Black Shale and the Green Shale facies. Note the very large range in values of both TOC and GP. This reflects the large diversity of the cyclically-interbedded organic facies. Data from UGS CRC files.

facies. The geochemical logs for the Marsing 16 core (Fig. 3-11), which plot the values in the cross plots as a function of depth, show interesting patterns. Most obvious are the four cycles expressed in values of TOC, HI, and the OSI. These cycles match only in part the stratigraphic subdivisions of Wiggins and Harris (1994); refer to Figure 2-6. The most organic carbon- and hydrogen-rich rocks are associated with the intervals identified as marginal lacustrine. These intervals also have the higher residual oil saturations. Note that TOC and $(S1/TOC) \times 100$ are displayed on log scales. The siliciclastics-carbonate, open-lacustrine succession has only Type II and Type III kerogens and low oil saturation index. There are just three instances of OSI higher than 100, and these spikes are in the 200 to 600 range (Fig. 3-11). Examination of the core photographs for these spikes failed to disclose their source. Examination of the actual core would be needed. It is clear, however, that the residual oil saturations are not sufficiently high to characterize the Green River Formation sampled by this core as a potential shale oil resource. The low OSI values could indicate low thermal maturity of the source rocks, related to their shallow depth of burial, or migration of once-present mobile oil out of the rock. The average Tmax (see Fig. 3-11) is just at the lower oil-generative window threshold.

Core samples from the southeast part of the basin are primarily from the Middle and lowest Upper Green River Formation. The samples are very hydrogen-rich and dominantly Type I kerogens (Figs. 3-12 and 3-13) and their TOC content is exceptionally high. Consequently, these Middle and Upper Green River strata are very good to excellent source rocks (Fig. 3-14). A few of the samples from the WOSCO EX-1 and

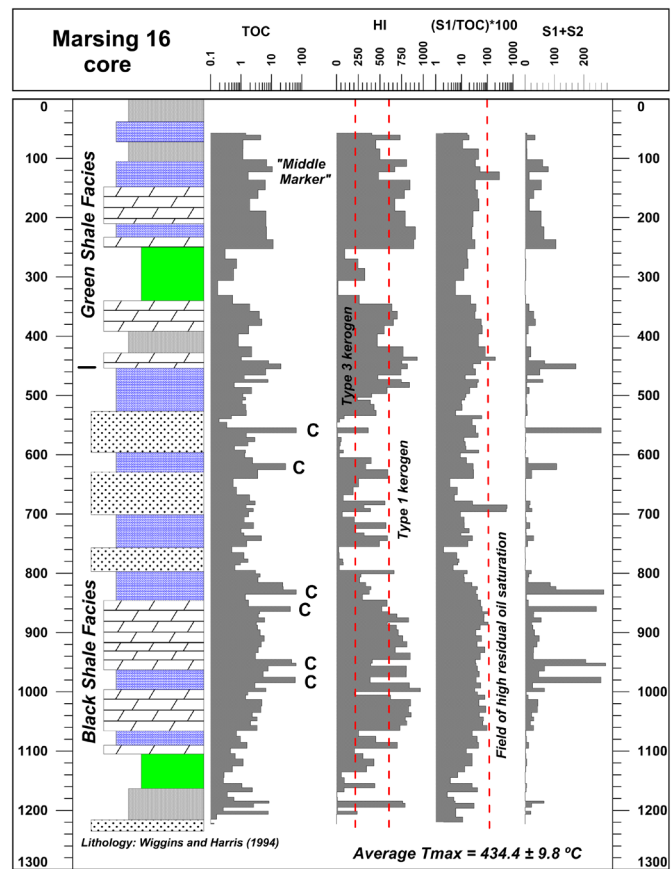


Figure 3-11: Organic geochemical log of the lower Green River Formation in the Marsing 16 core in the southwest Uinta Basin. Depth in feet; "C" indicates coal beds. Data from Wiggins and Harris (1994) and UGS CRC files. See text for discussion.

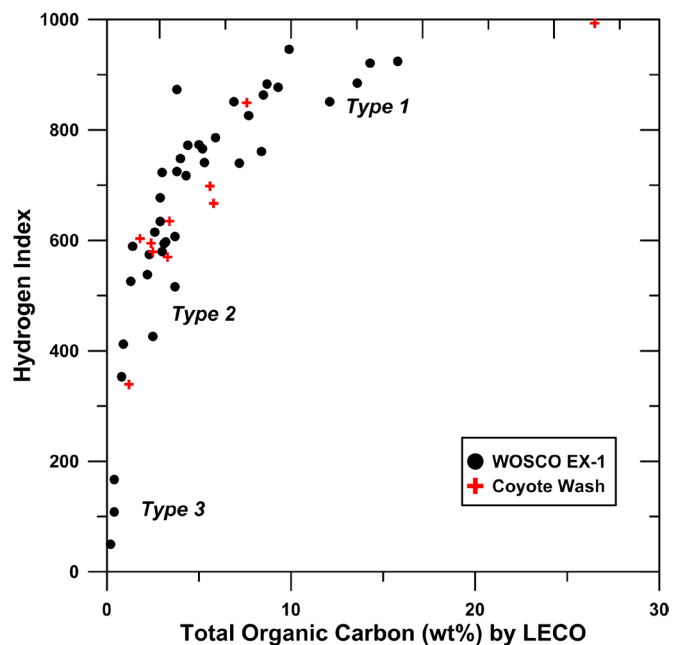


Figure 3-12: TOC vs. hydrogen index for Parachute Creek Member samples in cores from the southeast Uinta Basin. Data from Dean and Anders (1991).

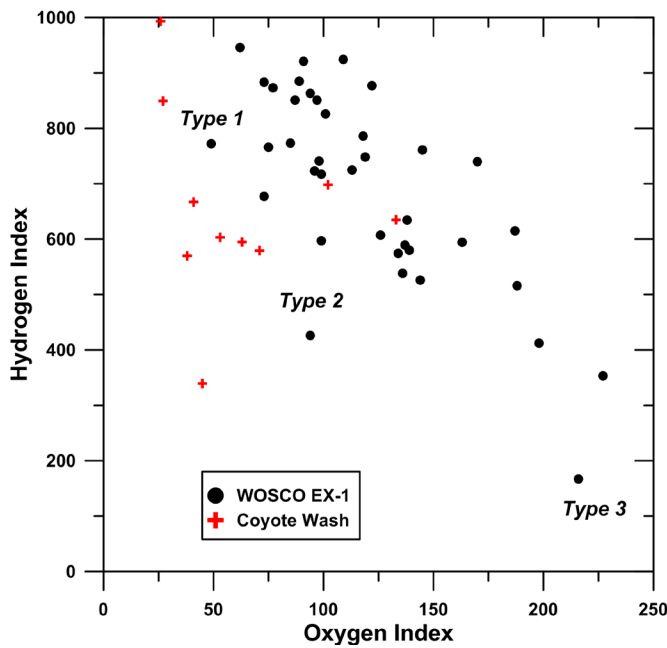


Figure 3-13: Van Krevelen plot for the Parachute Creek Member core samples in the southeast basin. Note the predominance of Type I and Type II kerogens at this higher stratigraphic level, at least in this axial part of the basin. Data from Dean and Anders (1991).

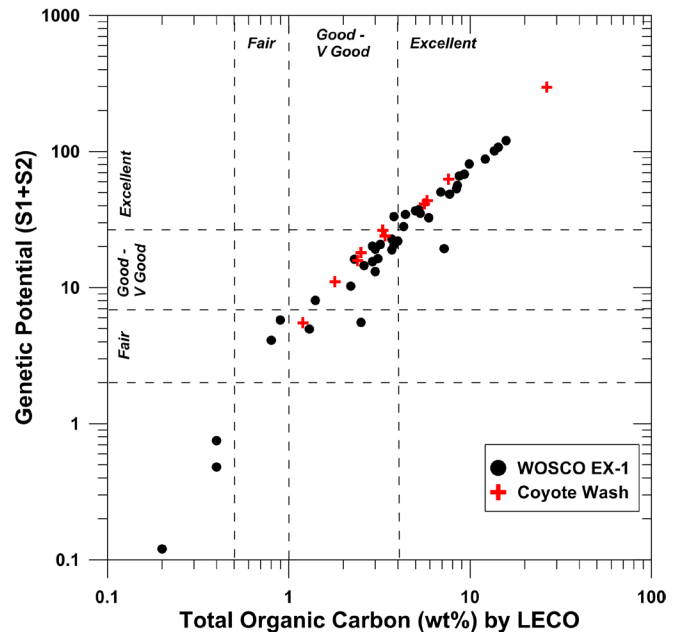


Figure 3-14: TOC vs. genetic potential of the Parachute Creek Member core samples indicating the overall good to excellent quality of the source rocks. It is known that these are low maturity rocks, although T_{max} or R_o measurements are not available for the samples. Data from Dean and Anders (1991).

Coyote Wash cores even have elevated values of OSI (Fig. 3-15). The geochemical log of the WOSCO EX-1 core (Fig. 3-16) shows a cyclic variation in geochemical parameters that corresponds to the alternating “rich-“ and “lean-“ intervals. In the intervals in which TOC is greatest, the HI and genetic potentials (S1+S2) are greatest. The OSI is uniformly low except in one two-sample interval centered at a depth of 2,415 feet (Fig. 3-16) in which the index exceeds 200 mg HC/g TOC. These samples are in the B-groove interval (Fig. 2-5) lacking quality source rock. Bitumen-saturated tuff beds, such as that observed in a nearby well (Fig. 3-17) are described throughout the core (Robinson and Cook, 1975), but this is not one of them. Dean and Anders (1991) appear not to have sampled any of the bitumen-impregnated tuffs since no such units appear in the programmed pyrolysis data in the geochemistry log. The very high oil saturation suggests the tuff bed is a conventional reservoir bed.

Robinson and Cook (1975) extracted oil from the WOSCO EX-1 core with solvents and analyzed the oil to determine its principal liquid chromatography fractions, the Saturate-Aromatic-Resin-Asphaltine (SARA) components. They found that the quantity of solvent-extracted oil ranged from negligible to 5.1 wt%. In the bitumen-impregnated tuffs, the solvent-extracted oil quantity was in the 2.9 to 7.5 wt% range, with one exceptional sample at 93.9 wt%. The oils are richest in resins (55.4% average), branched alkanes (25.7%), and asphaltenes (11.9%). Normal alkanes and aromatics, generally dominant components in normal oils, are unusually low at 3.8% and 3.2%, respectively. These oils appear very immature. The relatively low concentration of solvent-extractable oil makes the

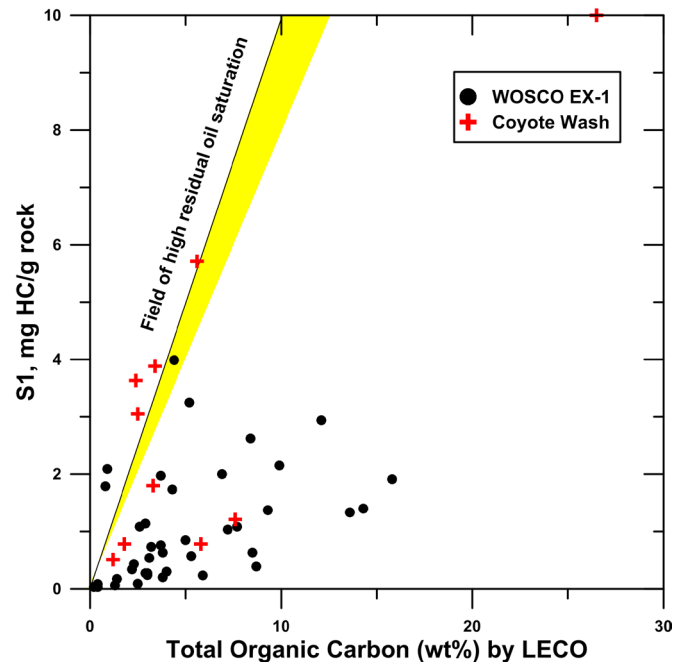


Figure 3-15: TOC vs. S1 for Parachute Creek Member core samples in the southeast basin. Note that a few of the EX-1 and Coyote Wash samples have values of oil saturation index (OSI) greater than 100. The yellow field indicates OSI values in the range 80-100 mg HC/g TOC. Data are from Dean and Anders (1991). See text for discussion.

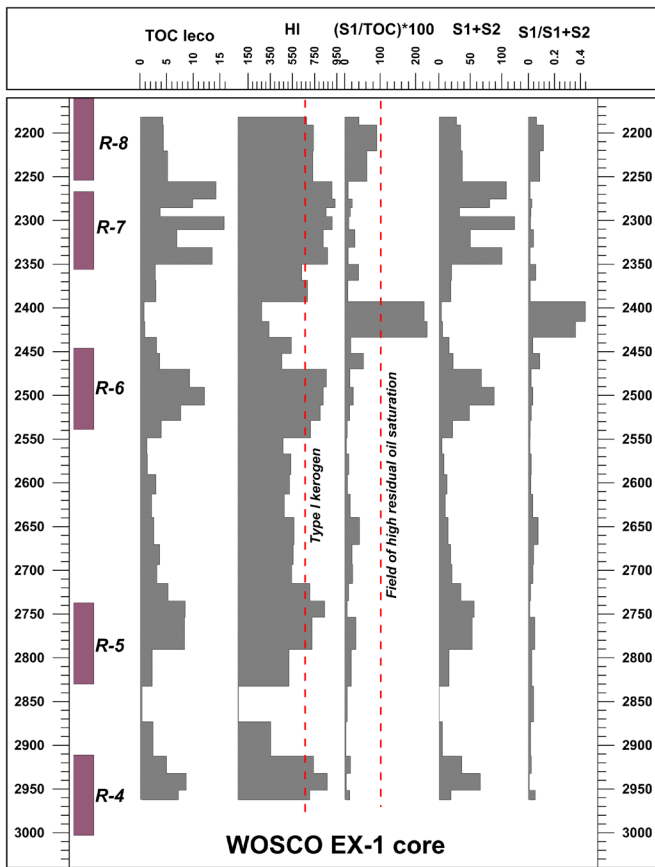


Figure 3-16: Organic geochemical log for the upper Green River Formation in the WOSCO EX-1 core in the southeast Uinta Basin. Depths in feet. See text for the description.

rock, despite the high TOC and HI, a poor candidate for a shale oil resource given the current level of thermal maturity.

Dean and Anders (1991) published independently measured LECO TOC and Fischer assays of oil yield in gallons per ton (GPT) for the WOSCO EX-1 core. A regression analysis of these data yields an algorithm for converting Fischer assay values to organic richness:

$$TOC = 0.42308 (GPT) + 0.34154 \quad R^2 = 0.9934$$

The 14X-22-46 and 16X-23D-36 cores from the Starvation Reservoir area (Fig. 3-3) west of Duchesne capture select intervals from the middle and upper Green River Formation. The 14X-22-46 core samples the Black Shale facies and the 16X-23D-36 core samples portions of the interval from the lower R-8 through R-5, including the Mahogany Zone (R-7). The cores have a mix of kerogen types, and relative to other core samples, lower than expected HI and TOC (Figs. 3-18 and 3-19). These low values could relate to thermal maturity, which is indicated to be in or near “peak oil”. Nevertheless, the rocks are good to excellent source rocks (Fig. 3-20). Several of the core samples have OSI values that approach and even exceed 100 (Fig. 3-21). The one sample in Figure 3-21



Figure 3-17: Bitumen impregnated tuff bed in the upper R-6 oil shale interval in the Skyline 16 core. The tuff bed is just 2 inches thick. The core is southeast of the WOSCO EX-1 core in 10-11S-25E; UTM E 661445, UTM N 4415109.

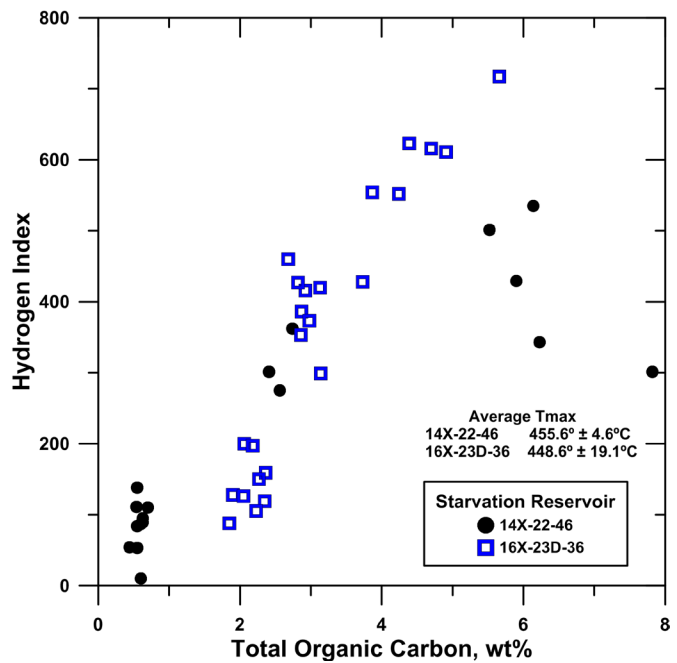


Figure 3-18: TOC vs. hydrogen index for fresh Green River Formation core samples from two wells near Starvation Reservoir in the southwest basin. Data from UGS CRC files.

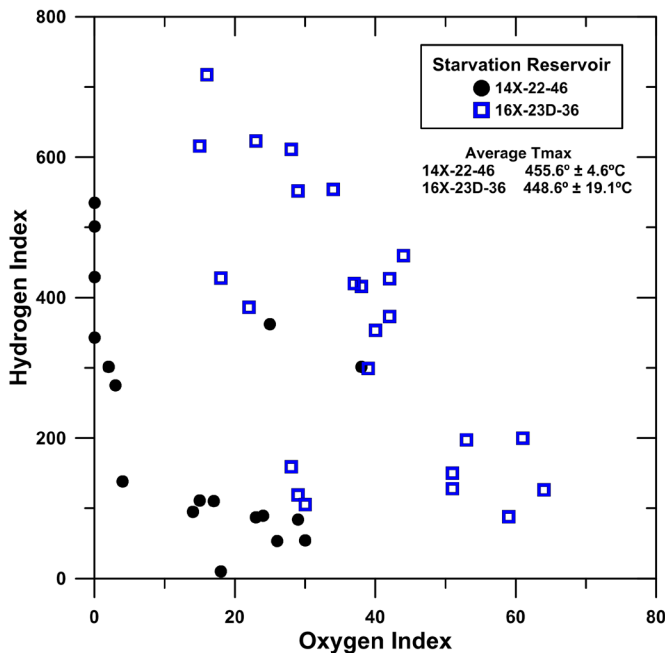


Figure 3-19: Van Krevelen plot for fresh Green River Formation core samples from two wells near Starvation Reservoir in the south-west basin. The samples represent a broad range of kerogen types, but dominantly Type II kerogens. Data from UGS CRC files.

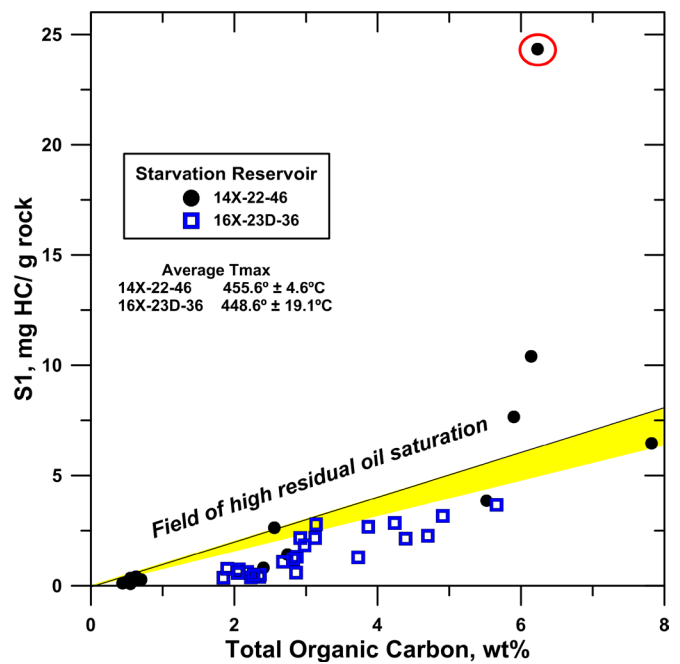


Figure 3-21: TOC vs. S1 from programmed pyrolysis analysis for Green River cores in the vicinity of Starvation Reservoir. Note that three of the samples have OSI values greater than 100, but other samples fall into the 80-100 field, shown in yellow. One sample (red circle) has an exceptionally high value. See text for discussion. Data from UGS CRC files.

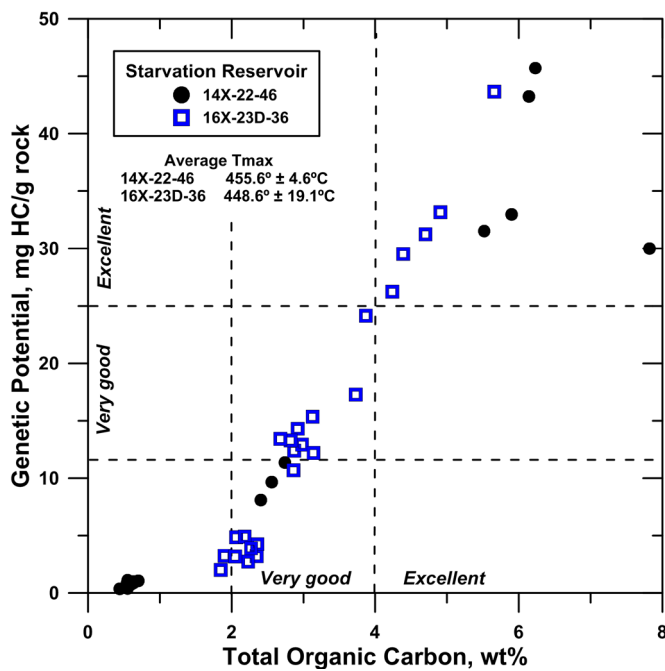


Figure 3-20: TOC vs. genetic potential for Green River Formation core from wells near Starvation Reservoir. The samples are of good and very good to excellent source rocks. Data from UGS CRC files.

circled in red has an OSI value of 390 suggesting an oil-impregnated reservoir bed, but without further information on the 14X-22-48 core, it is not possible to know with certainty.

The cores from the six wells in the Altamont-Bluebell field have been in storage for several decades since the wells were drilled and the present condition of the core is not known, except for Norling 1-9B1 and Virgil Mechem 1-11A2, both of which are still in good condition. Well reports contain limited information about the stratigraphic level of the Green River Formation cored. However, for the limited tops reported, the Norling 1-9B1 core samples appear to be in the Mahogany Zone. Note the large number of samples with Type I kerogen (Fig. 3-22 and 3-23). The same is possibly true of the DR Long 2-19A1E core, however these samples are primarily Type II kerogen. The Olsen U1-12A2, Virgil Mechem 1-11A2, Chasel 1-81A1 and Lamiq-Urrity 1-8A2 cores sample the lower Green River Black Shale facies. Programmed pyrolysis values indicate that the kerogen is dominantly Type II (Figs. 3-22 and 3-23), with the exception of many samples from the Norling 1-9B1 and Virgil Mechem 1-11A2 cores. Source rock quality is fair to very good (Fig. 3-24); only the Norling 1-9B1 core is an excellent source rock. Despite the relatively low quality of the source rock compared to other cores presented above, many of the core samples from a variety of wells have elevated residual oil saturations, several with an OSI in excess of 100 (1:1 line in Figure 3-25).

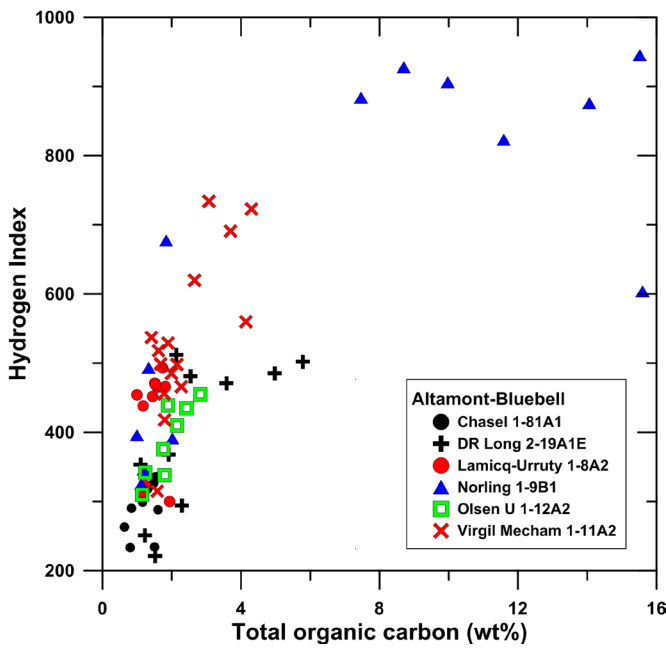


Figure 3-22: TOC vs. hydrogen index for six older cores of apparent open lacustrine facies Green River Formation from wells in the northern Altamont and Bluebell fields. Data from USGS CRC files.

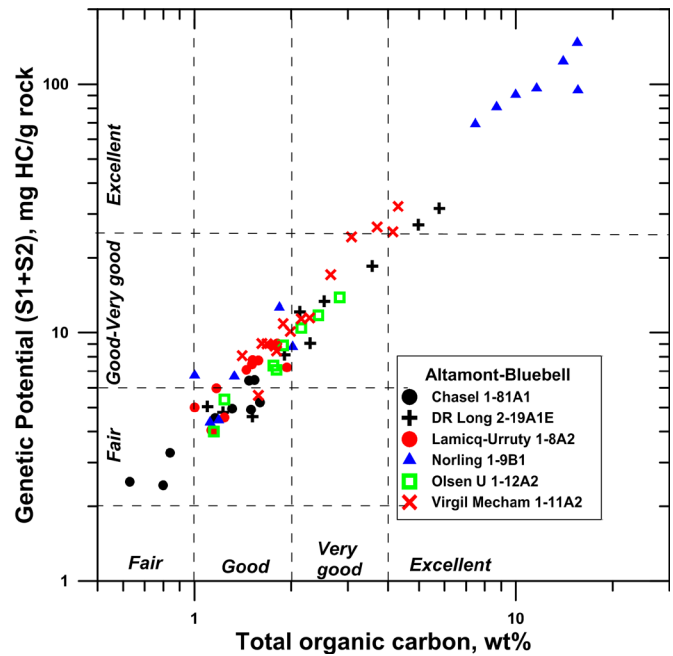


Figure 3-24: TOC vs. genetic potential for deep core samples from the northern Altamont and Bluebell fields. The core samples are rocks having fair to excellent source potential. The Norling 1-9B1 well, which is to the southwest of the others, has sampled rocks with the highest source potential. Data from USGS CRC files.

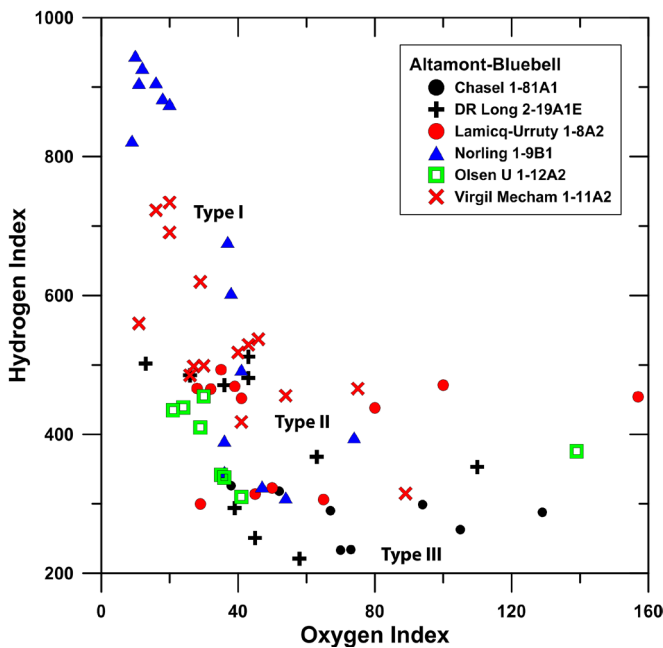


Figure 3-23: Van Krevelen plot of core samples in the deep northern Altamont and Bluebell fields. It is noteworthy that no Type III kerogen is observed in this sample suite in apparent open lacustrine facies rocks from near the basin axis. The kerogens are predominantly Type II, with Type I represented in just two wells. Data from USGS CRC files.

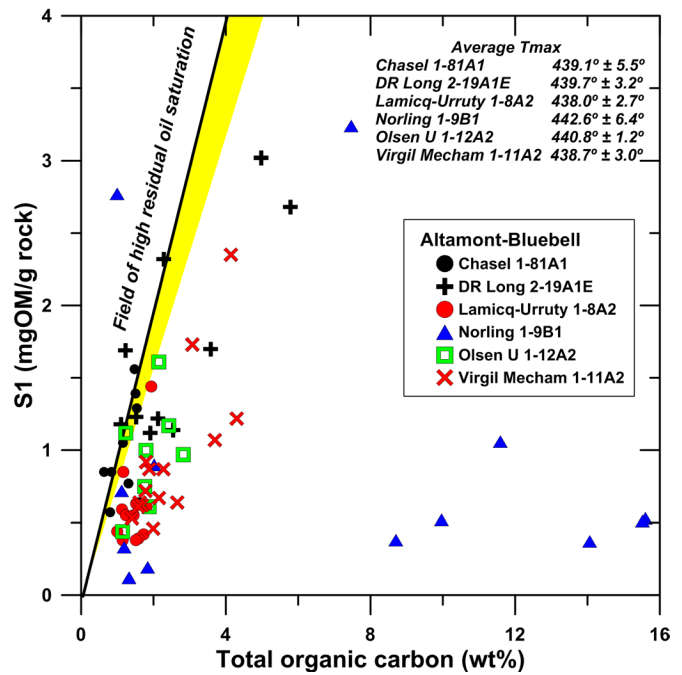


Figure 3-25: TOC vs. S1 for deep core samples from the northern Altamont and Bluebell fields. Many of the core samples have OSI values greater than 80 (yellow field), but only a few exceed 100. These rocks could have potential for a shale oil resource play. Data from USGS CRC files.

In the Norling 1-9B1 core (Mahogany), free or mobile oil occurs in bioclastic limestone or sandstone lenses and in open fractures (Fig. 3-26). The fractures are commonly short and strata bound, as depicted in Figure 3-26, but oil also fills many long subvertical fractures that are partially closed by calcite. Similar fractures are not observed in the Virgil Mechem 1-11A2 core (lower Black Shale).

Organic Maturity and Anomalous Formation Pressure

It is generally accepted that even in the deeper part of the Uinta Basin at the Altamont-Bluebell field, the Mahogany oil shale bed is situated above the normal oil generative window for a Type II kerogen, whereas the pre-Eocene portions of the basal Green River Black Shale have thermal maturities of about 1.1–1.2% vitrinite reflectance (R_o) (Anders and others, 1992; Nuccio and others, 1992), sufficient for generation of oil and associated gas. Closer to the basin margins, the level of thermal maturity in the Green River Formation decreases such that in the western Natural Buttes area it is merely 0.75% R_o at the Eocene-Paleocene boundary beneath the Black Shale. All but the lower Black Shales of the Green River Formation in the deeper parts of the Uinta Basin are immature with respect to hydrocarbon generation. It should be noted that the Green River Formation has a limited num-

ber of actual measurements of vitrinite reflectance, so prior basinwide thermal maturity estimates are poorly constrained.

The programmed pyrolysis data gathered for this study suggest a different situation, at least for the western part of the basin in the area of the greater Altamont-Bluebell field. Here cores that sampled the upper parts of the Green River Formation have T_{max} values characteristic of the “early mature” oil window (Fig. 3-27). In wells near the Starvation Reservoir, core samples from all levels of the Green River Formation have T_{max} values indicating “peak oil” levels of maturity, equivalent to R_o of 0.65% to 0.9% (Peters and Cassa, 1994).

What is certain is that the maturity levels at the base of the Green River Formation (lower Eocene) will not exceed those determined from measured R_o (Fig. 3-28) at the base of the underlying Mesaverde Formation (Upper Cretaceous). Thermal maturation simulations for a limited number of wells in the Uinta Basin (Nuccio and Roberts, 2003) predict maturities for the lower part of the Green River Formation in the northwest half of the basin in the oil, and even, the dry gas, window (Fig. 3-29). Entry into the oil window is modeled earlier than 20 Ma (Fig. 30).

As presented above, a large portion of the kerogen in the Green River Formation can be characterized as Type I. Therefore, thermal maturity of the hydrogen-rich source rocks may be



Figure 3-26: The occurrence of oil in Norling 1-9B1 core as fracture filling and/or oil-impregnated lenses of bioclastic limestone or sandstone with relatively higher porosity than the adjacent lime mudstone source rock. The core was photographed in October 2012 at the USGS CRC, Denver.

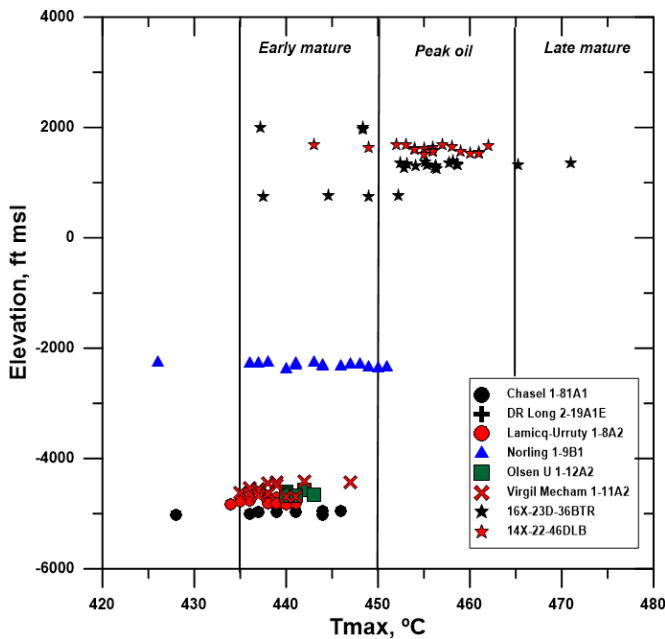


Figure 3-27: Measured values of T_{max} plotted against the elevation, not depth, of the core samples from wells in the greater Altamont-Bluebell field. There is a counterintuitive relationship in which the samples with highest elevations have the highest T_{max} values and the presently deepest samples have the lower values of T_{max} . See text for discussion. Data from USGS CRC files.

constrained if closed-system, hydrous pyrolysis experiments on the Green River Black Shale (Ruble and others, 2001; Lewan and Roy, 2010) provide the best description of the reaction kinetics of this source rock (Fig. 3-31). The very large activation energy determined from the experiments of 68.7 kcal/mole and relatively small frequency factor (A_0) of $1.65 \times 10^{32} \text{ my}^{-1}$ suggest that the onset of oil generation from the Green River Black Shales will be delayed to about 0.75% R_o . The peak of oil generation would be at the equivalent of about 1.0 R_o and oil and gas generation would occur together over a relatively narrow generative window. A separate gas generative window, if even relevant in the Green River Black Shales, would have been reached only in the very deepest parts of the Uinta basin, if at all.

At normal depths of production, overpressuring occurs throughout the Uinta Basin (Nelson, 2002, 2003). The highest overpressures (Figs. 3-32 and 3-33) are encountered in the Altamont-Bluebell district at depths greater than 10,000 ft (Bredehoeft and others, 1994). As this also is the basin center, the top of the overpressured region is within the lower Green River/Wasatch Formation. In this part of the basin the interval of maximum pressure gradient (0.60–0.80 psi/ft) is about 4000 ft thick and extends to near the top of the Upper Cretaceous. This overpressured zone is considered to be associated with the active generation of oil and associated gas from the Lower Black Shale of the Green River Formation (Bredehoeft and others, 1994). There may be an alternative explanation for the observed overpressures, as will be discussed in the final chapter.

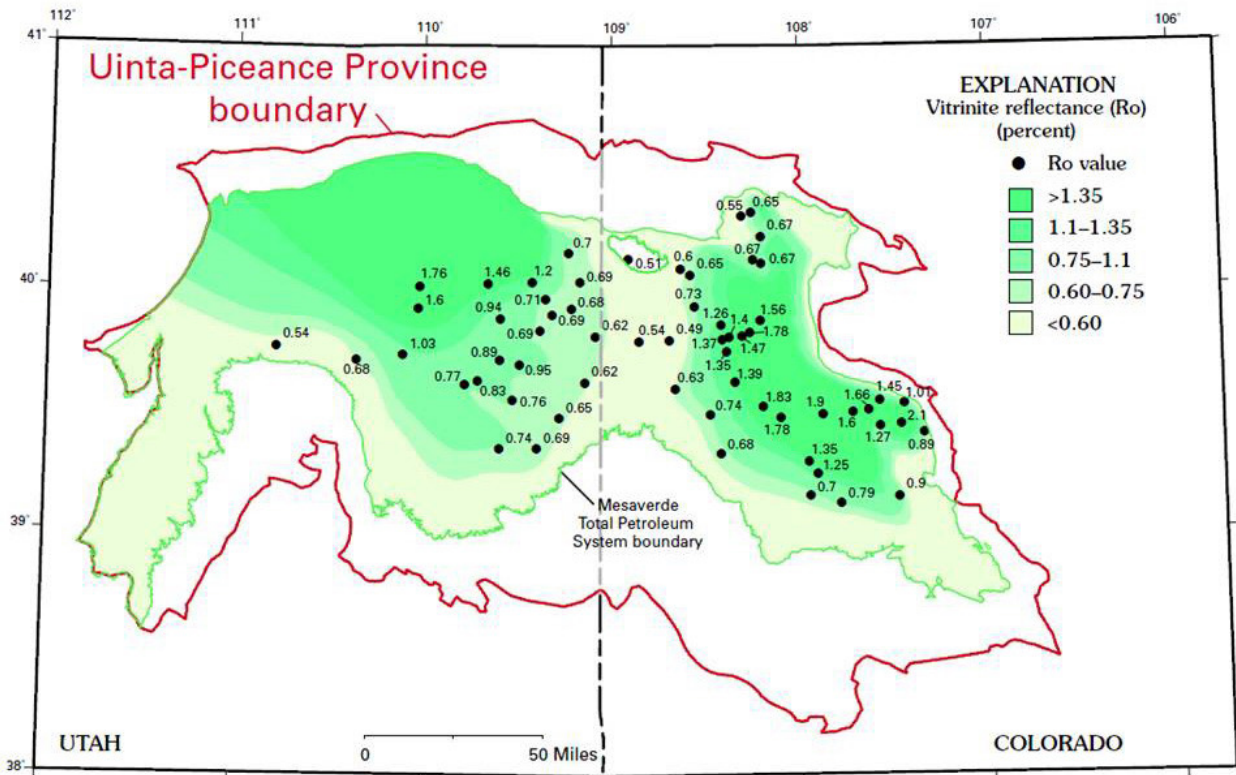


Figure 3-28: Measured vitrinite reflectance (R_o) values from near the base of Mesaverde-top of Mancos Shale contact in the Uinta and Piceance Basins (Nuccio and Roberts, 2003). These values from thousands of feet below the base of the Green River Formation establish a floor on R_o in this younger source rock.

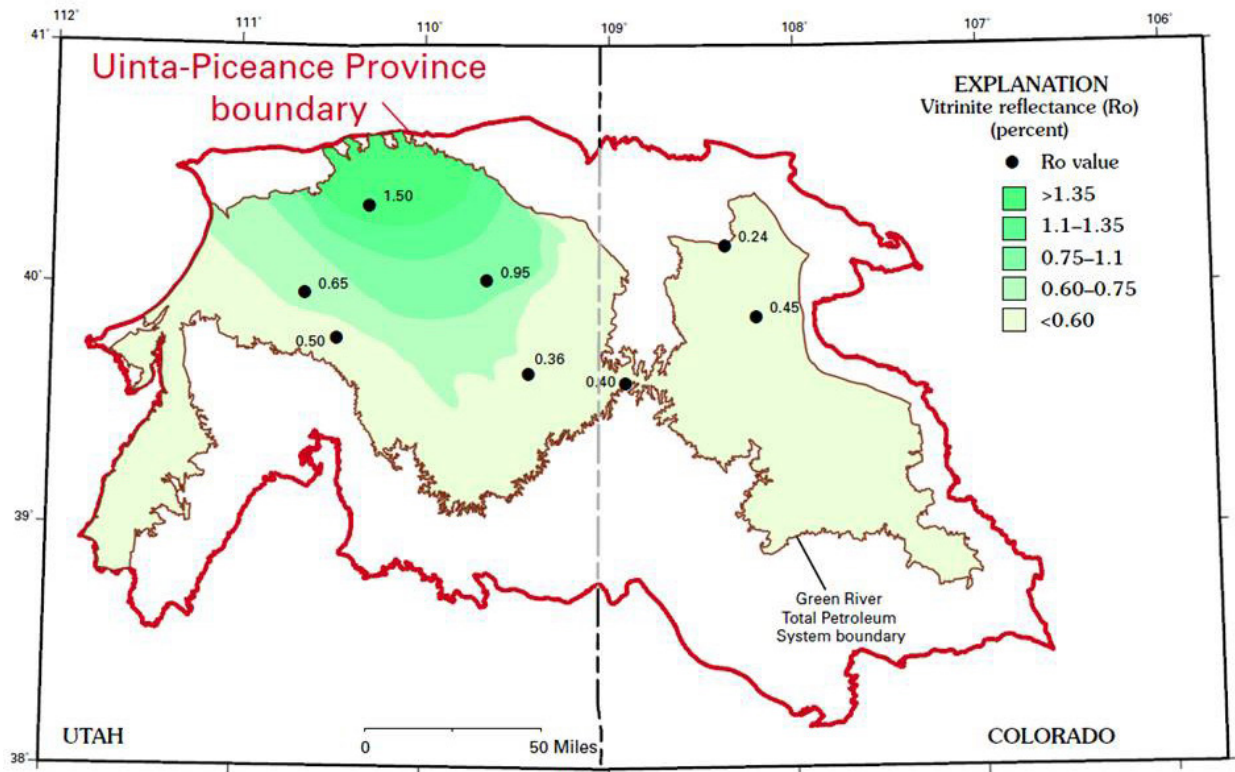


Figure 3-29: Simulated vitrinite reflectance (R_o) values for the lower Green River Formation based on five modeled deep wells in the Uinta Basin (Nuccio and Roberts, 2003). Note that the R_o isopleths are constructed to generally conform to those for the deeper base Mesaverde Group. Considering the small number of simulated wells (5), there is only limited geologic justification for such a construction.

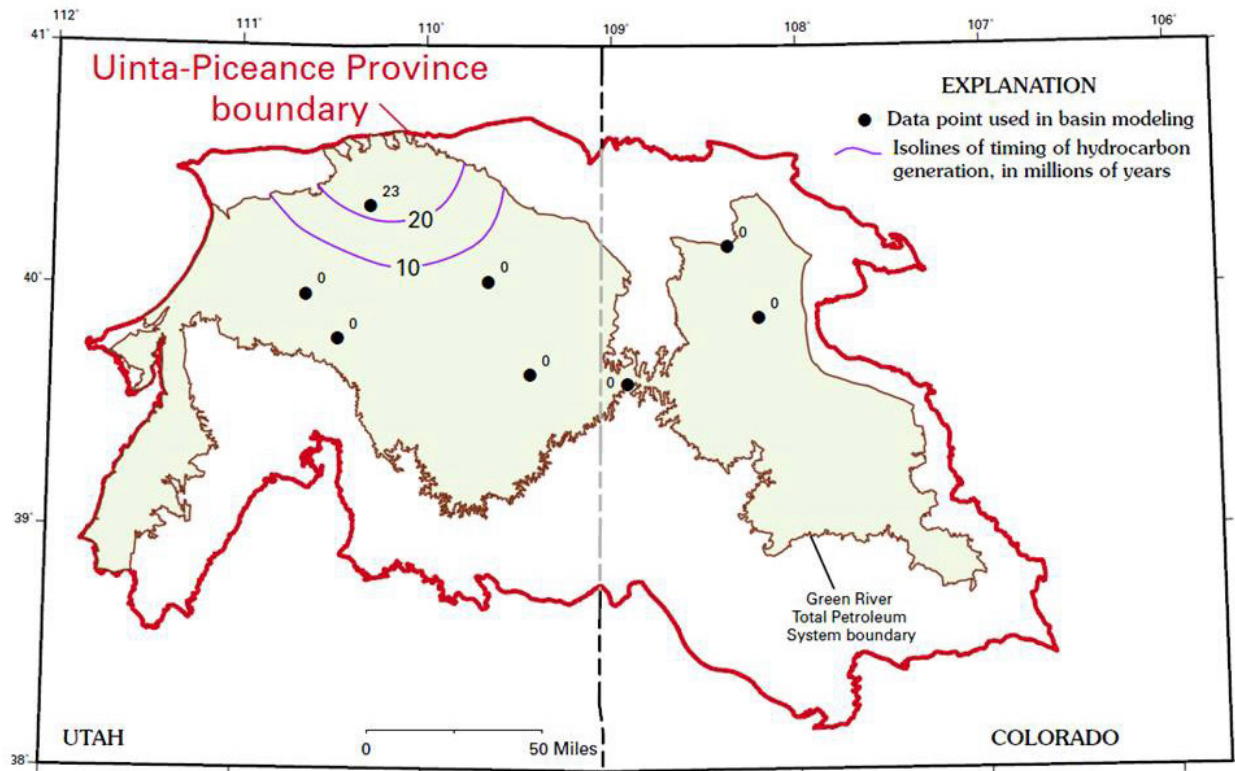


Figure 3-30: Simulated "time-triggers" representing the time in millions of years before the present for entry of the lower Green River Formation into a thermal maturity window representing "significant oil and gas generation" (Nuccio and Roberts, 2003). The simulations would suggest earliest entry into the oil generative window in the Neogene for only a small portion of the Uinta Basin.

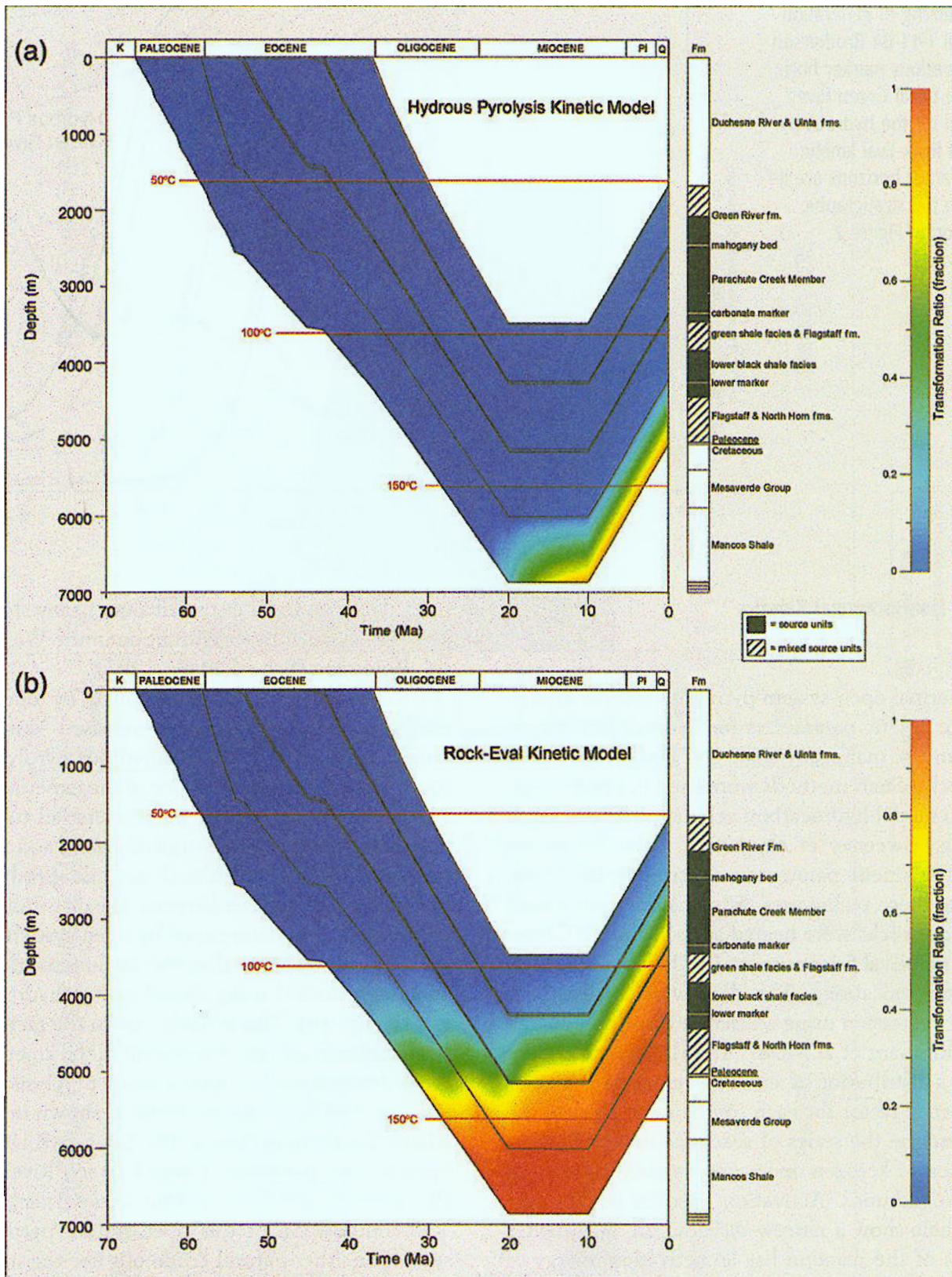


Figure 3-31: Burial history curves and organic maturity simulations for two alternative models for the Brotherson 1-11-B4 well (API 4301330052) in township 2S-4W (Ruble and others, 2001). This is the northernmost of the modeled wells shown in Figure 3-27. The UTM coordinates of the well are E 559583 N 4464084. See text for the full description. AAPG©2001, reprinted by permission of the AAPG whose permission is required for further use.

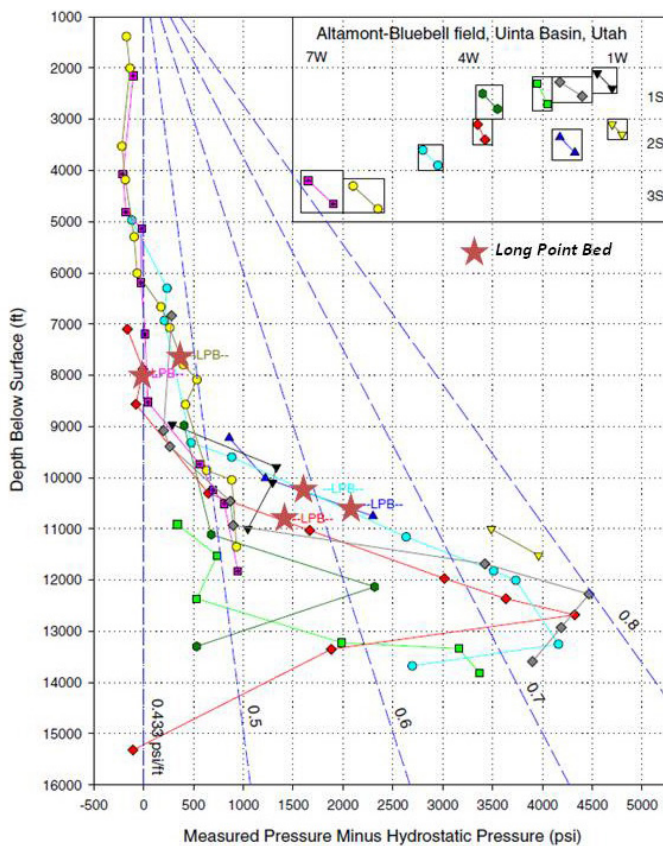


Figure 3-32: Overpressure-depth profiles determined from drill-stem test data in deep wells in the northern Altamont field (Nelson, 2003). Many of the wells have anomalous pressures approaching lithostatic (0.8 psi/ft). These anomalous pressures are observed in the Lower Member of the Green River Formation and down into the Wasatch (Colton) Formation. The red stars indicate the position of the Long Point Bed, a marker within the Lower Member, along each excess pressure curve. The highest overpressures are within the Wasatch (Colton) Formation.

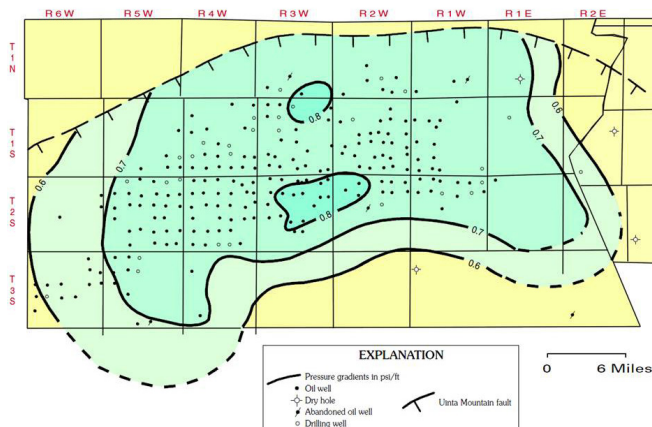


Figure 3-33: Map showing values of anomalous formation pressure gradients (psi/ft) measured in drill-stem tests in the Altamont-Bluebell field reported by Lucas and Drexler (1975). The fault bounding the area of anomalous formation pressures on the north is the Uinta Basin Boundary Fault. The figure is from Dubiel (2003).

4. NUMERICAL SIMULATIONS OF ORGANIC MATURATION

Given the limited number of direct measurements (R_o) of organic maturation of the Green River Formation in the Uinta Basin, it was considered prudent to undertake numerical simulation using the Platte River Associates BasinView-3D™ modeling software. This highly sophisticated and versatile simulator was loaned to this UGS-sponsored research project by Dr. Jay Leonard, President of Platte River Associates (PRA).

In a normal 1-D numerical simulation (Waples, 1994) using a program such as the PRA BasinMod-1D™ there are three principal components.

1. By assigning measured depths and presumed geologic ages to formation tops encountered in a well, it is possible to construct a *burial history curve*. This is the trajectory of burial of the formation boundaries as a function of time. With the assignment of sediment intervals deposited, but subsequently removed by erosion, the trajectory also captures the “uplift” of the formation tops.
2. With the assignment of a value of heat flow, or alternatively the geothermal gradient, the burial history curve is converted to a *temperature history curve* that plots against geologic time the increase in ambient temperature of stratigraphic markers during burial and crustal cooling accompanying exhumation.
3. The thermal trajectories provide ambient temperatures for calculation of thermal maturities for the various stratigraphic markers (or intervals) using the Arrhenius equation. This semi-empirical expression characterizes the quasi-first-order chemical reactions involved in the conversion of kerogen to liquid hydrocarbons and natural gas. The *rate* of the organic reactions (cracking of large molecules in kerogen to the smaller molecules in hydrocarbons) is a function of temperature; the higher the temperature, the faster the reactions proceed. Thus, the conversion of kerogen to hydrocarbons is a function of both temperature and time. This is what the simulations are calculating and expressing as *transformation ratios* or equivalent measures of thermal maturation of organic matter in the buried sediments.

When wells with stratigraphic tops are not available in a part of the basin where an organic maturation simulation is desired, modelers will construct a “synthetic well” with tops reflecting the known formation thicknesses for the region. This is the principal behind the PRA BasinView-3D™ simulator.

BasinView-3D™ uses either structure surfaces or isopach maps for each of the stratigraphic horizons in the basin (or

part of a basin) to construct an array of “synthetic wells” that then are modeled individually as normal 1-D simulations. The results of the simulations for each of the “synthetic wells” are then gridded and expressed as isopleth maps. This way the modeler can rapidly simulate the spatial variations in organic maturity and other model output parameters for a very large area and at a very fine resolution. Typically, the model runs for this study involved over 9000 nodes or “synthetic wells” with a one kilometer spacing taking just over ten minutes each to generate. The time involved in generating the simulations is short, but the time involved building and refining the models can be considerable.

Simulations were carried out for just the northern half to two-thirds of the Uinta Basin, the area bounded by UTM (NAD83) Eastings 500000 and 660000 and Northings 4430000 and 4485000 (Fig. 4-1). To the extent possible, the area of the basin simulated is south of the Basin Boundary Fault. This is the deepest part of the basin, and the part with a highest proportion of open lacustrine facies source rocks.

Model Input Parameters

The set of input parameters used in these particular simulations are: (1) the *structure surface and isopach grids* (in meters) that define the stratigraphic units constructed using Surfer 10™ and Surfer 11™, (2) the absolute age of bounding surfaces of the stratigraphic units and/or geologic events, (3) *kerogen kinematics* from Ruble and others (2001) and default kerogen parameters built into BasinMod-1D™ and Basin-View-3D™, (4) *initial TOC* of the designated “source rock” units determined from the information presented in Chapter 3, (5) *heat flow values* for the Uinta Basin reported in Chapman and others (1984), and (6) *generalized lithology* mixes for the individual model intervals. The simulators allow a variety of other variables, such as petrophysical properties of the rock

units, to be specified by the modeler. In all instances, the PRA default values of these second-tier parameters were accepted. The model-specific input parameters are described below.

The Green River Formation is divided into seven model elements designated GR-1 to GR-7. The bounding surfaces for each of the units is shown in Table 4-1 along with the ages assigned to each surface. Most of the surfaces are defined by presumed basin-wide events making them everywhere the same age. A few, most notably the top of the Green River Formation (GR-1), are time-transgressive. For the purpose of the simulations, all surfaces are treated as time-constant. The source of the data for constructing the surface and determining its absolute age is presented in the figure captions for each of the surface maps (Figs. 4-2 through 4-9).

In earlier trial model simulations the grids used were constructed with Surfer 10™. In general, these grids extended beyond the region of well top control in the data sets gridded. The result was large regions lying north of the Basin Boundary Fault having clearly meaningless simulation results. So for the final set of five simulations (iterations using the same input surfaces and ages) presented in this report, a new set of Green River Formation grids was constructed using a feature in Surfer 11™ (beta), “*blank convex hull when gridding*”, that limits the grid nodes to just the region containing control values. The new grids reduce the area covered by the simulations, but they should assure more accurate output. The surface maps in Figures 4-2 through 4-9 were constructed using these same Surfer 11™ grid files. These input Surfer grid files can be found in the Digital Appendix C.

In the Uinta Basin, the strata overlying the Green River Formation have little commercial value for fossil fuels. Nevertheless, it is surprising how little information exists on the regional stratigraphy of this “overburden” succession. Well tops have been compiled for many of the marker beds within

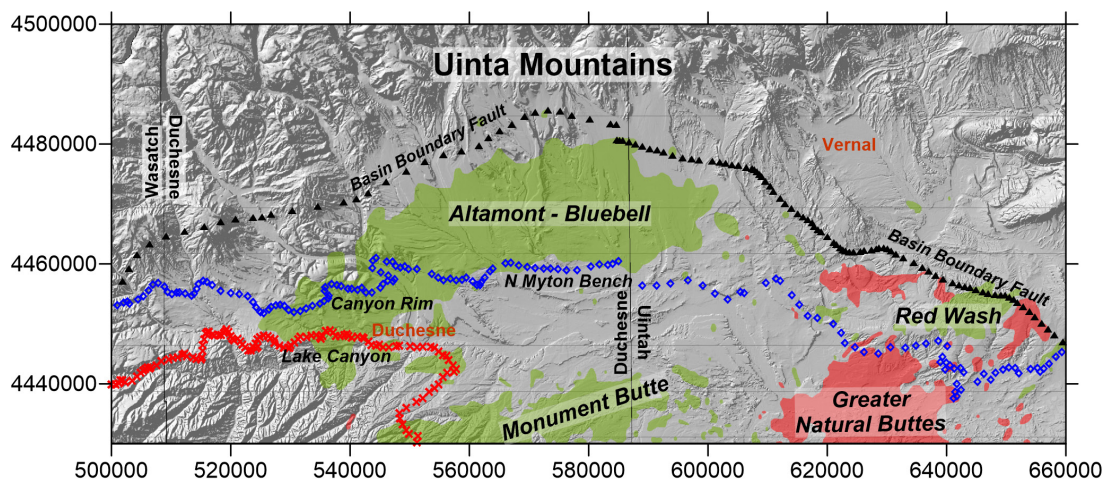


Figure 4-1: Basemap for the modeled portion of the Uinta Basin showing the location of the Basin Boundary Fault, the larger fields producing oil from the Green River Formation (green areas, red areas are natural gas fields), the county lines, and major towns. The blue line marks the southern erosional edge of the Duchesne River Formation and the red line marks the southern erosional edge of the Uinta Formation, south of which the uppermost Green River Formation is exposed at the surface. The geographic coordinates are meters in UTM NAD83, Zone 12.

Table 4-1: Organic maturation model events

<u>Age/Duration</u>	<u>Unit/Haitus</u>	<u>Surface or Interval</u>
0.0 Ma		Present-day ground surface
0.50–0.0 Ma	E-2	Erosion II isopach (high rate; 70% of total erosion)
10.0–0.50 Ma	E-1	Erosion I isopach (slow rate; 30% of total erosion)
20.3–10.0 Ma		Post- Bishop Conglomerate pediment lag or hiatus
20.3 Ma	----- Tbc	Top of Bishop Conglomerate surface (reconstructed)
30.5 Ma	----- Tdr	Gilbert Peak geomorphic surface (projected; age: Kowallis and others, 2008)
40.0 Ma	----- Tu	Top of Uinta Fm surface (age: Prothero, 1996)
47.0 Ma	----- GR-1	Top Green River Fm surface (age: Prothero, 1996)
48.9 Ma	----- GR-2M	Top of Mahogany Zone surface
49.3 Ma	----- GR-3	Top of B-groove (base Mahogany Zone) surface
50.3 Ma	----- GR-4	Top of L-5 interval surface
51.6 Ma	----- GR-5	Base of R-4 interval surface
53.9 Ma	----- GR-6	Top of Carbonate Marker surface (top lower Black Shale)
54.0 Ma	----- GR-7	Base of Long Point Bed surface (base Douglas Creek Mbr)
55.3 Ma	-----	Base of Ostracodal Limestone surface (base lower Black Shale)

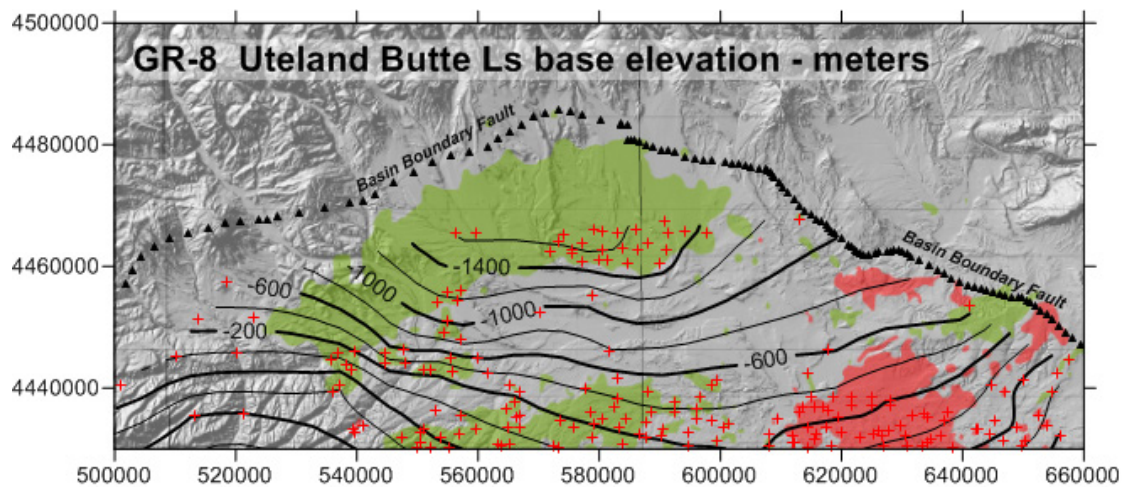


Figure 4-2: Structure map relative to mean sea level (msl) of the base of the Ostracodal Limestone or Uteland Butte Limestone. This is the effective base of the Green River Formation. This surface forms the bottom of the model. Red crosses indicate well locations with surface tops. Well tops source: U.S. Geological Survey; refer to Johnson and Roberts (2003). The contour interval (CI) is 200 meters.

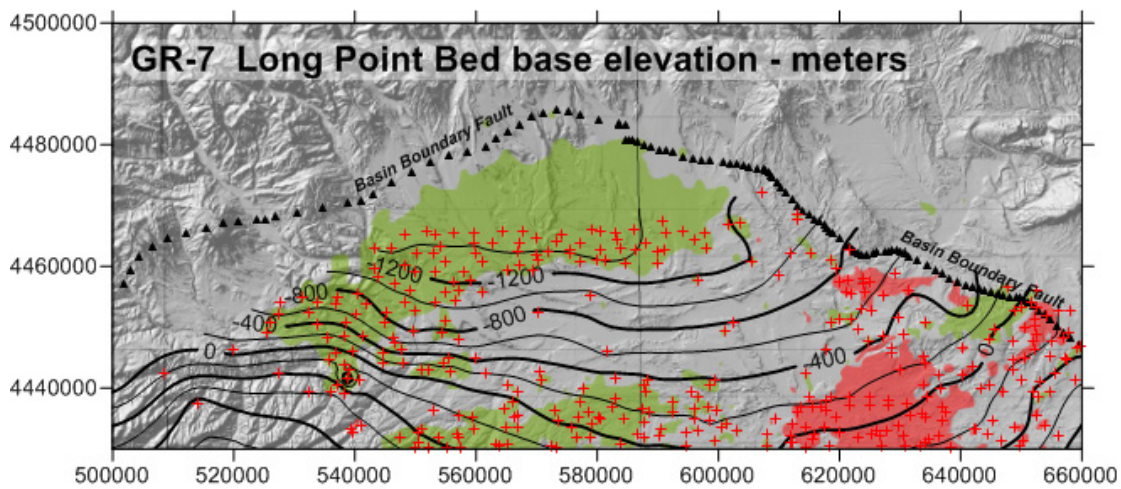


Figure 4-3: Structure map (msl) of the base of the Long Point Bed, the base of the Douglas Creek Member. This is the top of the GR-7 model element. Red crosses indicate well locations with surface tops. Well tops source: U.S. Geological Survey; refer to Johnson and Roberts (2003). CI = 200 m

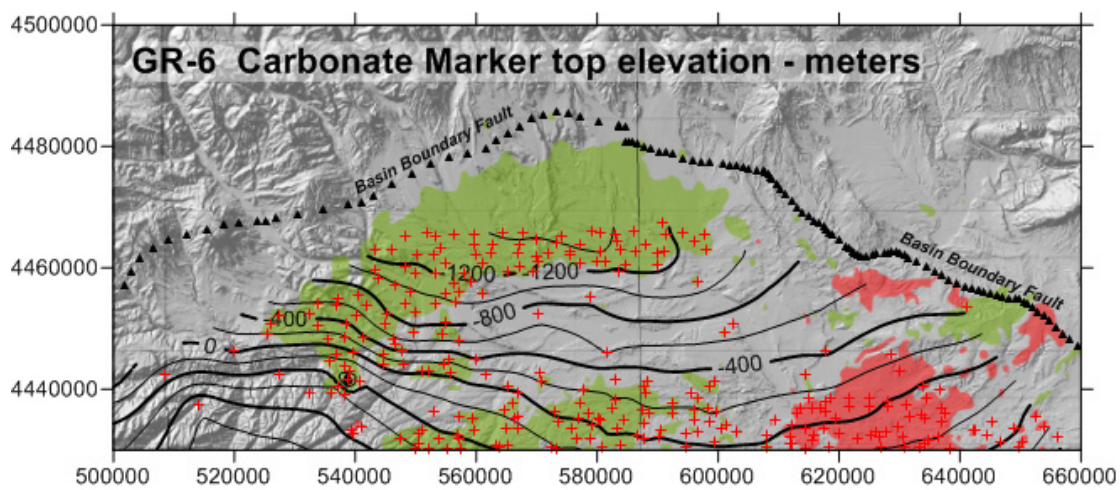


Figure 4-4: Structure map (msl) of the top of the Carbonate Marker, the effective top of the Black Shale Facies or Lower Green River Formation. This is the top of the GR-6 model element. Red crosses indicate well locations with surface tops. Well tops source: U.S. Geological Survey; refer to Johnson and Roberts (2003). CI = 200 m

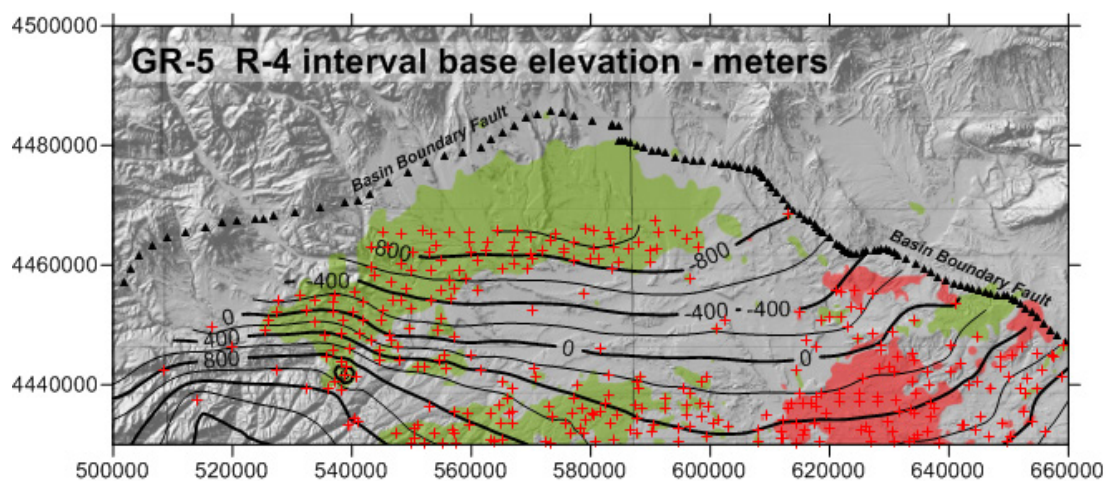


Figure 4-5: Structure map (msl) of the base of the R-4 interval of the Parachute Creek Member and top of the GR-5 model element. Red crosses indicate well locations with surface tops. The age of the surface is 51.6 Ma (Birgenheier and Vanden Berg, 2011). Well tops source: Utah Geological Survey. CI = 200 m

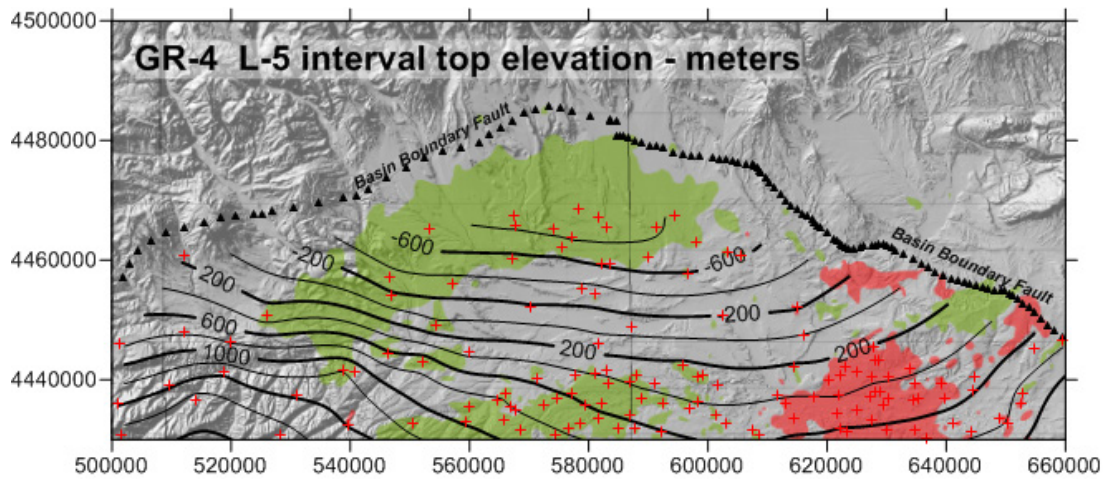


Figure 4-6: Structure map (msl) of the top of the L-5 interval of the Parachute Creek Member and top of the GR-4 model element. Red crosses indicate well locations with surface tops. The age of the surface is 50.3 Ma (Birgenheier and Vanden Berg, 2011). Well tops source: Utah Geological Survey. CI = 200 m

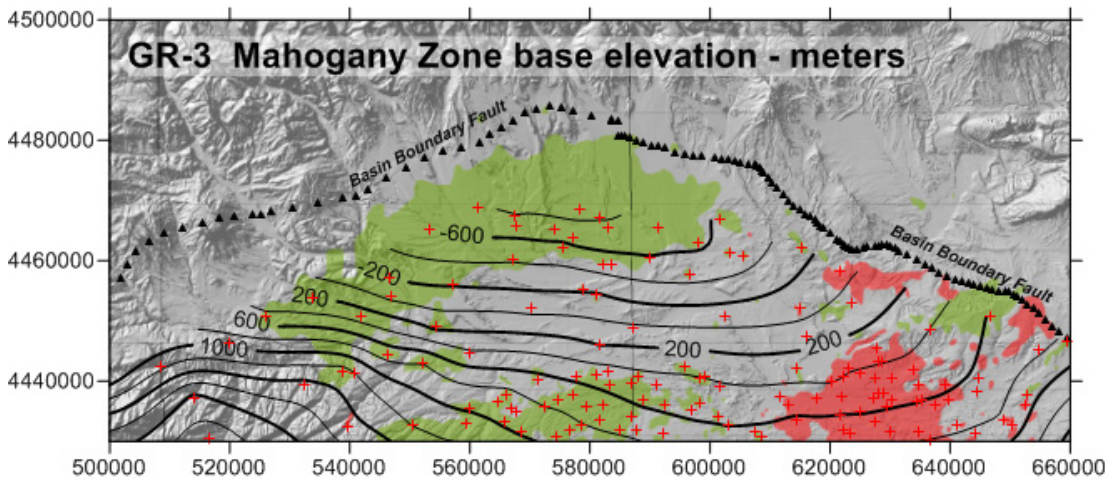


Figure 4-7: Structure map (msl) of the top of the B-groove interval of the Parachute Creek Member, which is the base of the Mahogany Zone (GR-2M), and top of the GR-3 model element. Red crosses indicate well locations with surface tops. The age of the surface is 49.3 Ma (Birgenheier and Vanden Berg, 2011). Well tops source: Utah Geological Survey. CI = 200 m

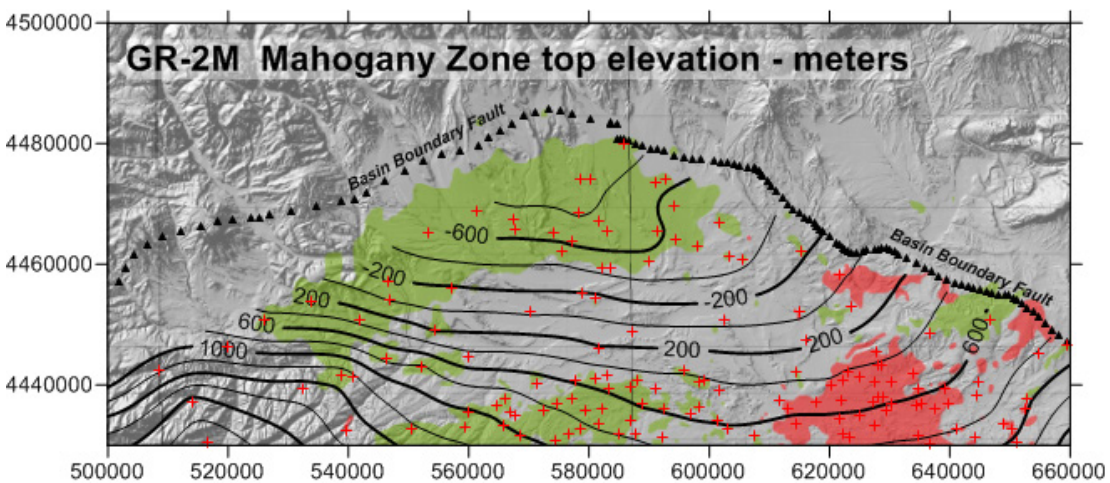


Figure 4-8: Structure map (msl) of the top of the Mahogany Zone (R-7) interval of the Parachute Creek Member and top of the GR-2M model element. Red crosses indicate well locations with surface tops. The age of the surface is 48.9 Ma (Birgenheier and Vanden Berg, 2011). Well tops source: Utah Geological Survey. CI = 200 m

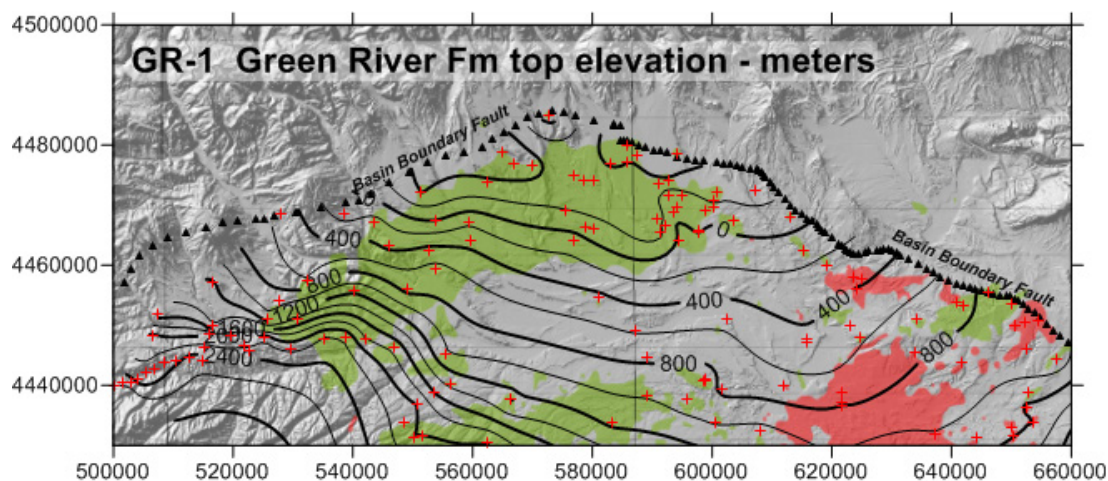


Figure 4-9: Structure map (msl) of the top of the Green River Formation and top of the GR-1 model element. Red crosses indicate well locations with surface tops. The age of the surface reported by Prothero (1996) to be 47.0 Ma, but Smith and others (2008b) indicate that it is a time-transgressive surface ranging in age from 47 Ma in the eastern part of the basin to 44 Ma in the west, where lacustrine conditions lingered longest. Well tops source: Utah Geological Survey. CI = 200 m

the Green River Formation, but there are no such compilations for the formations overlying the Green River Formation or even the top of the Green River itself. The overburden is an essential stratigraphic element driving thermal maturation, so it was necessary for this project to construct structure maps for this succession, starting with the top of the Green River Formation.

The transition from lacustrine-playa strata of the uppermost Green River Formation into the overlying fluvial mudflat red mudstone and channel sands of the Uinta Formation is gradual. The tops of Green River Formation recorded in well completion reports are commonly inconsistent, even between adjacent wells. As explained in Chapter 2, the structure map for the top of the Green River Formation was constructed from tops extracted from published tops tables (Sprinkel, 2007), cross sections (Johnson, 2003), interpretation of plotted LAS files (see Digital Appendix A), as well as heavily edited tops compilations from DOGM well completion reports. An additional constraint on the top of the Green River Formation surface is the elevation of the mapped southern outcrop edge of the Uinta Formation on the Duchesne (Bryant, 2010), Price (Weiss and others, 2003), Seep Ridge (Sprinkel, 2009) and Vernal (Sprinkel, 2007) geologic maps. This diverse data set was used to construct the structure surface map in Figure 4-9.

The same sources were used to attempt construction of pre-erosion isopach maps for the overlying Uinta and Duchesne River Formation. However, here the control was even sparser. Early attempts at constructing conventional isopleth maps yielded unacceptable results. Consequently, indirect methods were adopted that in the end may be more reasonable. It was noted that the cluster of reliable thicknesses for the Uinta Formation in the Red Wash field area are in the range of 500–550 m (1640–1800 ft), whereas a similar cluster in the Bluebell and eastern Altamont fields are from 900–950 m (2950–3100

ft) thick. These values were used to create the synthetic isopach shown in Figure 4-10. The isopach grid was added to the grid for the top of Green River Formation (Fig. 4-9) to yield the structure surface for the top of the Uinta Formation (Tu; Fig. 4-11). The surface elevations were checked for consistency with the elevations of the southern outcrop edge of the Duchesne River Formation (blue line in Figure 4-10) observed on the Duchesne (Bryant, 2010) and Vernal (Sprinkel, 2007) geologic maps, and they were remarkably close.

The Duchesne River Formation is partly to completely eroded across nearly all of the Uinta Basin. Only along the south flank of the Uinta Mountains are there remnants where the Lapoint Member is overlain by the Starr Flat Member-Bishop Conglomerate. These are the only areas where there is the full, pre-erosion thickness of the formation preserved. Unfortunately, these are areas largely north of the Basin Boundary Fault where wells are few and far between. Hanson (1986) describes the base of the Starr Flat Member as the Gilbert Peak geomorphic surface, and the projection of this surface southward across the basin defines the top of the Duchesne River Formation. This surface was modeled by projecting the elevations of the base of the Starr Flat Member and/or the Bishop Conglomerate (Table 4-2), where remnant on the south flank of the Uinta Mountains, Little Mountain, Diamond Mountain plateau, and Blue Mountain plateau, gradually downward and outward across the basin. It is imagined that the Gilbert Peak surface was an arid-climate pediment like those of the modern Basin and Range Province. This reconstructed Gilbert Peak geomorphic surface is taken to be the same as the top of the Duchesne River Formation (Fig. 4-12).

The isopach for the Bishop Conglomerate (Fig. 4-13) is considered to be a conservative estimate of its original thickness. It is constructed by taking the thickness observed for the formation in the erosional remnants and projecting those

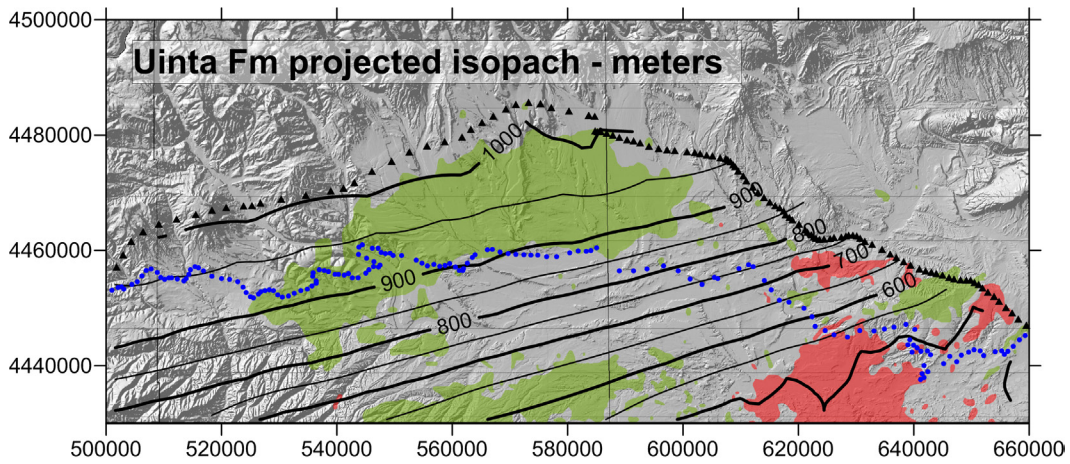


Figure 4-10: Generalized pre-erosion thickness of the Uinta Formation projected from areas of relatively reliable well control in the Red Wash and northeast Altamont-Bluebell fields where thicknesses are in the range of 500-550 m and 900-950 m, respectively. The blue line indicates the south outcrop edge of the Duchesne River Formation. South of this line to the outcrop edge of the Uinta Formation (red line) the observed thicknesses are reduced by erosional beveling. CI = 50 m

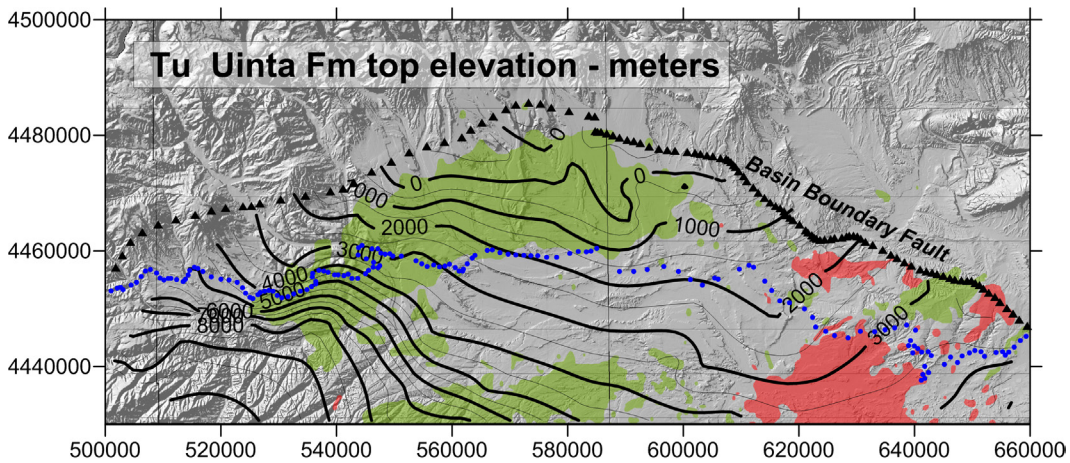


Figure 4-11: Structure map (msl) for the top of the Uinta Formation constructed by adding the pre-erosion isopach in Figure 4-10 to the top of Green River Formation structure surface (Figure 4-9). South of the Duchesne River Formation outcrop edge this surface projects southward above the present ground surface. Extensions of the surface north of the Basin Boundary Fault are artifacts of gridding that should be ignored. The age of the surface is 40.0 Ma (Prothero, 1996). CI = 500 m

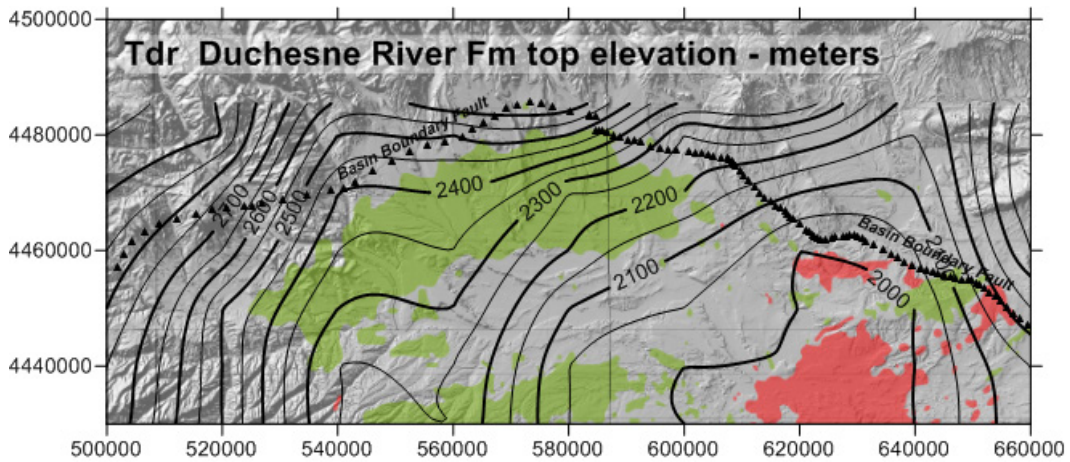


Figure 4-12: Generalized structure map (msl) for the surface representing the pre-erosion top of the Duchesne River Formation constructed by projecting the present elevations of the Gilbert Peak surface across the basin as though it were an arid-climate pediment flanking the Uinta and Split Mountain uplifts. As this surface is considered to post-date uplift of the mountains flanking the Uinta Basin, the extension of the surface north of the Basin Boundary Fault is intentional. The Duchesne River Formation does everywhere overlap this fault. The age of the surface is radiometrically dated as 30.5 Ma (Kowallis and others, 2005). See text for further discussion of the surface. CI = 50 m

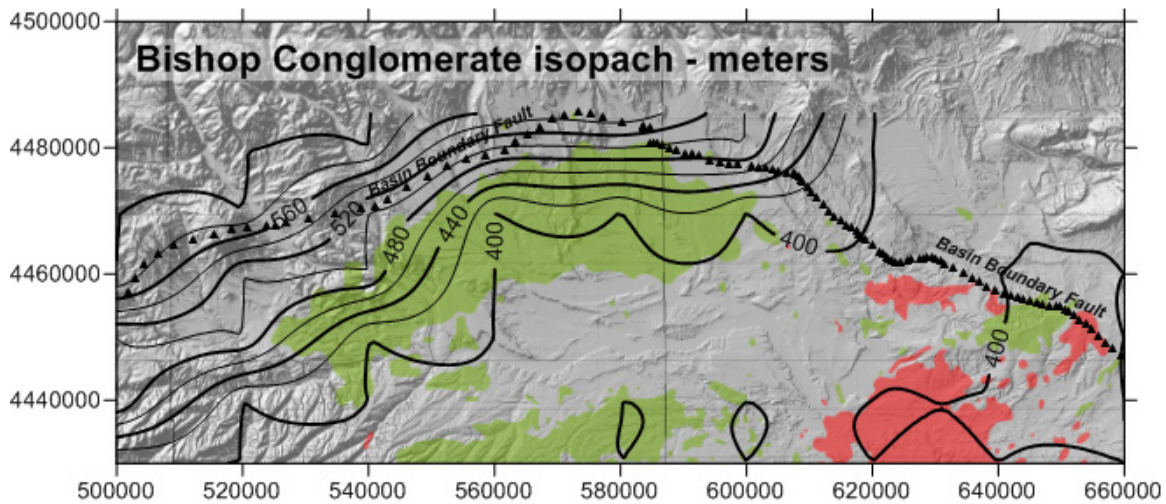


Figure 4-13: Generalized thickness of the pre-erosion Bishop Conglomerate constructed by projecting the maximum thickness of the Bishop Conglomerate-Starr Flat Member where preserved on the south flank of the Uinta Mountains southward into the basin as an arid-climate alluvial fan deposit. It is presumed that the unit was accumulating through the entire Oligocene and into the earliest Miocene, until about 20.3 Ma (Ogg and others, 2008). CI = 20 m

Table 4-2: Elevations in meters of the Gilbert Peak geomorphic surface and estimated thicknesses of the Starr Flat Member-Bishop Conglomerate determined from mapped contacts in erosional remnants in the Duchesne-Kings Peak (Bryant, 2010), Dutch John (Sprinkel, 2006), and Vernal (Rowley and others, 1985) geologic quadrangle maps. One meter = 3.28 feet.

Site	Name	Gilbert Peak elev, m	Bishop Congl. thick, m
A	Tabby Mtn W	2850	
B	Tabby Mtn	2750	
C	Dry Mtn	2250	
D	Round Mtn	3000	
E	Dry Ridge	2500	500
F	Lake Fort Mtn	2500-2750	500
G	Starr Flat	2750	650
H	Pole Mtn	2500-2750	500
I	Mosby Mtn	2500	450
J	Little Mtn	2250	400
K	Taylor Mtn	2750	
L	Diamond Mtn	2250	150
M	Jones Hole	2300	150
N	Blue Mtn plateau	2400	<100

thicknesses across the basin with minimal thinning. Again an intermountain arid-climate pediment deposit is envisioned, one that thins slightly away from the basin margins. The thickness in meters (Table 4-2) was determined by the difference in elevation between the base of the Starr Flat Member and the highest point underlain by the Bishop Conglomerate. Nearly everywhere patches of middle Pleistocene alluvium are mapped directly overlying the Bishop Conglomerate (Bryant, 2010; Sprinkel, 2006; Sprinkel, 2007). South of the Basin Boundary Fault, the Bishop Conglomerate has been completely removed by erosion.

For each formation with substantial erosion, BasinView-3D™ requires input of a grid representing the isopach of the portion of the formation lost to erosion. For the Uinta Formation, this isopach grid was constructed by subtracting the present-day ground surface (Fig. 4-14) from the top of Uinta Formation (Tu) surface (Fig. 4-11). The same procedure was used to calculate the isopach for the portion of the Duchesne River Formation lost to erosion. For this isopach it was necessary to add back the eroded Uinta Formation south of the Duchesne River outcrop limit. These two isopachs are displayed in Figures 4-15 and 4-16.

The total erosion after 10 Ma was determined by subtracting the present-day ground surface from the reconstructed top of the Bishop Conglomerate. The total erosion is separated into two separate isopach grids: Erosion 1 (Fig. 4-17) during the period 10–0.5 Ma representing 30% of the total erosion and Erosion 2 (Fig. 4-18) during the period 0.5 to 0 Ma representing the remaining erosion.

After running a variety of trial models to check the functioning of the simulator, five project models were run having the sets of variables indicated in Table 4-3. The models, designated A through E, were all identical except for the specific combination of variables related to the value of heat flow and the specific kerogen kinematics, as shown in the table. All models shared the same input surface elevation and isopach grids, model limits and node spacing, lithology mixes for the various stratigraphic units, initial TOC values for the designated source rock units, and a uniform surface temperature of 20°C.

Nearly all levels of the Green River Formation have potential to generate hydrocarbons. However, just four of the model units were treated as “source rock” units and assigned kerogen types with kinematics and values of “initial TOC”. The “initial TOC” values in all models are 15% for GR-2M, 10%

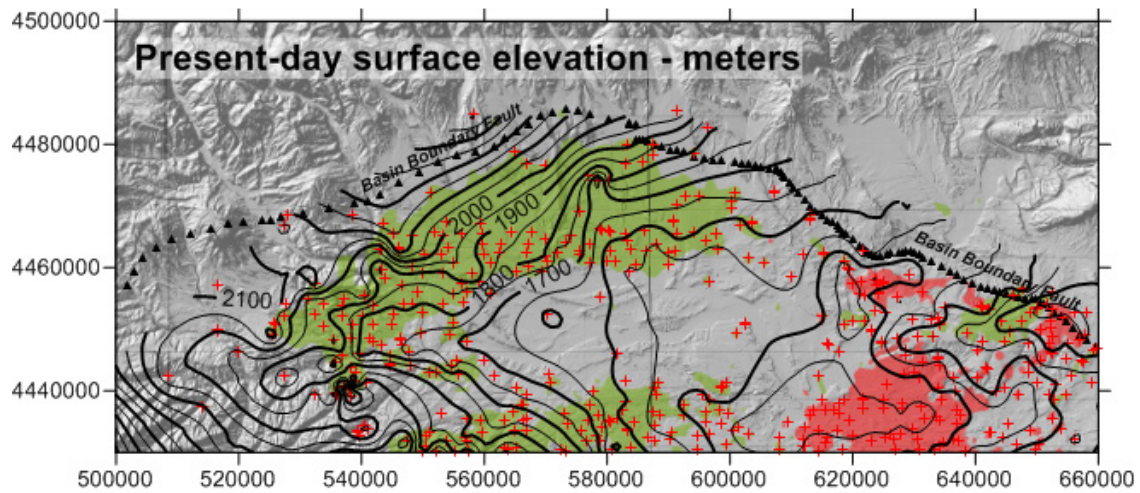


Figure 4-14: Generalized elevation (msl) of the present-day ground surface constructed from the ground elevations of wells used to construct the Green River Formation surfaces, rather than DEM data, in order to avoid potential simulation artifacts resulting from a large mismatch in grid densities. Data from Utah Geological Survey and Utah Division of Oil, Gas, and Mining. CI = 50 m

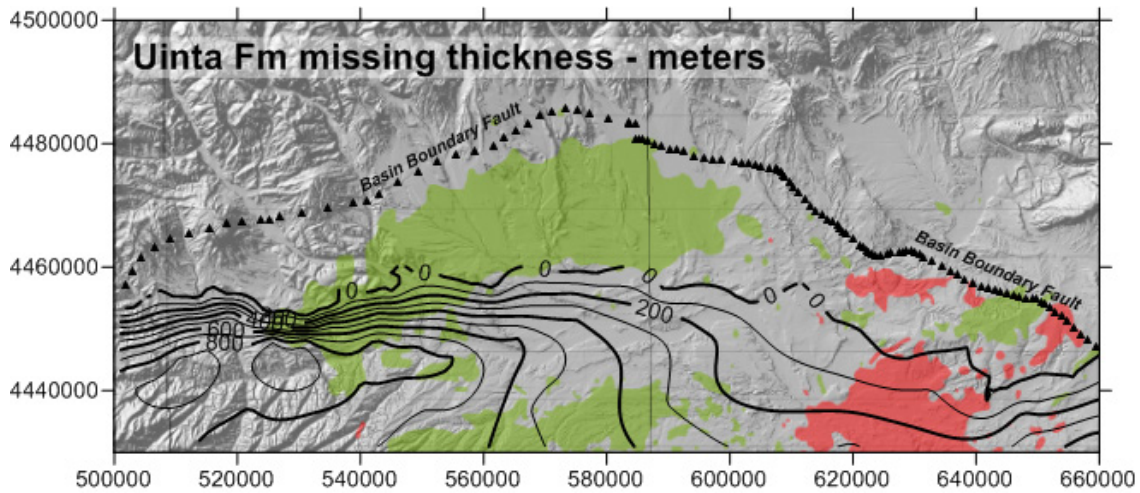


Figure 4-15: Thickness of the Uinta Formation removed by erosion after 10 Ma. The isopach grid was constructed by subtracting the present-day ground surface (Fig. 4-14) from the generalized top of Uinta Formation surface (Fig. 4-11). CI = 100 m

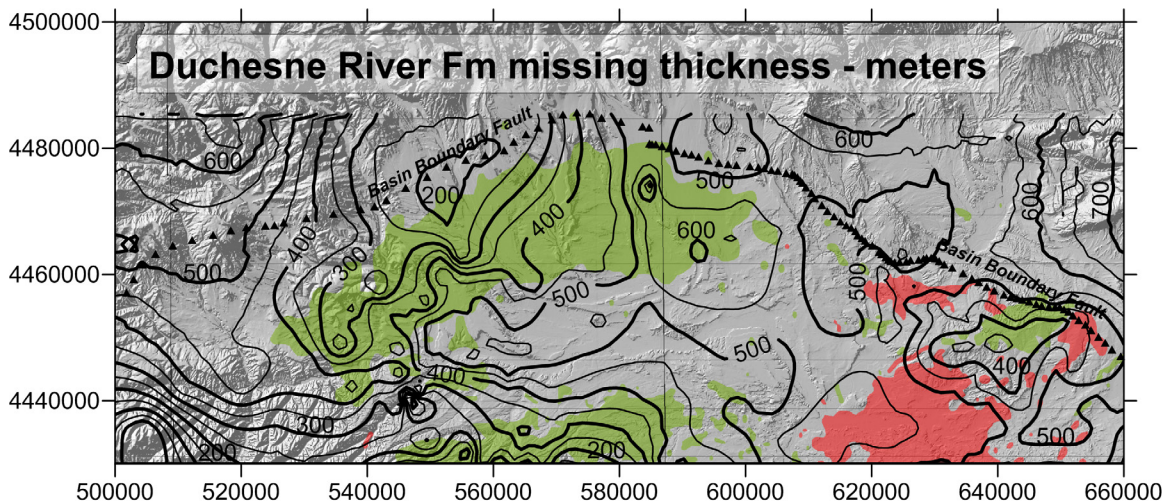


Figure 4-16: Thickness of the Duchesne River Formation removed by erosion after 10 Ma. The isopach grid was constructed by subtracting the present-day ground surface (Fig. 4-14) from the generalized top of the Duchesne River Formation (Fig. 4-12), then adding back the eroded Uinta Formation isopach (Fig. 4-15). CI = 50 m

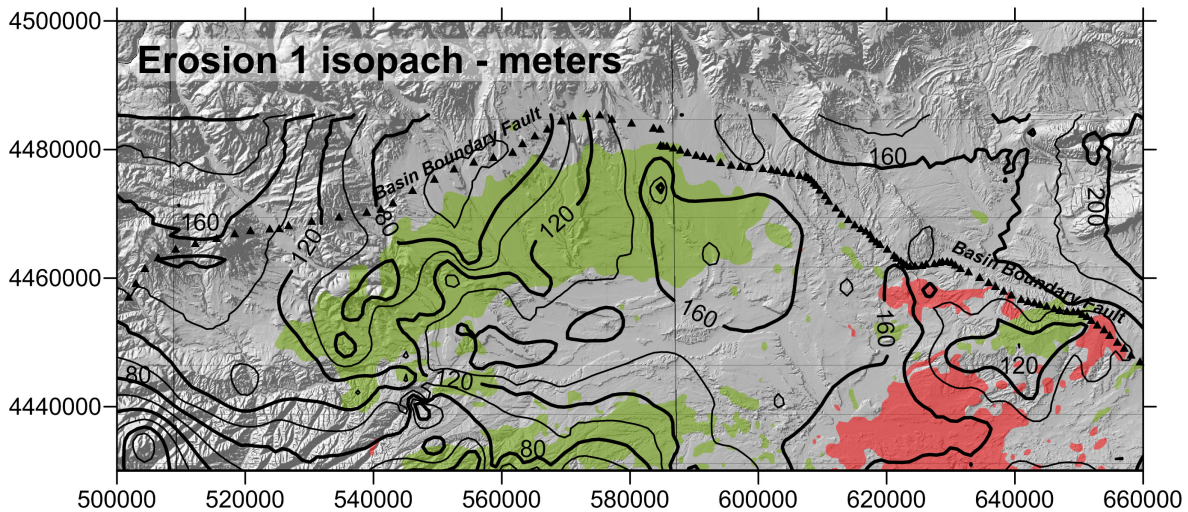


Figure 4-17: Model thickness of the erosion occurring between 10 and 0.5 Ma. This isopach represents 30% of the total erosion determined by subtracting the present-day ground surface (Fig. 4-14) from the reconstructed top of the Bishop Conglomerate. CI = 20 m

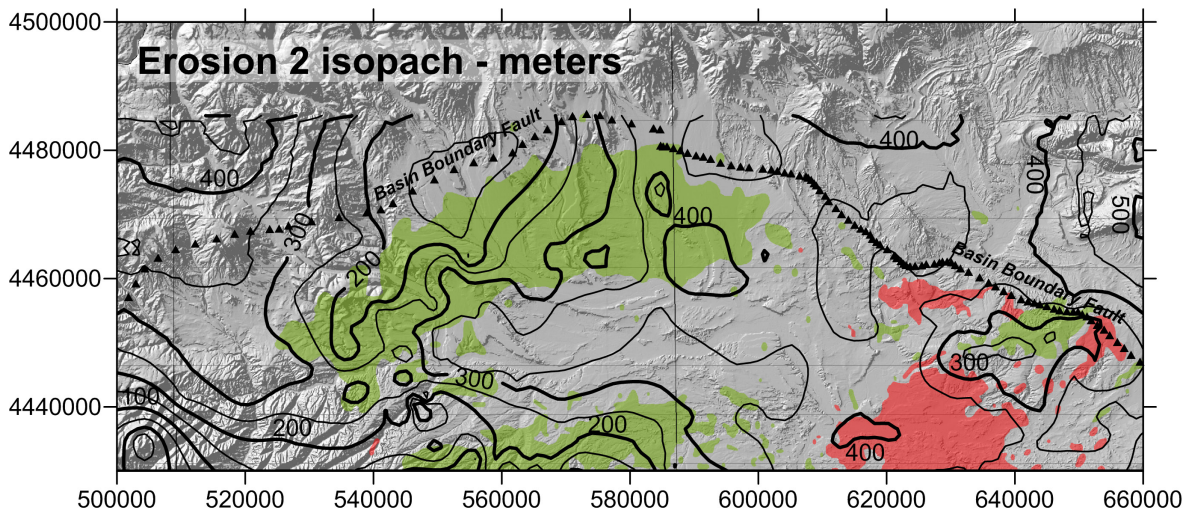


Figure 4-18: Model thickness of the erosion occurring between 0.5 and 0.0 Ma. This isopach represents 70% of the total erosion determined by subtracting the present-day ground surface (Fig. 4-14) from the reconstructed top of the Bishop Conglomerate. CI = 50 m

Table 4-3: Input variables for each of the five project models simulated, Model A through Model E. Model kinematics: RE and LLNL are from programmed pyrolysis, HP is from hydrous pyrolysis.

	Heat flow	Surface T, °C	GR-2M	GR-4	GR-6/7
Model A	52 mW/m ²	20	Mahogany RE	Mahogany RE	Black Shale RE
Model B	52 mW/m ²	20	Mahogany HP	Mahogany HP	Black Shale RE
Model C	52 mW/m ²	20	Type I, LLNL	Type I, LLNL	Type II, LLNL
Model D	57 mW/m ²	20	Mahogany RE	Mahogany RE	Black Shale RE
Model E	57 mW/m ²	20	Mahogany HP	Mahogany HP	Black Shale RE

for GR-4, and 5% for GR-6 and GR-7. Units GR-1, GR-3 and GR-5 are treated as “non-source rock” having no initial TOC.

Calculations requiring physical properties of rocks, such as thermal conductivity or average petrophysical properties, can draw on a set of default values related to standard lithologies. Alternatively, the user can specifically assign physical values to each rock unit when creating the model. Where the actual physical properties are not known, the user has the option of creating lithology mixes of the default lithologies. The lithology mixes used in all of the five project models are:

Tdr: 60% sandstone + 20% siltstone + 20% shale

Tu: 30% sandstone + 40% siltstone + 30% shale

GR-n “source rock”: 10% siltstone + 50% shale + 40% dolomite

GR-n “non-source rock”: 30% siltstone + 20% shale + 50% dolomite

The kerogen kinematics associated with the various kerogen types reported in Table 4-3 are specified in Table 4-4. The kerogen designated Type I, LLNL and Type II, LLNL are widely used kerogens published by the Lawrence Livermore National Laboratory and included in the kerogen type library in BasinView-3D™ and BasinMod-1D™. The other kerogen kinematics were determined by either RockEval programmed pyrolysis methods (RE) or hydrous pyrolysis (HP). They are published in Ruble and others (2001).

Chapman and others (1984) calculated geothermal gradients and heat flows across the Uinta Basin. They observed heat flow to decrease monotonically from 64 mW/m² in the southeast of the basin to 40 mW/m² in the extreme north along the Basin Boundary Fault. The average heat flow of 57 mW/m² (approximately equivalent to a geothermal gradient of 25°C/km) has been adopted in previous thermal maturation models (Sweeney, 1988; Ruble and others, 2001; Nuccio and Roberts, 2003) and is used in Models D and E in this study. However, this average heat flow is thought to be an artifact of high Quaternary erosion rates and unrealistically high for the Tertiary. The rapid exhumation of the basin in the mid and late Pleistocene would have the effect in the parts of the basin with major erosion of increasing geothermal gradients from which the heat flow is calculated. Rapid exhumation in recent time will have its greatest effect exactly where the higher heat flows are reported (Chapman and others, 1984). Models A, B and C used a more reasonable 52 mW/m². In hindsight, even this value may be too high.

The geographic limits for all models were from UTM (NAD83, Zone 12) Easting 500000 to 660000 and from Northing 4430000 to 4485000, with a node spacing of one kilometer. This resulted in over 9000 nodes (pseudowells) calculated for each simulation and a grid resolution of one kilometer.

Table 4-4: Kerogen kinematics used in the various project models; see Table 4-3. *E* is the activation energy and *Ao* is the frequency factor, both variables in the Arrhenius equation used to calculate the rate of thermally-driven conversion of kerogen to hydrocarbons. Different values of the parameters, in particular the activation energy, may apply to different mole fractions of the kerogen.

	fraction	E	Ao
Mahogany Shale	0.06	46	3.788 x 10 ²⁶ /my
RockEval	0.16	48	3.788 x 10 ²⁶ /my
	0.26	49	3.788 x 10 ²⁶ /my
	0.36	50	3.788 x 10 ²⁶ /my
	0.04	51	3.788 x 10 ²⁶ /my
	0.12	52	3.788 x 10 ²⁶ /my
Mahogany Shale	1.00	69	1.6505x 10 ²⁹ /my
Hydrous pyrolysis			
Black Shale facies	0.02	47	1.139 x 10 ²⁶ /my
RockEval	0.04	48	1.139 x 10 ²⁶ /my
	0.83	51	1.139 x 10 ²⁶ /my
	0.07	53	1.139 x 10 ²⁶ /my
	0.03	58	1.139 x 10 ²⁶ /my
Type I LLNL	0.07	49	1.6 x 10 ²⁷ /my
BMOD-1D	0.9	53	1.6 x 10 ²⁷ /my
	0.03	54	1.6 x 10 ²⁷ /my
Type II LLNL	0.05	49	9.5 x 10 ²⁶ /my
BMOD-1D	0.2	50	9.5 x 10 ²⁶ /my
	0.5	51	9.5 x 10 ²⁶ /my
	0.2	52	9.5 x 10 ²⁶ /my
	0.05	53	9.5 x 10 ²⁶ /my

Numerical Simulation Output Parameters

BasinView-3D™ is capable of generating a very large range of output parameters, each of which can be calculated in the simulation for any of the model stratigraphic units and associated times. Each parameter can be viewed as a graphic representation, a map, within the simulator, or exported as an array of x-y-z values formatted for any of several types of data mapping programs. Spatial variations in the burial history of different parts of the model can be visualized in synthetic 1-D burial history curves (Figures 4-19 and 4-20) that can be extracted as output graphics.

For this project, just five parameters were exported as Surfer™ grids: (1) transformation ratio, (2) vitrinite reflectance, (3) excess pressure (pressure in excess of hydrostatic), (4) oil generated (barrels per acre), and (5) time-triggers indicating time of entry of a specific stratigraphic unit into a particular

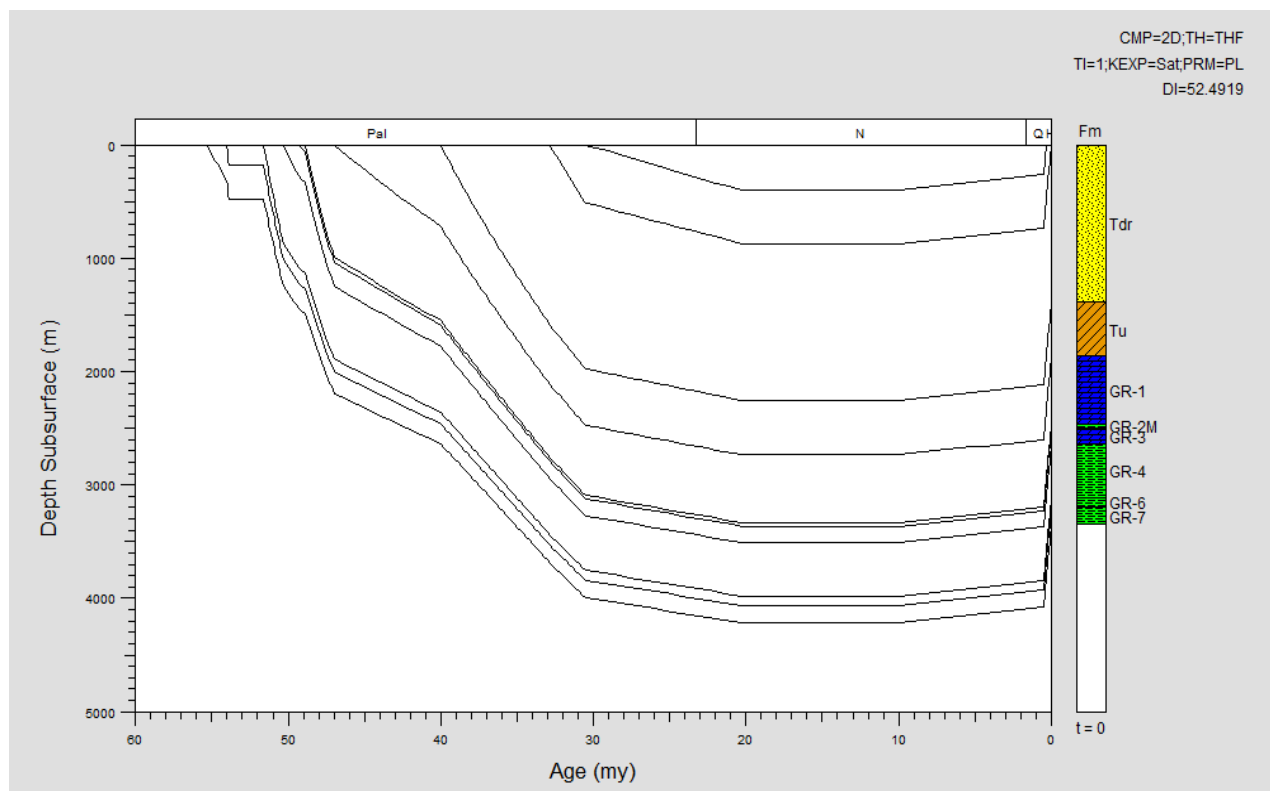


Figure 4-19: Burial history curves for a synthetic well in the northern Altamont-Bluebell field extracted from the BasinView-3D model. The base of the Green River Formation reaches a depth greater than 4000 m (13,000 ft). The well coordinates are Easting 579573, Northing 4468449.

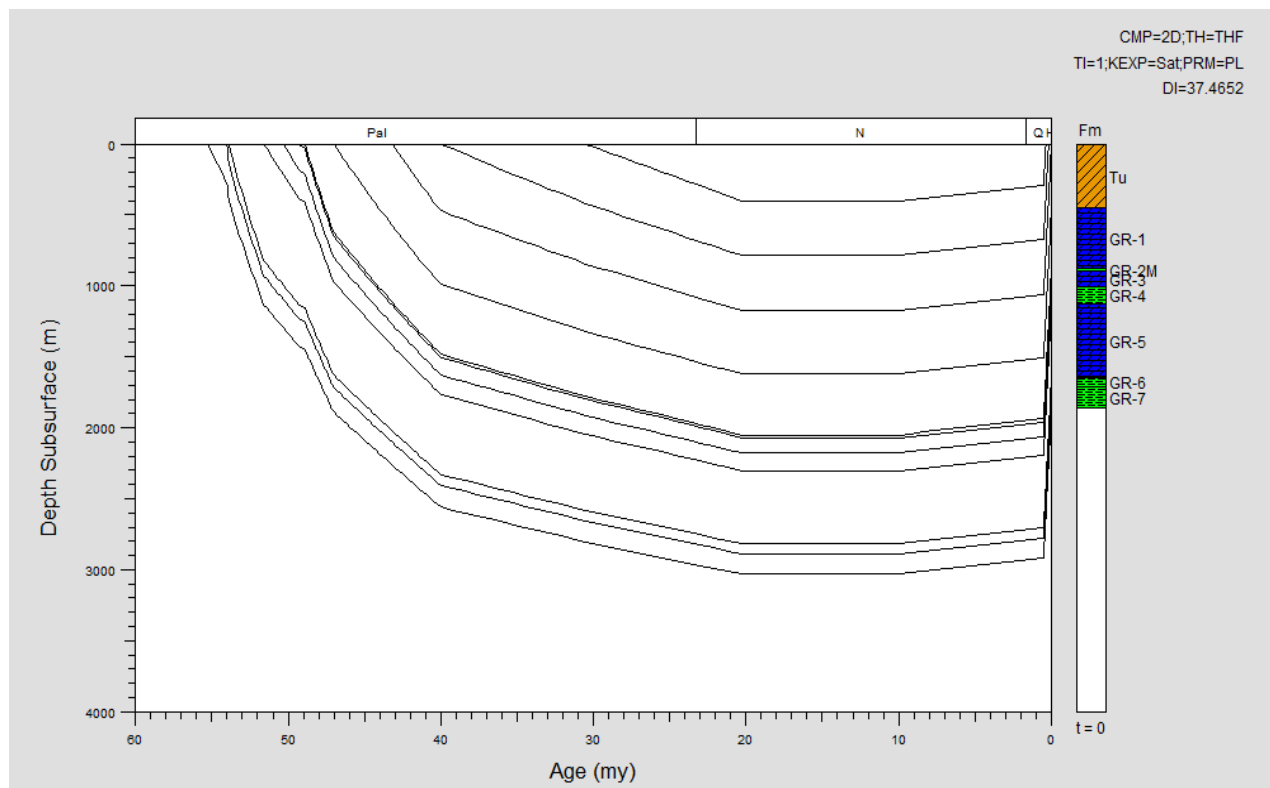


Figure 4-20: Burial history curves for a synthetic well in the northern Monument Butte field extracted from the BasinView-3D model. The base of the Green River Formation reaches a depth approaching 3000 m (10,000 ft). The well coordinates are Easting 585768, Northing 4434659.

organic maturity window. These parameters have been extracted for the assigned source rock units for various times (see Table 4-5).

The time-trigger maps provide a very direct means for visualizing the time of entry of different parts of the basin for a specific stratigraphic horizon into a particular maturity threshold. Figures 4-21 through 4-32 compare the simulations for Model A (52 mW/m²) with Model D (57 mW/m²). Understandably, the maturation threshold entry times are earlier by a few million years for the model run at the higher heat flow value. The simulations are shown for three stratigraphic horizons: (1)

the top of the Mahogany Zone, (2) the base of the Parachute Creek Member, and (3) the middle of the Black Shale facies in the Lower Green River Formation. What stands out in all simulation maps is that the time of entry into the oil window is very early, considerably earlier by as much as 30 million years compared to the simulation by Nuccio and Roberts (2003; Figure 3-29). Also the trend of the oil kitchen is parallel to the northwest segment of the Basin Boundary Fault and parallel to the isopach thick of the Green River Formation in Figure 2-12. Entry into all maturity thresholds is later in what is now the deepest part of the basin, the extreme north, compared with the areas to the southwest and especially near Duchesne.

Table 4-5: Chart of simulation output parameters exported as Surfer grid files for each of the models simulated, Model A through Model E. The grid files generated by the simulation can be found in Digital Appendix C in the folders for each individual model.

Transformation ratio	0 Ma	10.0 Ma	20.3 Ma	30.5 Ma
GR-2M	A B C D E	A B C D E	A B C D E	A B C D E
GR-4	A B C D E	A B C D E	A B C D E	A B C D E
GR-7	A B C D E	A B C D E	A B C D E	A B C D E

Vitritnite reflectance LLNL	0 Ma	10.0 Ma	20.3 Ma	30.5 Ma
GR-2M	A B C D E	A B C D E	A B C D E	A B C D E
GR-4	A B C D E	A B C D E	A B C D E	A B C D E
GR-7	A B C D E	A B C D E	A B C D E	A B C D E

Excess pressure (psi)	0 Ma	10.0 Ma	20.3 Ma	30.5 Ma
GR-2M	A B C D E	A B C D E	A B C D E	A B C D E
GR-4	A B C D E	A B C D E	A B C D E	A B C D E
GR-7	A B C D E	A B C D E	A B C D E	A B C D E

Oil generated (bbls per acre)	0 Ma
GR-2M	A B na D E
GR-4	A B na D E
GR-6	A B na D E
GR-7	A B na D E

Time triggers	Early mature	Mid-mature	Peak oil	Main gas
GR-2M	A B C D E	na B C D E	A na C D E*	
GR-4	A B C D E	na B C D E	A B* C D E*	
GR-7	A B C D E	na B C D E	A B C D E	A B C D E

* or Late mature

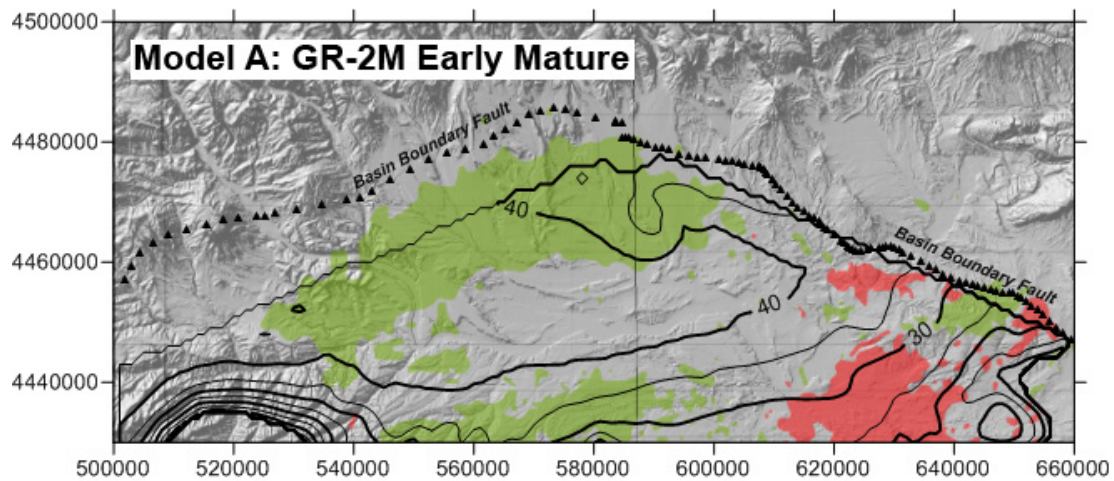


Figure 4-21: Time-trigger for entry of the Mahogany Zone (GR-2M) into the Early Mature oil window in Model A in which the heat flow is specified as the preferred 52 mW/m^2 . Note that a large portion of the GR-2M unit has entered the oil window even before end of deposition of the Uinta Formation. Early Mature is equivalent to vitrinite reflectance of 0.6–0.65% and T_{max} of 435° – 445°C (Peters and Cassa, 1994). $CI = 5 \text{ Ma}$

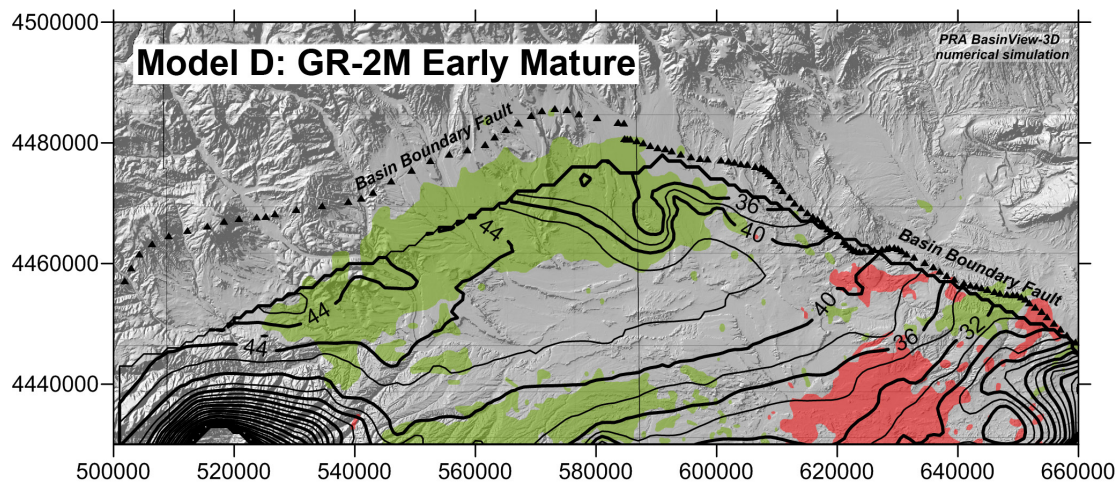


Figure 4-22: Time-trigger for entry of the Mahogany Zone (GR-2M) into the Early Mature oil window in Model D in which the heat flow is specified as the Uinta Basin average 57 mW/m^2 (Chapman and others, 1984). Note that at the slightly higher heat flow the entry into the oil window is a few million years earlier throughout the region modeled. It is possible that the simulation fails in the extreme southwest of the model area. $CI = 2 \text{ Ma}$

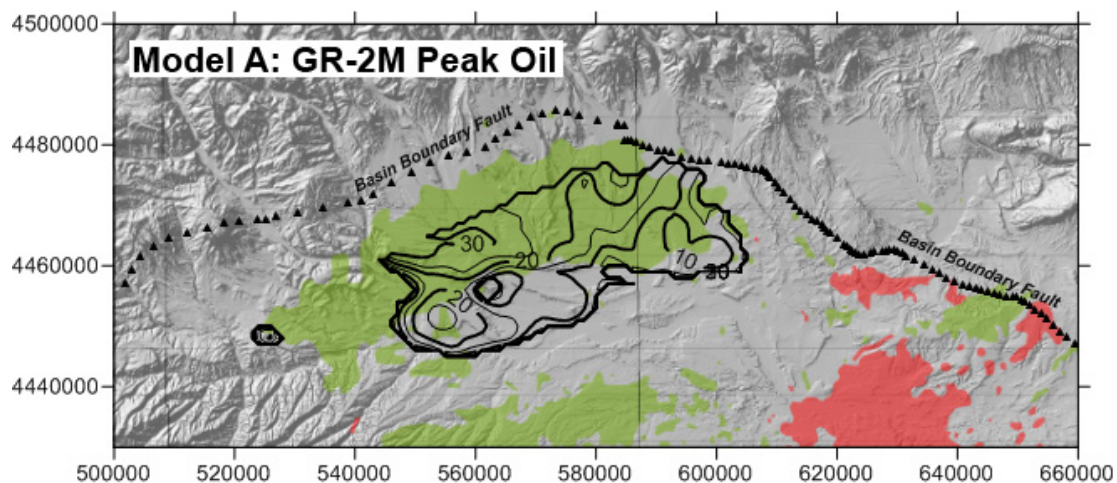


Figure 4-23: Time-trigger for entry of the Mahogany Zone (GR-2M) into the Peak Oil maturity window in Model A in which the heat flow is specified as the preferred 52 mW/m^2 . This area is spatially constrained to the deep axis of the basin in the region of the Altamont-Bluebell field. Peak Oil is equivalent to vitrinite reflectance of 0.65–0.9% and T_{max} of 445° – 450°C (Peters and Cassa, 1994). $CI = 5 \text{ Ma}$

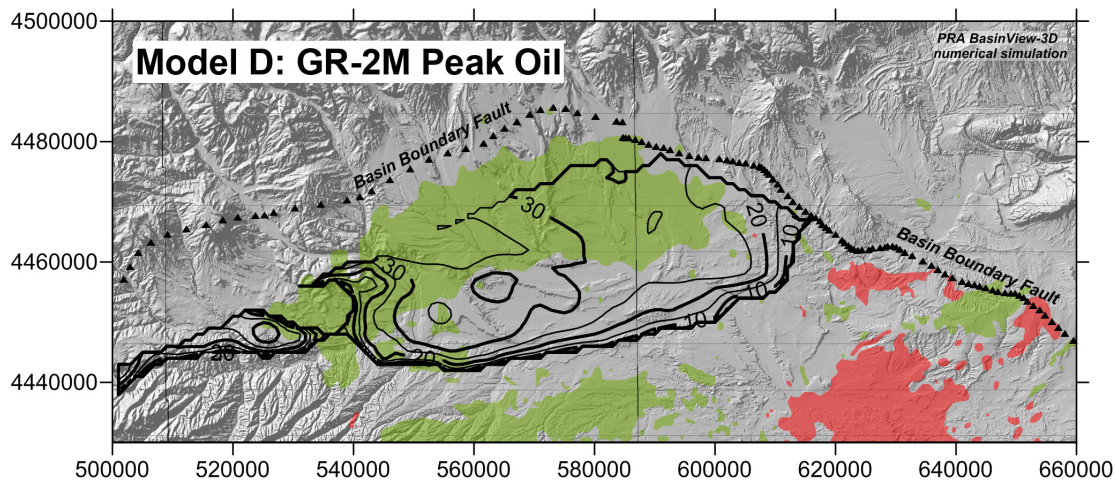


Figure 4-24: Time-trigger for entry of the Mahogany Zone (GR-2M) into the Peak Oil maturity window in Model D in which the heat flow is specified as the Uinta Basin average 57 mW/m^2 (Chapman and others, 1984). At this slightly higher heat flow the region of entry is larger and the time of entry is as much as 10 Ma earlier than for the lower value of heat flow. CI = 5 Ma

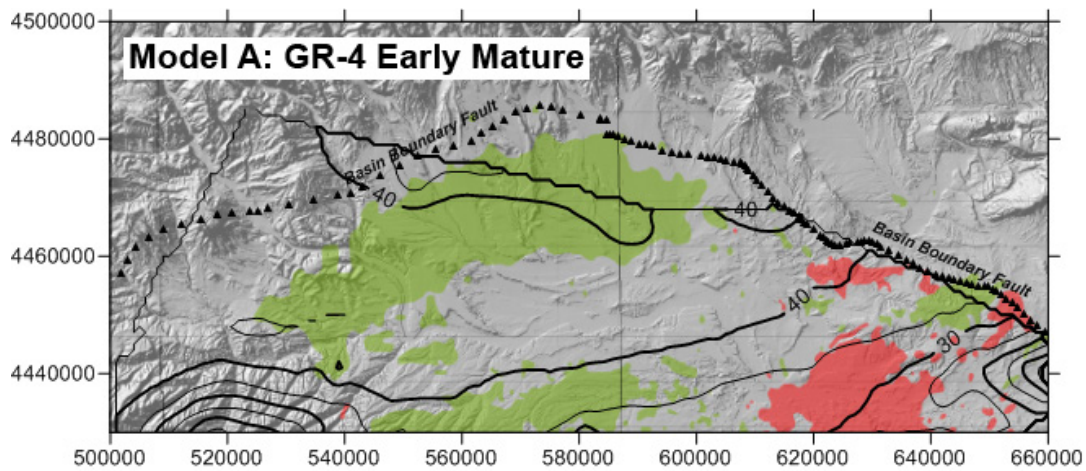


Figure 4-25: Time-trigger for entry of the lower Parachute Creek Member (GR-4) into the Early Mature oil window in Model A in which the heat flow is specified as the preferred 52 mW/m^2 . Virtually all of the north and central Uinta Basin is in the oil generative window at this stratigraphic level. Note that a single outlier “placed well” is pulling the simulation across the Basin Boundary Fault in the northwest. Isotherms north of the fault should be ignored. CI = 5 Ma

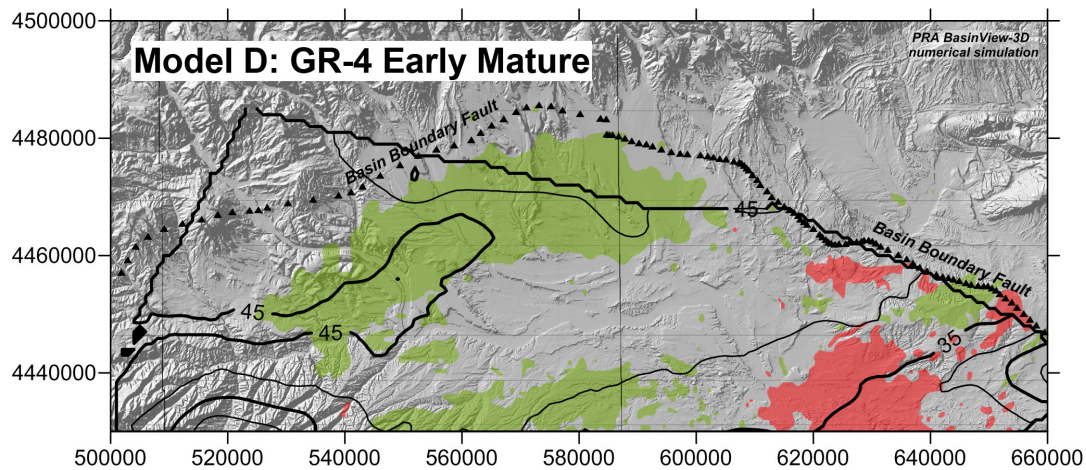


Figure 4-26: Time-trigger for entry of the lower Parachute Creek Member (GR-4) into the Early Mature oil window in Model D in which the heat flow is specified as the Uinta Basin average 57 mW/m^2 (Chapman and others, 1984). Note that the earliest entry into Early Mature in the southwest portion of the greater Altamont field, not the presently deepest part of the basin. CI = 5 Ma

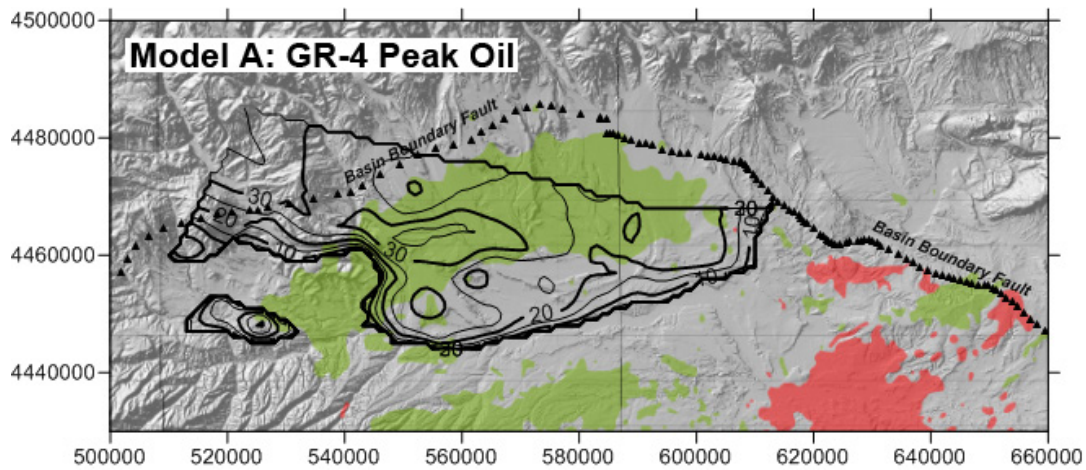


Figure 4-27: Time-trigger for entry of the lower Parachute Creek Member (GR-4) into the Peak Oil maturity window in Model A in which the heat flow is specified as the preferred 52 mW/m^2 . This area is spatially constrained to the deep axis of the basin in the region of the Altamont-Bluebell field, the portion of the field where anomalous formation pressures are observed (see figure 3-32). The 30 Ma isopleths might project across the gap in the simulation west of Duchesne. CI = 5 Ma

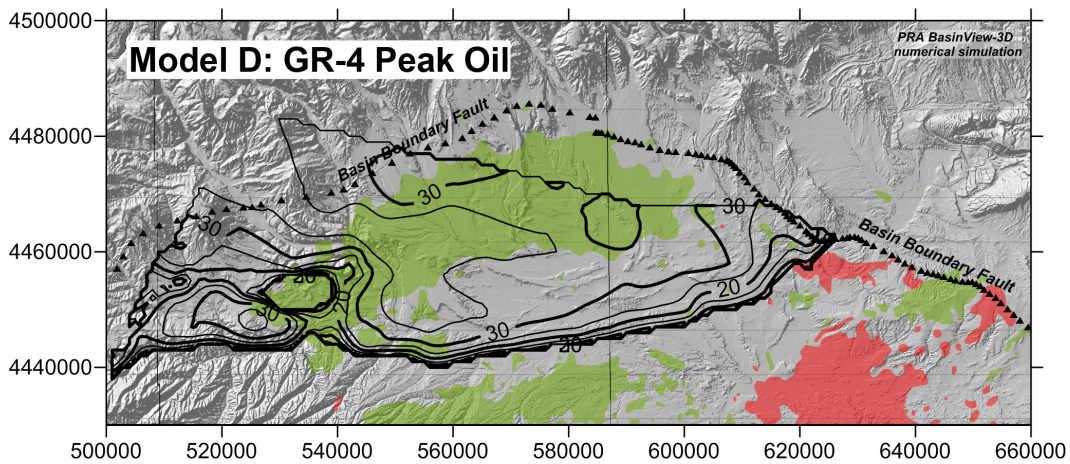


Figure 4-28: Time-trigger for entry of the lower Parachute Creek Member (GR-4) into the Peak Oil maturity window in Model D in which the heat flow is specified as the Uinta Basin average 57 mW/m^2 (Chapman and others, 1984). A possible flaw in the surfaces defining the GR-4 unit, possibly a small cross-over of the surfaces, is resulting in a hole in the simulation results for an area on the west side of the map. It could be acceptable to project the 35 Ma isopleths across the hole. CI = 5 Ma

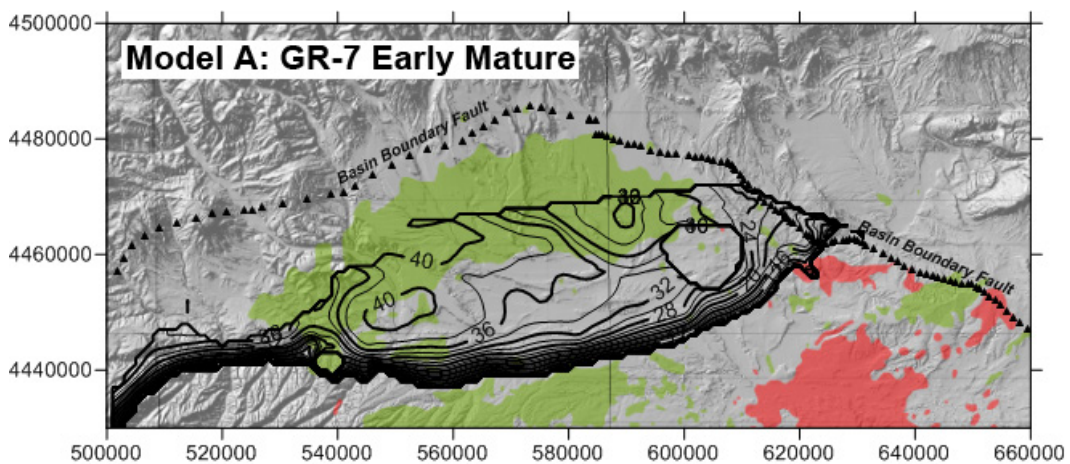


Figure 4-29: Time-trigger for entry of the Lower Green River Formation (Black Shale facies, GR-7) into the Early Mature oil window in Model A in which the heat flow is specified as the preferred 52 mW/m^2 . The circular void in the simulation east-central part of the map is due to a cross-over of model surfaces. CI = 2 Ma

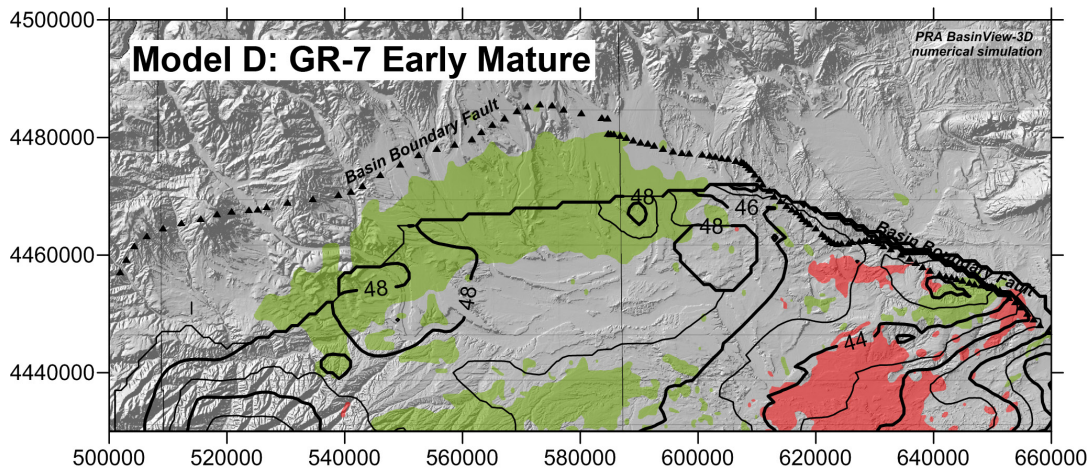


Figure 4-30: Time-trigger for entry of the Lower Green River Formation (Black Shale facies, GR-7) into the Early Mature oil window in Model D in which the heat flow is specified as the Uinta Basin average 57 mW/m^2 (Chapman and others, 1984). At this higher heat flow the deepest stratigraphic level of the Green River Formation is entering the oil generative window while the uppermost part of the very thick formation is still being deposited. Refer to Table 4-1. The circular void in the simulation in the east-central part of the map is due to a cross-over of model surfaces. CI = 2 Ma

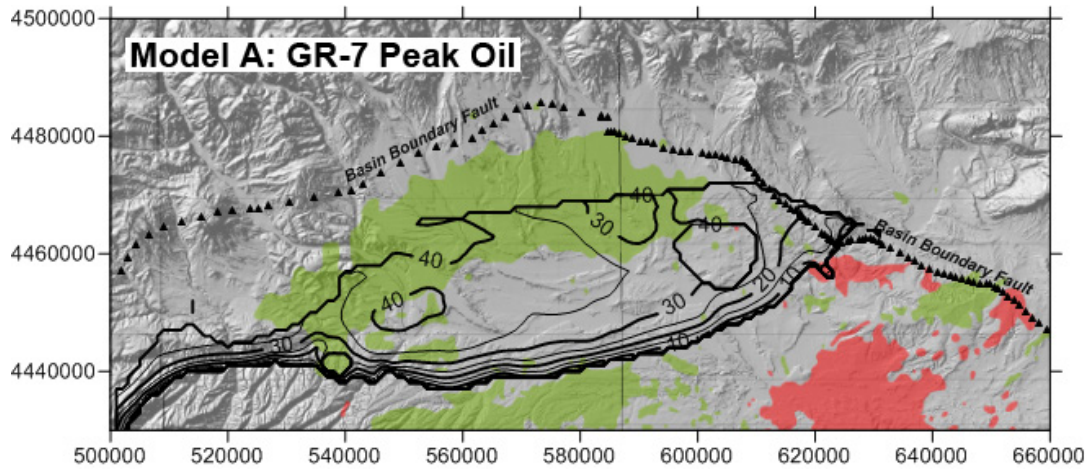


Figure 4-31: Time-trigger for entry of the Lower Green River Formation (Black Shale facies, GR-7) into the Peak Oil maturity window in Model A in which the heat flow is specified as the preferred 52 mW/m^2 . The circular void in the simulation in the east-central part of the map is due to a cross-over of model surfaces. CI = 5 Ma

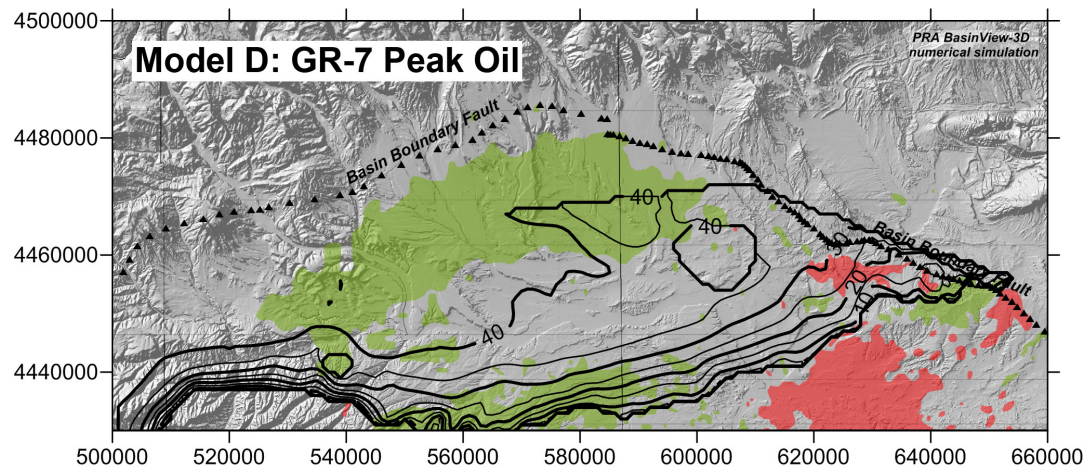


Figure 4-32: Time-trigger for entry of the Lower Green River Formation (Black Shale facies, GR-7) into the Peak Oil maturity window in Model D in which the heat flow is specified as the Uinta Basin average 57 mW/m^2 (Chapman and others, 1984). The circular void in the simulation in the east-central part of the map is due to a cross-over of model surfaces. CI = 5 Ma

The vitrinite reflectance (R_o -LLNL) maps (Figs. 4-33 to 4-44) depict the spatial distribution of simulated R_o using transformation ratio to R_o equivalencies developed at the Lawrence Livermore National Laboratory. The simulations were determined for the three stratigraphic horizons and four different times, 0 Ma, 10 Ma, 20.3 Ma and 30.5 Ma. The simulations are shown only for Model A, which generally match the R_o values in Anders and Gerrild (1984). Model D simulations are thought to be too high. As with the time-trigger maps, the oil kitchen is shown trending northeast, parallel to the northwest segment of the Basin Boundary Fault.

The maturity maps appear to be relatively insensitive to different model kerogen kinematics. Recall that Ruble and others (2001) propose that their Mahogany Shale activation energy would delay active oil generation of the Type I kerogen until a R_o maturity-equivalency of 0.75% is reached. However, it is definitely possible to see the effect of using the different kerogen kinematics in the simulations of oil generated. The results from using different kerogen kinematics are summarized in

Table 4-6. The simulations using activation energies for Type I kerogen based on programmed pyrolysis (RE) derived data predict large quantities of oil generated, whereas simulations using the activation energy for Type I kerogen based on hydrous pyrolysis predict only minimal oil generation. These are the results found by Ruble and others (2001) in their alternative 1-D simulations shown in Figure 3-31. If we accept the hydrous pyrolysis activation energy as the better descriptor for Green River Type I kerogen, the source rocks rich in Type I kerogen have just recently begun entering the oil generative window, which has significant implications for the Green River petroleum system.

Simulations of the excess (anomalous) pressure offer another way of looking at the question of time of entry into the oil generative window. The calculations of this parameter are very poor. Better calculations would have required assigning petrophysical properties, currently unknown, to the Green River rocks. However, what is observed in all of the simulations is that the area of anomalous pressures is large for the 0 Ma time

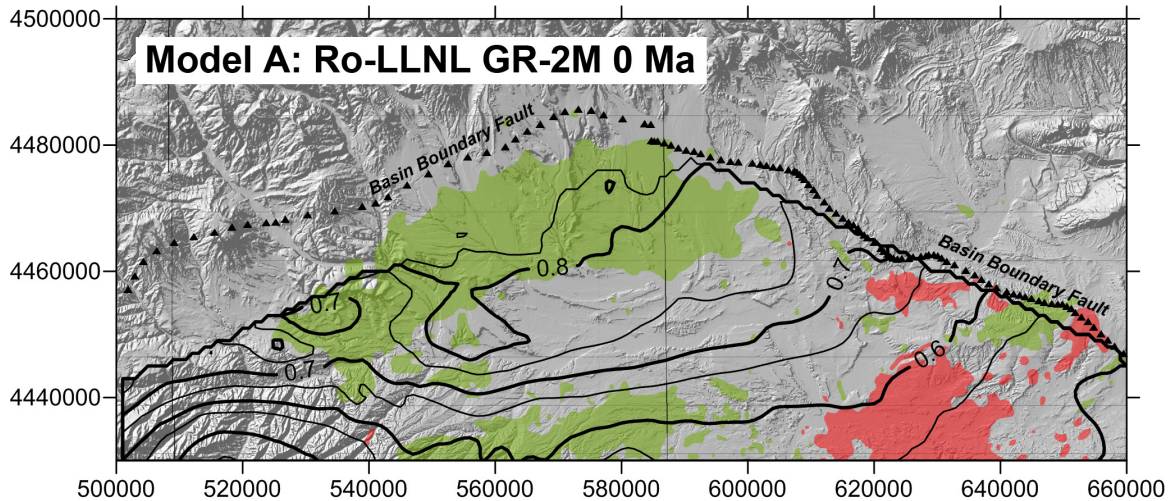


Figure 4-33: Simulated vitrinite reflectance values for the Mahogany Shale (GR-2M) at the present-time (0 Ma). $CI = 0.05\% R_o$.

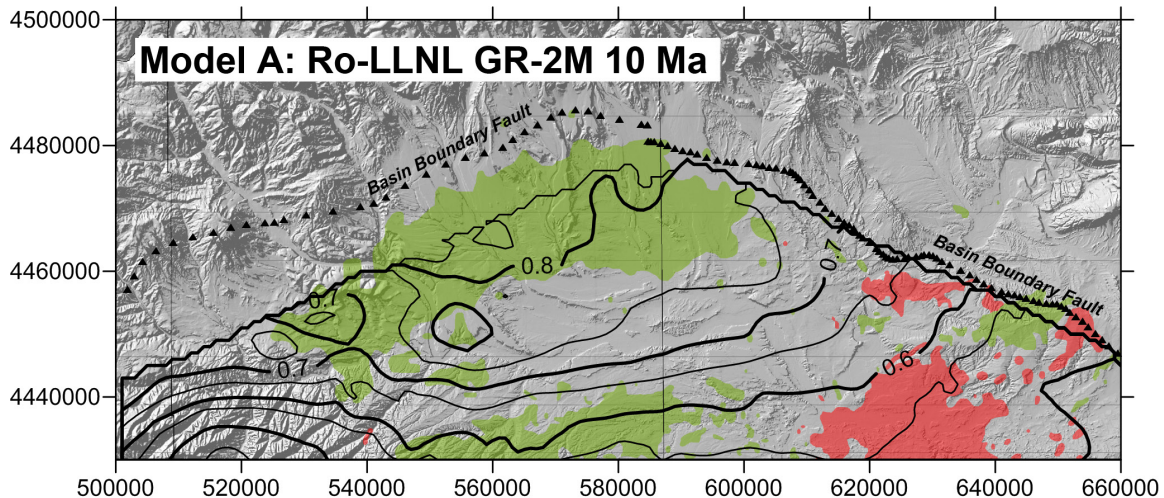


Figure 4-34: Simulated vitrinite reflectance values for the Mahogany Shale (GR-2M) at 10 Ma. $CI = 0.05\% R_o$.

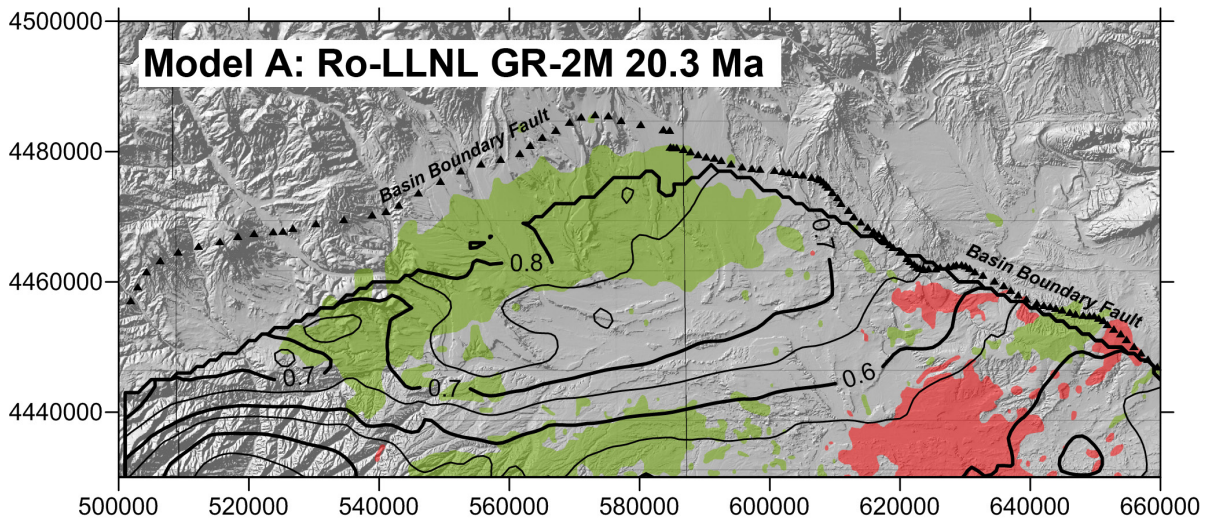


Figure 4-35: Simulated vitrinite reflectance values for the Mahogany Shale (GR-2M) at 20.3 Ma. $CI = 0.05\% R_o$

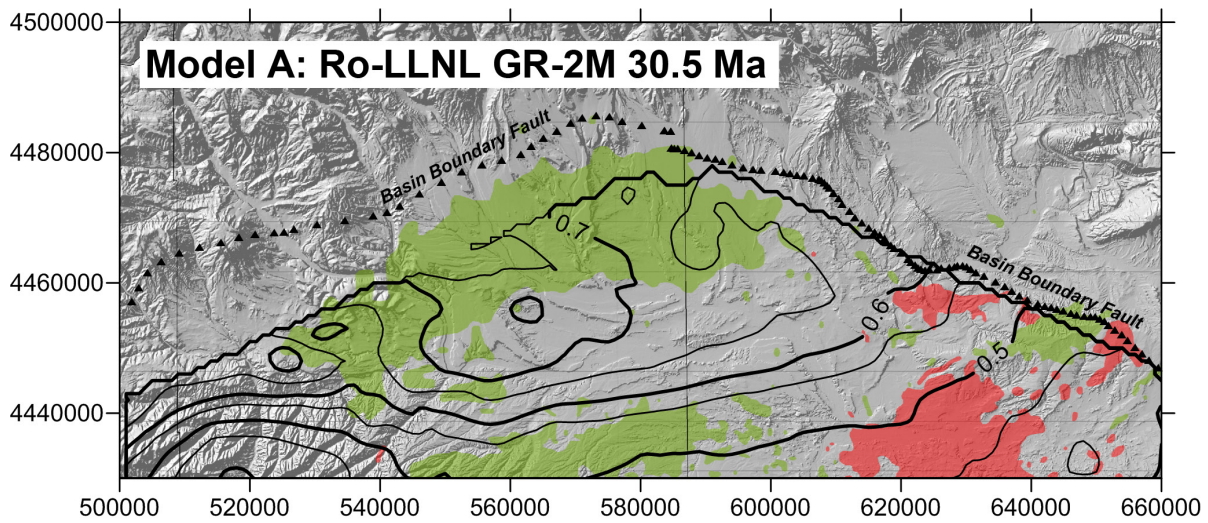


Figure 4-36: Simulated vitrinite reflectance values for the Mahogany Shale (GR-2M) at 30.5 Ma. $CI = 0.05\% R_o$

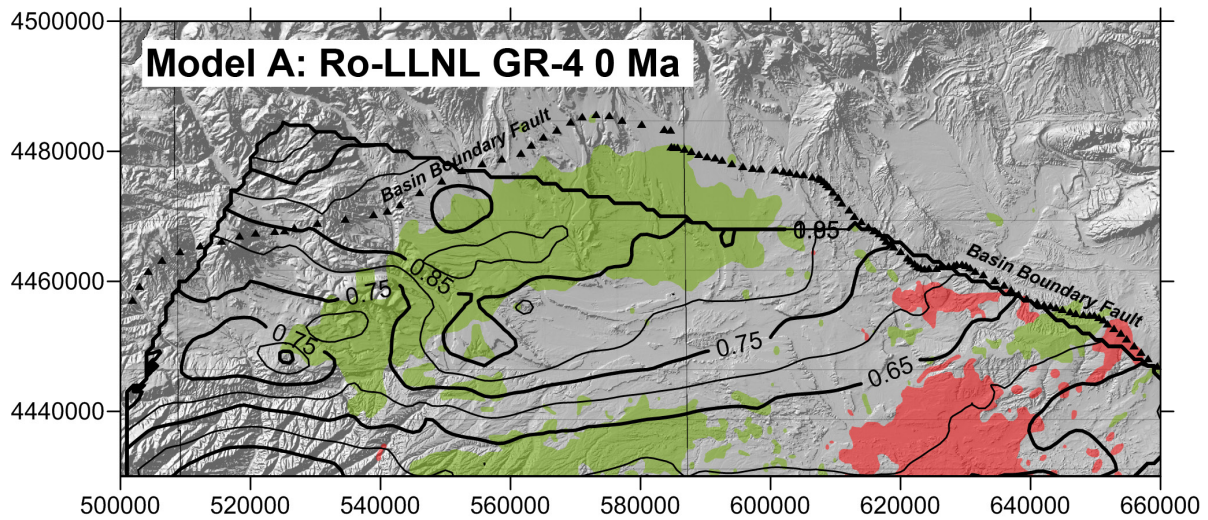


Figure 4-37: Simulated vitrinite reflectance values for the lower Parachute Creek Member (GR-4) at the present-time (0 Ma). Note that a single outlier “placed well” is pulling the simulation across the Basin Boundary Fault in the northwest. Isopleths north of the fault should be ignored. $CI = 0.05\% R_o$

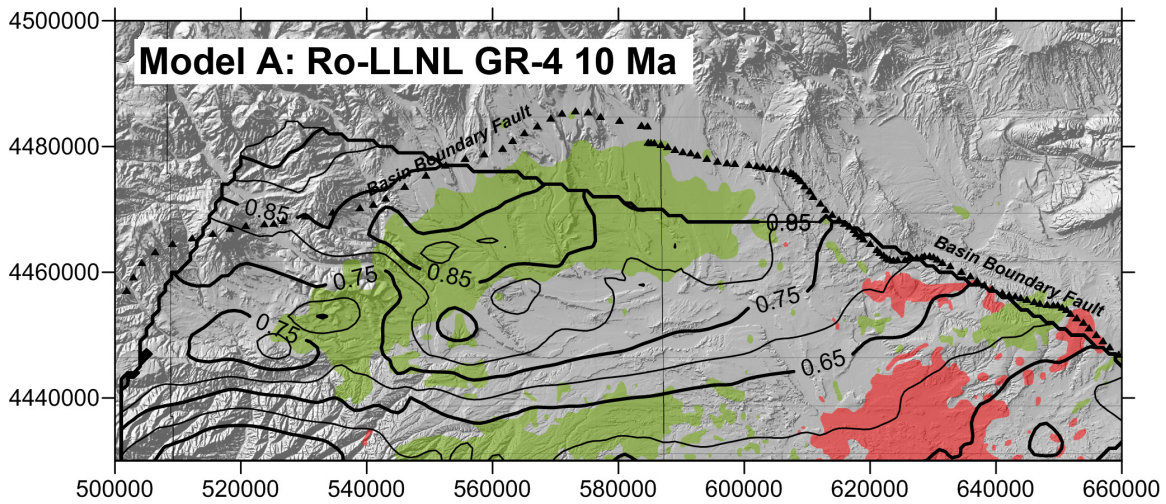


Figure 4-38: Simulated vitrinite reflectance values for the lower Parachute Creek Member (GR-4) at 10 Ma. Note that a single outlier “placed well” is pulling the simulation across the Basin Boundary Fault in the northwest. Isopleths north of the fault should be ignored. $CI = 0.05\% R_o$

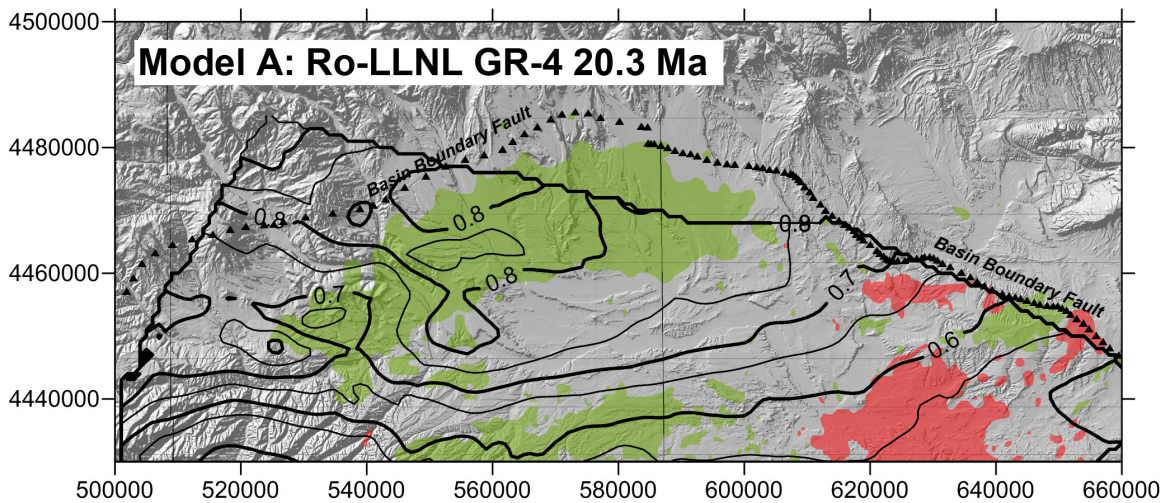


Figure 4-39: Simulated vitrinite reflectance values for the lower Parachute Creek Member (GR-4) at 20.3 Ma. Note that a single outlier “placed well” is pulling the simulation across the Basin Boundary Fault in the northwest. Isopleths north of the fault should be ignored. $CI = 0.05\% R_o$

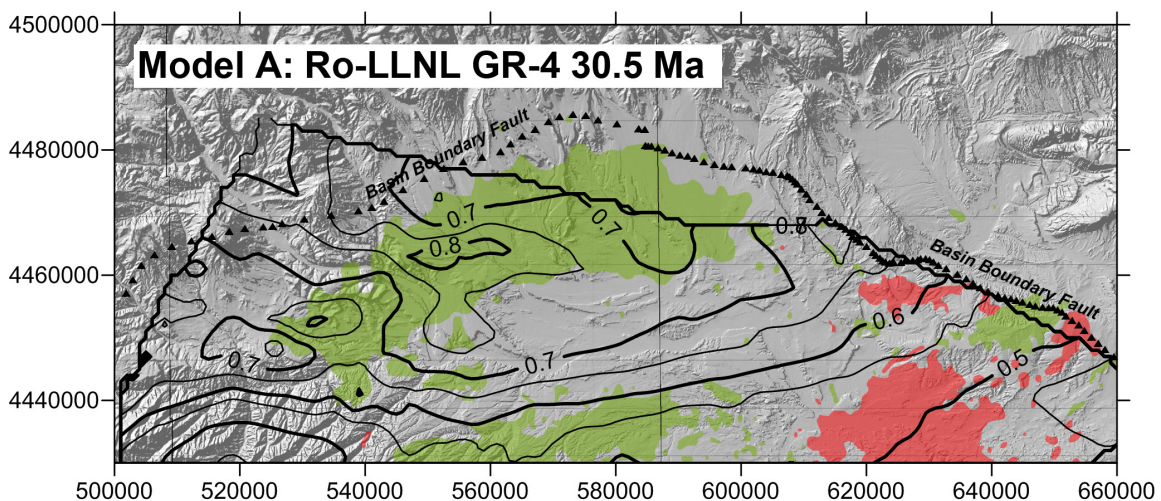


Figure 4-40: Simulated vitrinite reflectance values for the lower Parachute Creek Member (GR-4) at 30.5 Ma. Note that a single outlier “placed well” is pulling the simulation across the Basin Boundary Fault in the northwest. Isopleths north of the fault should be ignored. $CI = 0.05\% R_o$

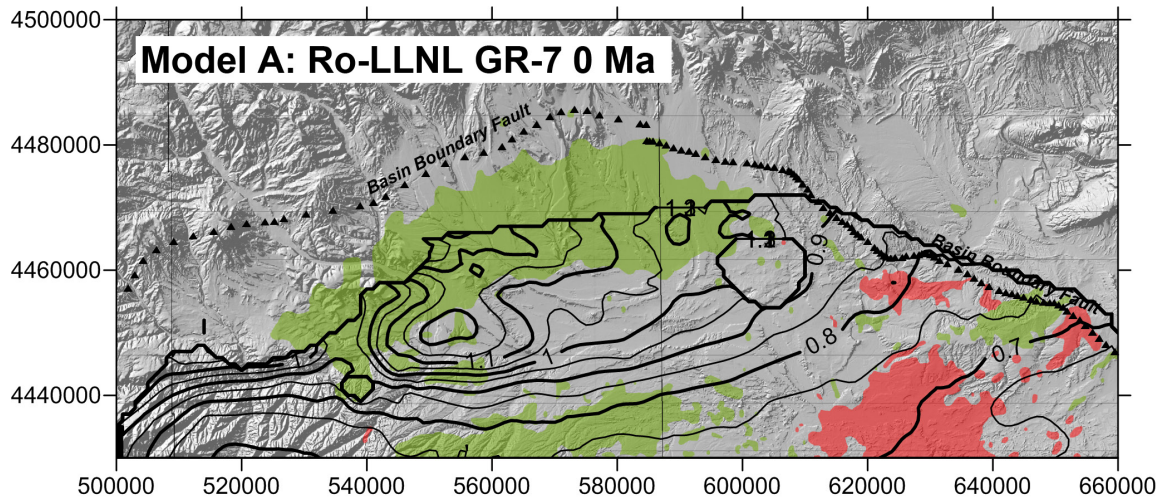


Figure 4-41: Simulated vitrinite reflectance values for the Black Shale facies (GR-7) at the present-time (0 Ma). The circular void in the simulation in the east-central part of the map is due to a cross-over of model surfaces. $CI = 0.05\% R_o$

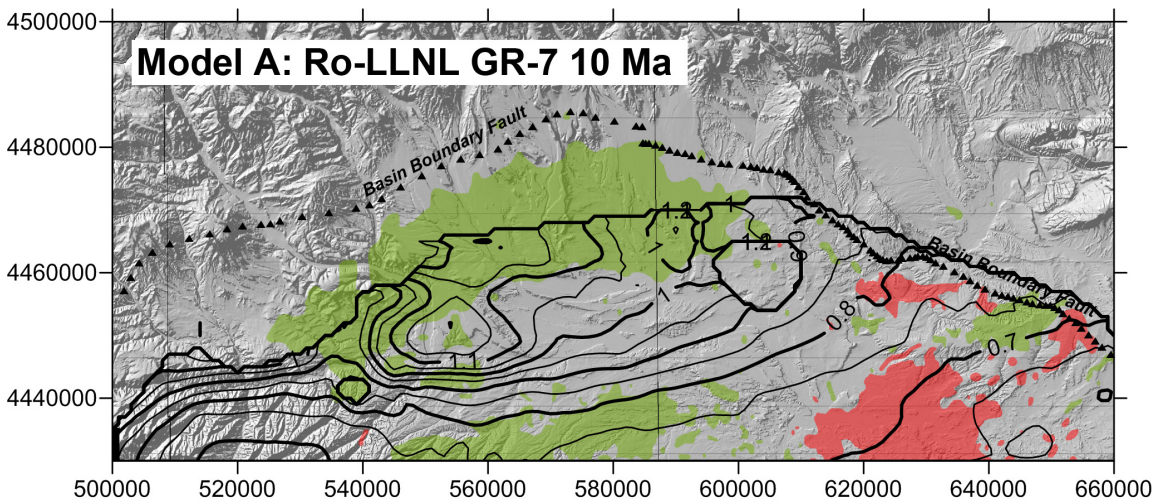


Figure 4-42: Simulated vitrinite reflectance values for the Black Shale facies (GR-7) at 10 Ma. The circular void in the simulation in the east-central part of the map is due to a cross-over of model surfaces. $CI = 0.05\% R_o$

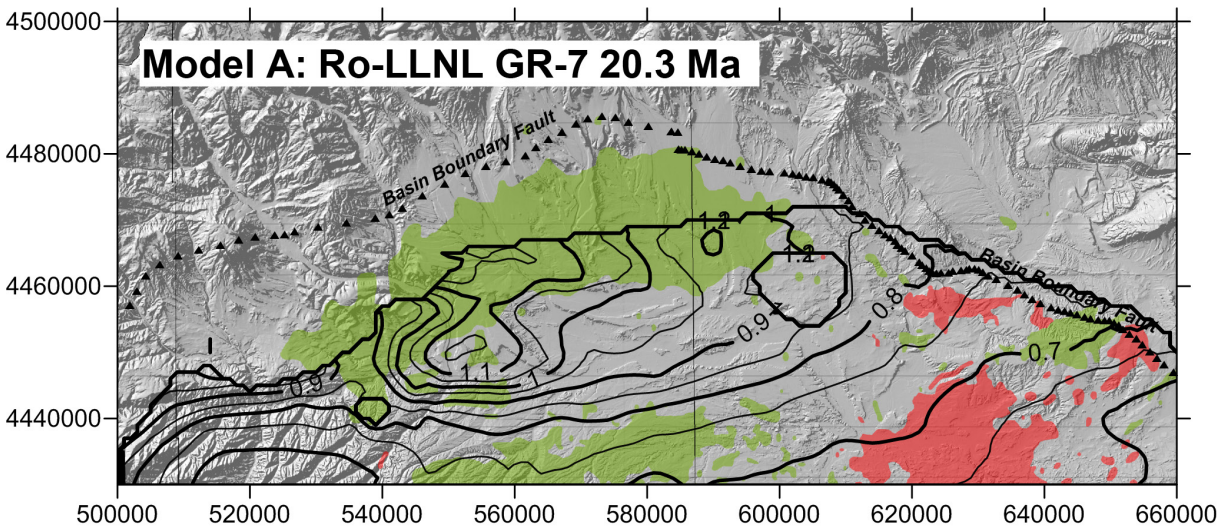


Figure 4-43: Simulated vitrinite reflectance values for the Black Shale facies (GR-7) at 20.3 Ma. The circular void in the simulation in the east central part of the map is due to a cross-over of model surfaces. $CI = 0.05\% R_o$

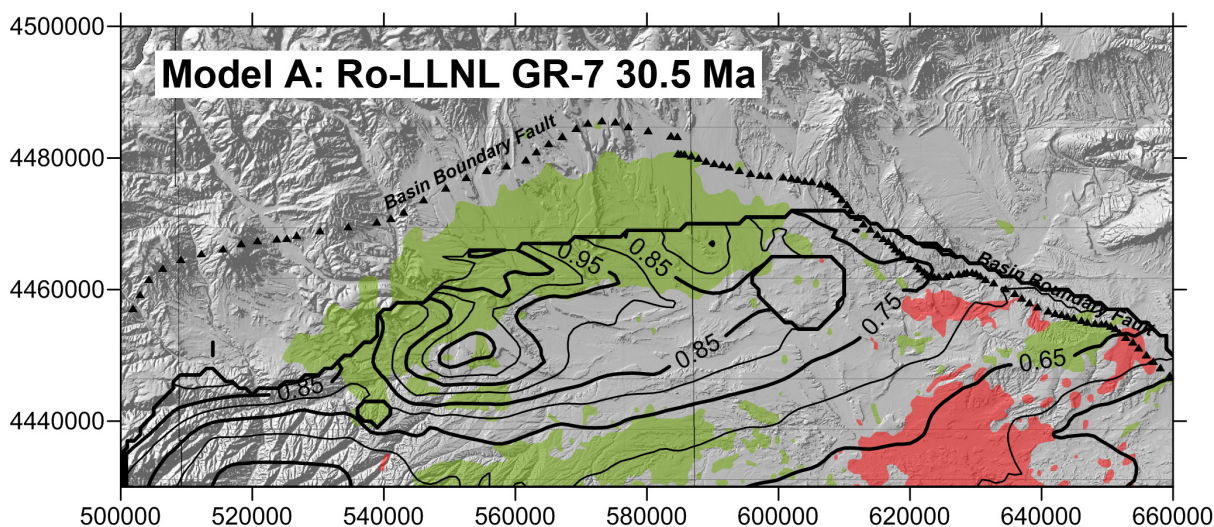


Figure 4-44: Simulated vitrinite reflectance values for the Black Shale facies (GR-7) at 30.5 Ma. The circular void in the simulation in the east central part of the map is due to a cross-over of model surfaces. $CI = 0.05\% R_o$

Table 4-6: The maximum values of oil generated in barrels of oil per acre in simulations for the different models. Note that Model A and B and D and E use different kinematics, Type I kerogen kinematics determined from open-system programmed pyrolysis (RockEval) versus closed system hydrous pyrolysis. The kerogen kinematics are identified by stratigraphic interval and source: RE (open-system RockEval) and HP (closed-system hydrous pyrolysis) from Ruble and others (2001) and LLNL (a commonly used BasinView 3-D default). MBO is units of thousand barrels per acre.

	Oil generated - maximum value, MBO				Model kerogen kinematics			Heat flow
	GR-2M	GR-4	GR-6	GR-7	GR-2M	GR-4	GR-6/7	
Model A	7,000	5,600	420	650	Mahogany RE	Mahogany RE	Black Shale RE	52 mW/m ²
Model B	0.0013	0.014	420	650	Mahogany HP	Mahogany HP	Black Shale RE	52 mW/m ²
Model C	na	na	na	na	Type I, LLNL	Type I, LLNL	Type II, LLNL	52 mW/m ²
Model D	8,000	6,500	480	850	Mahogany RE	Mahogany RE	Black Shale RE	57 mW/m ²
Model E	0.0125	0.15	480	850	Mahogany HP	Mahogany HP	Black Shale RE	57 mW/m ²

(Fig. 4-45) and quite small for previous times (Figs 4-46 and 4-47). There are two ways to interpret this observation. Either the higher anomalous pressure at the present is due to volume expansion of reservoir hydrocarbons related to the recent and rapid exhumation (unloading) of the basin, or it relates to the relatively recent entry of the Type I kerogens into the oil generative window.

5. DISCUSSION

In a conventional petroleum system, oil moves by buoyancy drive from source to trap through a carrier system, a network of permeable carrier beds, faults and fractures, and/or along unconformities. The oil generated in the “kitchen” leaves the tight source rocks by pressure-driven diffusion and Darcy flow (England, 1994), commonly aided by local fracturing caused by volume expansion of kerogen converting to bitumen and oil. The volume of oil that moves in this “primary” migration is just that portion generated that is not held in the source rock by sorption on and within the organic matter present or trapped behind nanno-size pore throats. Not all of the oil gen-

erated is free to migrate into the carrier network, only that portion that is not “irreducible” (Pepper, 1991).

Where the carrier system is non-existent or highly inefficient, the oil remains entrapped in the source-rock succession. This situation results in an unconventional continuous petroleum accumulation, a potential shale oil resource play. Typical shale oil resource plays are self-contained petroleum systems having ineffective carrier systems that severely restrict oil generated in the source rocks from migrating outward or upward into traps in reservoirs external to the oil kitchens. Consequently, oil backs up into any and all pore space in the source rock succession, even creating fracture storage space where over-pressures approaching lithostatic (0.8 psi/ft) occur. Relatively tight rocks that normally never would be considered reservoirs can have high oil saturations and oil-in-place. Hydrocarbon charge is pervasive across a large area, but one with poorly delineated boundaries. No distinct oil-water contacts are recognized and there is little water production, yet water occurs up dip from the oil accumulation. Normally, shale oil plays have low recovery factors (< 10%),

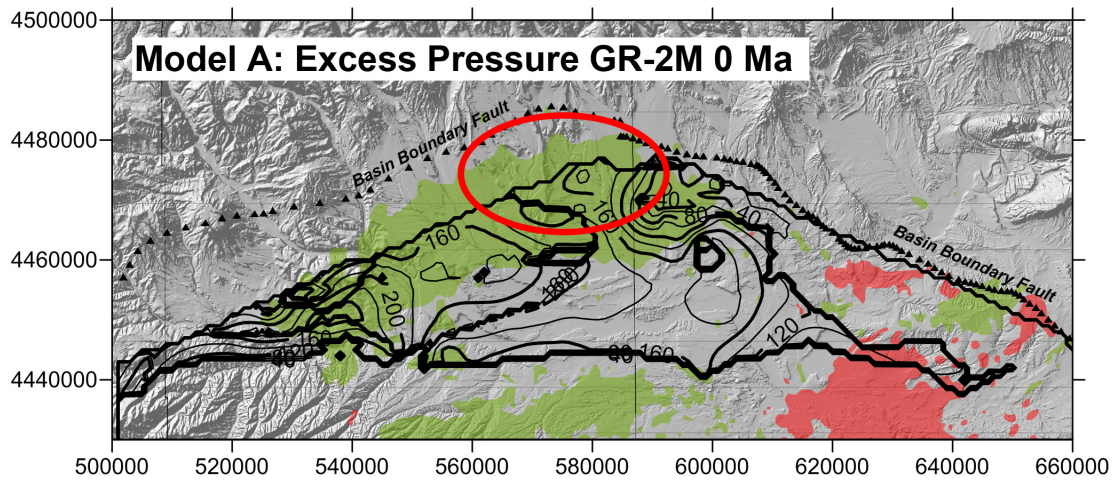


Figure 4-45: Field of Excess Pressure (pressure in excess of hydrostatic) in the Mahogany Zone (GR-2M) at the present, 0 Ma. Units are pounds per square inch (psi). Calculation of this parameter is sensitive to the petrophysical properties of the lithologies assigned. Consequently, the map should be seen as a qualitative representation of anomalous pressures. The red ellipse encloses the region of very high anomalous pressures reported by Lucas and Drexler (1975) and Nelson (2002). Contour interval is 20 pounds per square inch (psi).

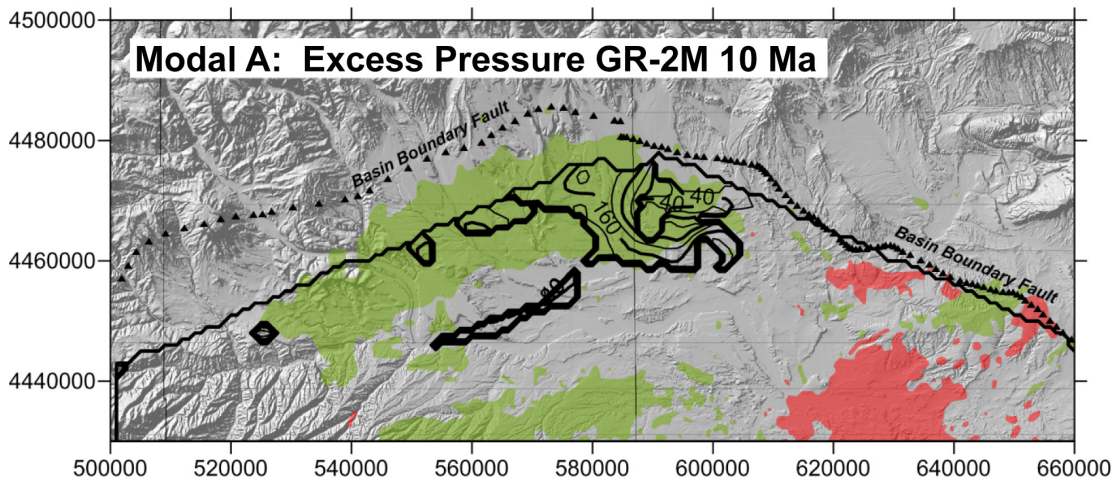


Figure 4-46: Field of Excess Pressure (pressure in excess of hydrostatic) in the Mahogany Zone (GR-2M) at the onset of exhumation, 10 Ma. Units are pounds per square inch (psi). CI = 20 psi

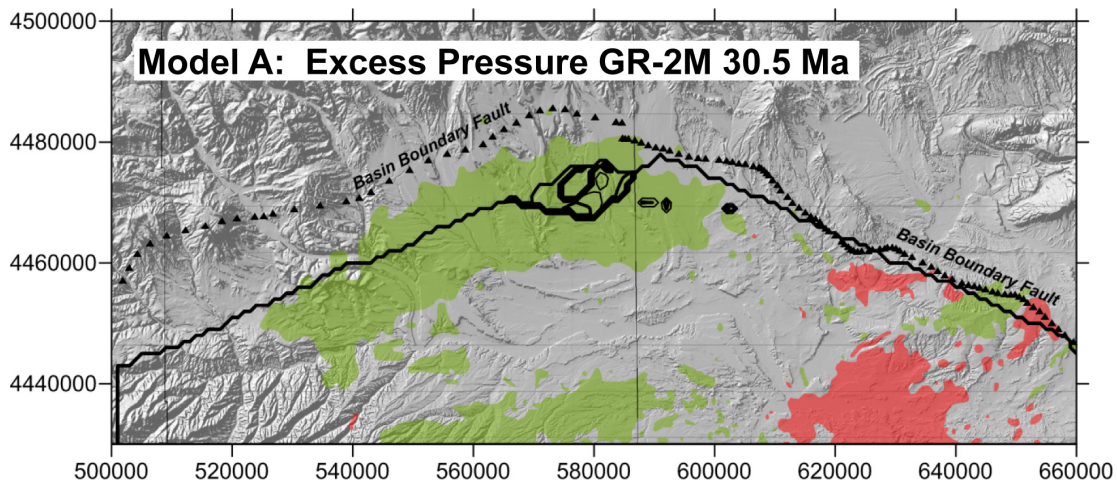


Figure 4-47: Field of Excess Pressure (pressure in excess of hydrostatic) in the Mahogany Zone (GR-2M) at the end of deposition of the Duchesne River Formation, 30.5 Ma. Units are pounds per square inch (psi). Although the Mahogany Zone is generating liquid hydrocarbons at this time, there is very limited area with overpressure. CI = 10 psi

despite the very large oil resource in-place. This is due to the very low permeability of the tight rocks that serve as the reservoirs. In a shale oil resource play these tight oil reservoirs are what are exploited by horizontal wells and hydraulic fracture stimulation. The universal characteristics of a shale oil resource play are (1) oil saturations in excess of irreducible and (2) formation pressures in excess of hydrostatic (0.43 psi/ft), but commonly approaching lithostatic (Jarvie, 2012). Otherwise, the plays, or even parts of the same play, can be quite distinct.

Although the actual source-rocks can yield commercial quantities of oil, as in the Eagle Ford play (Fig. 3-4), it is commonly the case that the productive reservoir intervals are interbedded within or are in proximity to the mature source rocks. This is the situation in the Bakken (Fig. 3-5) and Niobrara plays (Jarvie and others, 2011; Sonnenberg, 2011), where the target reservoirs for well completion are the organic matter-poor and slightly more porous carbonates and siliciclastics adjacent to the organic-rich source beds. The source rocks are commonly too tight to yield high oil rates and they retain the residual oil too tenaciously. These low-TOC reservoirs have high oil saturations compared to their organic carbon content, that is, high values of OSI. Additionally, they are characterized by low S1, S2 and HI values.

The Green River Formation in the Uinta Basin has many characteristics typical of an ideal shale oil resource play. It is a world-class oil-prone source rock. In nearly all parts of the basin there are many thousands of net feet of Type-I and Type-II kerogen-rich calcareous mudstones, many intervals which have average total organic carbon contents of 5–10%, or greater. In the north-central and western parts of the basin, a substantial part of the formation is currently in the oil-generative window. A large volume of the formation has reached “peak oil”. Furthermore, organic maturation simulations done in this study using PRA BasinView-3D™ (see Chapter 4) indicate early entry into the oil-generative window. In the northwest parts of the basin, the lower Green River Formation was generating oil even before the end of the Eocene and slowing of sediment accumulation in the basin. Anomalous formation pressures are observed in the Green River Formation across much of the basin. In the area of the greater Altamont-Bluebell field in the northwest of the basin, the abnormal pressures are nearly lithostatic (0.6 to 0.8 psi/ft). The Green River Formation is, unquestionably, a superb petroleum system responsible for very large cumulative production of conventional oil and associated natural gas, and an even larger unexploited, immobile, heavy-oil resource (Schamel, 2013). But that very fact may limit its prospects as a significant shale oil resource play.

The pattern of cyclical, climate-driven lacustrine deposition of the Green River Formation was such that porous siliciclastics and shoreline bioclastic carbonates extend across most of the basin, even into the basin depocenter in the north and northwest. These relatively porous strata, in part, served as effective carrier beds for oil generated in this kitchen area to

migrate laterally up dip to the south and east to charge the producing Green River oil fields (Monument Butte, Red Wash, among many others) and the vast oil sand deposits of the Tavaputs Plateau (Schamel, 2013). These oil accumulations are outside of the Green River oil-generative window. In contrast, oil production in the northwest quadrant (Altamont-Bluebell field and its southwest extensions) is from thick porous sandstone and carbonate (Uteland Butte) beds intercalated with thermally-mature source rocks.

The northwest depocenter of the Uinta Basin is where Green River open-lacustrine facies rocks dominate (Fig. 2-1), the formation is thickest (Fig. 2-13), the greatest part of the formation is in the oil generative window (Figs. 4-33 to 4-44), and the lower parts of the formation are overpressured (Figs. 3-32 and 3-33). Cores in this area have sandstone and porous carbonate lenses within the organic-rich calcareous mudstone that consistently are oil impregnated (Figs. 2-12 and 3-26). It is here that the Green River Formation has potential as a shale oil resource play, especially in intervals isolated from effective oil carrier systems.

A central element of this study is the basinwide modeling of thermal maturation carried out using BasinView-3D™ to create a grid of numerical simulations for synthetic wells with one kilometer spacing. Simulations were done for the northern two-thirds of the basin, the deeper and known petroleum generative area. The formation tops for generating the synthetic wells are derived from the contour map grids displayed in the structure maps in Chapter 2. The surfaces are constrained by a large number of wells up through the Mahogany Zone across the region modeled. However, the configuration of higher surfaces, partially eroded in the south, was reconstructed from a combination of well tops and surface projections, or by other means described in Chapter 4. The burial history model of the basin incorporated into the simulations has the following phases.

- Rapid sediment accumulation of the Green River, Uinta, and Duchesne River Formations during the Eocene, coincident with the Laramide uplift of the Uinta Mountains.
- A brief period of peneplanation in the early Oligocene (30.5 Ma) during which the Gilbert Peak geomorphic surface formed. This surface then was buried beneath a thin veneer of Bishop Conglomerate, laid down slowly until the early Miocene (20.3 Ma). There is no indication that the thick Oligocene-age volcanoclastic deposits found west of the Uinta Mountains ever reached the Uinta Basin.
- A long period (20.3 to 10.0 Ma) during which pediments covered the basin at the extreme northern extent of the southern segment of the Green River drainage and little sediment was added or removed.

- Exhumation of the basin began slowly at about 10.0 Ma, but then accelerated 500,000 years ago when the southern Green River segment captured its northern segment, thus dramatically lowering the local base level. Stream capture and greatly accelerated erosion rates are both likely tied to the onset of mountain glaciation in the region.

The Green River Formation was deposited rapidly in the early Eocene, buried under a thick succession of fluvial sediments (Uinta and Duchesne River Formations) by the end of the Eocene-early Oligocene, and then remained buried until the middle Pleistocene. The details of this scenario, with documentation, are presented in Chapter 2.

As described in Chapter 4, the numerical simulation of organic maturation is based on temperature history curves for a grid across the basin. These, in turn, are derived from the measured depths and known or estimated geologic ages of basin-wide stratigraphic markers, and from plausible heat-flow values at the time of basin infilling. At each grid node, the Arrhenius equation is used to calculate the rates of conversion of kerogen to bitumen, liquid hydrocarbons, and natural gas from the temperature history curves. The rates of conversion, in turn, are integrated into transformation ratios in space and time. The transformation ratio expresses the portion of initial kerogen converted to hydrocarbons (0.0 for no hydrocarbons to 1.0 for complete conversion of the kerogen, leaving only a pyrobitumen or graphite residue). BasinView-3D™ converts the transformation ratio to conventional measures of organic maturity, such as vitrinite reflectance equivalent or time-of-entry of a specific stratigraphic datum into a maturity threshold, “time-triggers” such as entry into the “peak-oil” window.

In order to visualize the variations in thermal maturation throughout the thick Green River Formation, simulations were run for three surfaces at the bottom, middle and top of the source-rock bearing part of the formation. These surfaces are: (1) the base of the lower Black Shale or Uteland Butte Limestone (55.3 Ma); (2) the base of the R-4 or the lower Green Shale interval (51.6 Ma); and (3) the top of the Mahogany Zone (48.9 Ma). In order to visualize the changes in thermal maturation of each of these three reference horizons over time, simulations were run for four times in the past: 1) 35.5 Ma, the end of basin infilling marked by the early Oligocene Gilbert Peak geomorphic surface; 2) 20.3 Ma, the end of Bishop Conglomerate deposition in the early Miocene; 3) 10.0 Ma, the estimated initial onset of basin exhumation; and 4) 0.0 Ma or the present-day. Thermal maturations were calculated for each of the three reference horizons at each of the four times in five different simulations run using different heat flow values and kerogen kinematics (see Table 4-3). The simulations are displayed either as times of entry into different thermal maturation windows, such as “early oil” or “peak oil” (Figures 4-21 through 4-32) or as equivalent vitrinite reflectance (R_o) values (Figures 4-33 through 4-44).

In general, the simulations indicate that in the area of the greater Altamont-Bluebell field, the lower Black Shale enters the “peak oil” window already by 40 Ma to 30 Ma. By present-day in the same area, the lower Black Shale has reached the “late oil” or early “wet gas” window. A similar pattern is observed for the lower Green Shale and the Mahogany Zone, only the maturation windows are slightly lower and the times of entry are slightly later, as would be expected. Generation of oil in the Green River source rocks is occurring close to or shortly following the end of sediment infilling of the Uinta Basin, and after that time there is only a slight increase in thermal maturation. Given that thermal maturation is a function of both time and temperature, the generation of hydrocarbons would have continued, albeit at slow rates, up into the Pleistocene and the onset of very rapid exhumation of the basin.

The active generation of hydrocarbons commonly is considered to be a cause of abnormal formation pressure (Spencer, 1987; Law and Spencer, 1998; Swarbrick and others, 2002). However, as noted by Osborne and Swarbrick (1997), it is the rapid generation and/or desorption of natural gas that is the more effective cause of large excess pressures. Furthermore, overpressures are inherently unstable and will dissipate unless continuously maintained. In the more thermally mature portions of the Uinta Basin, in particular the greater Altamont-Bluebell field (Fig. 3-33), late generation of natural gas by cracking of kerogen and residual oil, together with gas expansion due to rapid exhumation, may be the cause of the extremely high abnormal formation pressures observed in the lower Black Shale and underlying Wasatch Formation (Figure 3-32). If true, the overpressure is a recent and transient phenomenon related to sudden unroofing of a gas-charged petroleum system.

Lacustrine basins are ideal settings for the accumulation and preservation of organic matter, especially large volumes of hydrogen-rich kerogen, and Lake Uinta was no exception. The Green River Formation is widely recognized as a world-class source-rock succession for conventional oil and associated natural gas resources. Nevertheless, there is a general paucity of standard organic geochemical analyses of Green River source rocks in the public domain. For this study, there were only 15 wells for which programmed pyrolysis data were available from the literature and from UGS and USGS files (Table 3-1). However, from these 15 wells, nearly all with core samples, there were a total of 312 separate programmed pyrolysis analyses. Fortunately, 222 of the geochemical analyses from 9 cores (Table 5-1) in the western half of the basin had been run within the past five years by the same highly-reliable laboratory. The other analyses are more than a decade old and perhaps less reliable. Given that the cores are from all portions of the basin (Fig. 3-1) and sampled virtually all of the organic-rich portions of the Green River Formation, these analyses form a reliable basis for characterizing the source rocks.

There are two salient aspects of the organic geochemistry of the Green River Formation. The first relates to the wide range

Table 5-1: Summary of average values and standard deviations for selected geochemical parameters measured on Green River Formation core samples in the western part of the Uinta Basin. The values presented are for the data plotted in Figures 5-1 to 5-3. Township-Range is Salt Lake meridian.

Well name	T-R	TOC	HI	Tmax	OSI	OSI max	#	Depth range, ft
Chasel 1-81A1	1S-1W	1.2 ± 0.4	287.4 ± 37.6	439.1±5.5	86.5 ± 27.7	135	9	10639 - 10705
DR Long 2-19A1E	1S-1W	2.6 ± 1.6	381.5 ± 112.5	439.7 ± 3.2	80.0 ± 37.1	138	11	9163 - 9716
Olsen U1-12A2	1S-2W	1.9 ± 0.6	388.1 ± 54.3	440.8 ± 1.2	52.0 ± 14.9	90	8	10495 - 10603
Lamiq-Urrity 1-8A2	1S-2W	1.4 ± 0.3	412.6 ± 76.5	438.0 ± 2.7	42.3 ± 16.9	73	12	10833 - 10951
Virgil Mecham 1-11A2	1S-2W	2.0 ± 1.0	536.6 ± 115.2	438.7 ± 3.0	38.5 ± 10.6	57	15	10348 - 10634
Norling 1-9B1	2S-1W	8.4 ± 7.9	654.0 ± 254.2	442.6 ± 6.4	32.3 ± 76.5	277	18	7497 - 7618
16X-23D-36BTR	3S-6W	3.2 ± 1.0	377.0 ± 187.4	453.6 ± 7.7	46.4 ± 21.0	89	22	3887 - 5150
14X-22-46DLB	4S-6W	2.5 ± 2.6	215.4 ± 166.7	455.6 ± 4.6	79.7 ± 86.9	391	18	5480 - 5625
Marsing 16 BkSh	10S-8E	3.4 ± 4.9	440.8 ± 280.6	437.1 ± 4.5	46.9 ± 88.8	580	82	460 - 1165
Marsing GrSh	10S-8E	4.2 ± 4.6	599.4 ± 249.2	433.6 ± 5.5	50.5 ± 61.0	292	27	57 - 450

of kerogen types present within organic-carbon-rich mudstones in the formation (Fig. 3-1). These vary from humic and algal coals to exceptionally hydrogen-rich sapropel, each characteristic of a different part of the lake environment from shoreline to near-perennial lake center. Despite the range of kerogen types observed, cross-plots of total organic carbon (TOC) vs. genetic potential (GP) indicate that, on the whole, the rocks are good to excellent source rocks (Figures 3-10, 3-14, 3-20, and 3-24). Average TOC values for the nine cores in the western part of the basin are in the range 1.2 wt% to 8.4 wt% (Table 5-1), all in the good to excellent range (Peters and Cassa, 1994). Only a few of the samples analyzed would be classified as fair or poor. Furthermore, the kerogens generally are quite hydrogen-rich with average values of hydrogen index (HI) in the range 287 to 654 mg HC/g TOC, but with large standard deviations indicative of the variability in kerogen type (Table 5-1).

The second notable aspect of the geochemistry is the widespread cyclicality of geochemical properties (Figs. 3-11 and 3-16), particularly TOC and HI. The range of kerogen types is indicated in the large values of standard deviation associated with the average HI values (Table 5-1). Climatically driven rise and fall of Lake Uinta drove the expansion and contraction of the shoreline to lake center depositional settings that, in turn, determined the dominant kerogen types preserved. Indeed, it is this cyclicality, alternating organic-rich and organic-lean intervals, that is used as the basis for delineating Green River Formation stratigraphy in the central portions of the basin (Vanden Berg, 2008).

Given the paucity of measured vitrinite reflectance (R_o) values for the Green River Formation, Tmax from programmed pyrolysis is the only widely available indicator of thermal maturity. Tmax values for cores in the western half of the basin are in the “early oil” and “peak oil” maturity windows (Fig. 3-27) as delimited by Peters and Cassa (1994). Just a few samples fall into the “late oil” field. Average Tmax values for the cores, other than Marsing 16, are in the range 486°C to 456°C (Table 5-1). The Green and Black Shale intervals in Marsing

16 with average values of 434°C and 437°C, respectively, are at the threshold into the “early oil” generative window. Tmax values from cuttings reported by Anders and Gerrild (1984) from the greater Altamont-Bluebell area (Fig. 3-3) are in the same range as the more recent analyses from cores: Dustin 1 (451°C), Cedar Rim 3 (451°C), and Ute Tribal 1-6 (453°C).

In Figure 3-27, we observe a curious, counterintuitive inversion of Tmax values in that the shallower samples (higher elevations) are the more mature, whereas the deeper samples are less mature. It is significant that the wells with the shallower and more mature Tmax values are in the southwest portion of the basin close to the Book Cliffs. What we are seeing is evidence for northward tilting of the Green River section following the imprint of maximum thermal maturity. Given that generation of hydrocarbons is simulated to have continued into the late Pliocene-Pleistocene, this tilting and erosional stripping of the southwest corner of the basin presumably is very recent. One plausible explanation for this northward tilt is isostatic rebound of the entire northern portion of the Colorado Plateau, including the San Rafael Swell and the present south rim of the Uinta Basin, due to exhumation of all or large parts of the thick Mesozoic section once burying the area south of the Uinta Basin.

The thermal maturity indicated from Tmax values is lower than that predicted from the thermal maturation simulations presented in Chapter 4 and discussed above. It is possible that the heat flow value of 52 mW/m² used for the simulations was unrealistically high, even though it represented the low end of present-day measured heat flow in the Uinta Basin. A lower paleo-heat flow for the rapidly filling sedimentary basin is plausible, as would be a higher value during the present. Recent, rapid erosional unroofing of the basin would result in a temporarily distorted thermal profile that would yield a higher-than-historic heat flow value.

Alternatively, the Tmax value thresholds for the thermal maturation windows from Peters and Cassa (1994) might not be relevant for the lacustrine source rocks of the Green River

Formation. For instance, it has been shown that the onset of oil generation for the hydrogen-rich (Type I-II) Bakken Shale is reached at T_{max} of 425°C, and that by 450°C, the source rock is passing into the wet gas generative window (Jin and Sonnenberg, 2012). The onset of oil generation in the marine Type 2-S Monterey Shale kerogen is at even lower maturities, T_{max} in the 410° to 425° range (Jarvie, 2012). However, as discussed in Chapter 3, the reaction kinetics for the Green River hydrogen-rich (Type I) source rocks may be such that the onset of oil generation is delayed to about 0.75% R_o (Ruble and others, 2001; Lewan and Roy, 2010). The peak of oil generation would be at the equivalent of about 1.0 R_o and oil and gas generation would occur together over a relatively narrow generative window. A separate gas generative window, if even relevant in the Green River organic-rich mudstones, would have been reached only in the very deepest parts of the Uinta Basin, if at all. If, indeed, Green River Type I kerogens have a delayed entry into the oil generative window, then the maturity windows would be expected to shift towards higher T_{max} thresholds, not lower ones.

When the thermal maturity of a Type I or Type II kerogen increases, the HI decreases. As oil is generated, hydrogen is concentrated in the hydrocarbon phase, which generally is expelled from the source rock, thus depleting its hydrogen. The decrease in HI tracks the increase in transformation ratio to the point where the remaining kerogen and any residual oil cracks into natural gas. Low HI values are associated with the gas generative window. This is reflected in the maturity trajectories commonly shown in Van Krevelen plots (Fig. 3-1) for the different kerogen types. A cross plot of T_{max} vs. HI is a convenient tool for examining the decline in HI with increasing source rock maturation. However, such a plot for the 222 core analysis in the western basin (Fig. 5-1) fails to demonstrate any obvious decrease in HI with increasing thermal maturity, as measured by T_{max} . There is a very large scatter in HI values. The very high HI values in the “early mature” window are from cores (Marsing 16 and Norling 1-9B1) that have generated at least some petroleum.

As discussed in Chapter 3, very few samples of Green River core have OSI values greater than the 80–100 range, the empirical threshold for oil to be readily expelled from the source rock (Jarvie, 2012). At lower OSI values, liquid hydrocarbon is retained in the rock, largely by sorption to kerogen or trapped behind nanno-pore throats. However, a majority of the core samples have OSI values that fall just below this threshold (Fig. 5-2). The average OSI for the cores in Table 5-1 range from 32 to 86, but with large standard deviations. This observation raises the interesting possibility that during programmed pyrolysis runs this residual oil is advancing the appearance of the S2 peak, thereby resulting in a lower than expected T_{max} value. The “bound oil” is not expelled as “free oil” at lower temperatures to form the S1 peak, but it could be released during kerogen pyrolysis that forms the S2 peak. Such “bound oil” could also result in a larger S2 peak and thereby a larger HI value than what would be generated

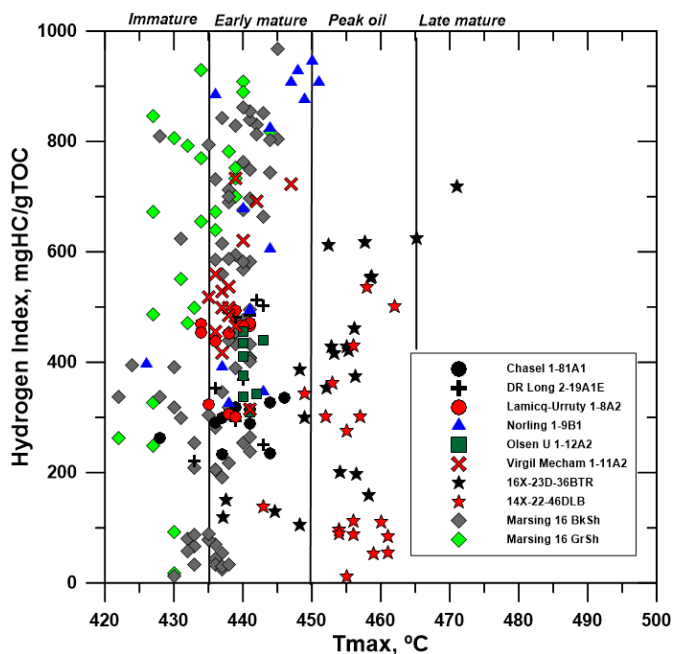


Figure 5-1: Programmed pyrolysis T_{max} values plotted against hydrogen index for core samples of Green River Formation source rocks in the western Uinta Basin. The vertical lines are thermal maturity thresholds for T_{max} values reported in Peters and Cassa (1994).

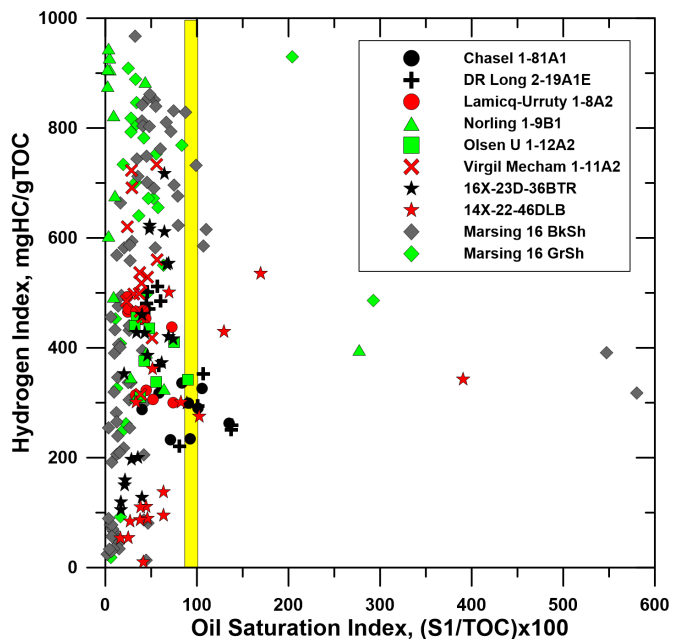


Figure 5-2: Programmed pyrolysis oil saturation index (OSI) values plotted against hydrogen index for core samples of Green River Formation source rocks in the western Uinta Basin. The vertical yellow bar is the empirical threshold for retention of oil in tight source rocks (Jarvie, 2012). Higher OSI values are one of the key characteristics of productive shale oil plays.

by the kerogen alone. If so, this could also account for the anomalously low Production Index (PI) readings, less than 0.1, for many of the Green River core samples (Fig. 5-3). HI derived from programmed pyrolysis is $(S_2/TOC) \times 100$; $PI = S_1/(S_1 + S_2)$. Larger S_2 values increase HI, but decrease PI. Jin and Sonnenberg (2012) also report substantial quantities of residual oil in the organic-rich mudstones of the Bakken Shale. In the absence of an independent measure of thermal maturity, such as vitrinite reflectance, this explanation for slightly lower than expected T_{max} thermal maturities remains a “working hypothesis”. However, it is possible that due to the presence of “bound oil”, T_{max} values of 425° and 450°C approximate the actual limits for the oil generative window in the Green River Formation. This would be more consistent with the known petroleum characteristics of the formation and the thermal maturation simulations using the heat flow value of 52 mW/m².

A very important observation derived from the programmed pyrolysis data (Fig. 5-2 and Table 5-1) is that the Green River organic-rich mudstones have OSI values that are too low to make them candidates for a self-sourcing shale oil reservoir. What oil they contain is “bound oil”, not free to migrate readily from rock to well, even when the rock is fracture stimulated. As discussed in Chapter 3, the few high values of OSI (Table 5-1) are likely associated with thin, relatively porous, commonly-fractured, oil-impregnated interbeds within the source rock intervals, as shown in Figures 3-17 and 3-26. These more porous, permeable and brittle beds are the potentially productive oil reservoirs.

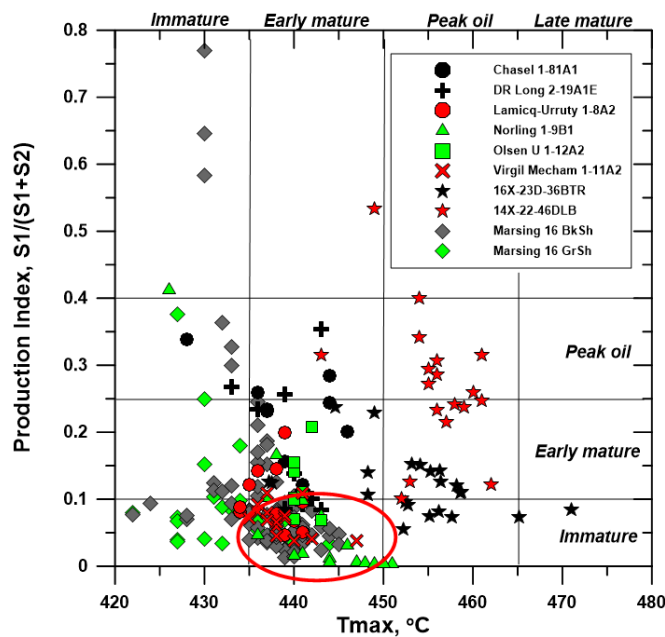


Figure 5-3: Programmed pyrolysis T_{max} values plotted against production index (PI) for core samples of Green River Formation source rocks in the western Uinta Basin. The vertical and horizontal lines are thermal maturity thresholds for T_{max} and PI values, respectively, as reported in Peters and Cassa (1994). The red ellipse highlights the cluster of anomalously low PI values.

Typically, shale oil resource plays are discovered by drilling and appropriate well completions, not through the study of cores. The scientific investigations follow production and serve the purpose of targeting “sweet spots” and enhancing recovery. This is likely to be the situation with the Green River Formation in the Uinta Basin as well. Within and along the margins of the greater Altamont-Bluebell field, several operators have been finding success with intensive hydraulic fracture completions and have begun to exploit specific reservoir targets with horizontal wells, even within what can be regarded as “source rock” intervals. If the formation responds in a way that would be expected of a typical shale oil resource play, for all intents and purposes, it is one.

The Cedar Rim and Altamont fields (Fig. 5-4) were delineated in 1969 and 1970; the Bluebell field is just a decade older. Only a few years later, Lucas and Drexler (1973) identified the Altamont-Bluebell field as an “oil accumulation near the center of a deep basin”, an example of a then newly-recognized “group of deep-basin, organic-shale-related, overpressured accumulations” having significant hydrocarbon potential. They attribute to the Altamont-Bluebell field characteristics that subsequently have come to identify a basin-centered, continuous resource play. These include:

- difficulty in defining field limits laterally and vertically because the trap is stratigraphic with no simple down-dip water levels or facies boundaries to the productive horizons,
- multiple thin productive zones with abnormally high fluid pressures, and
- very low matrix porosities enhanced by post-lithification fractures.

The initial development of the Altamont-Bluebell field was by vertical wells targeting sandstone lenses encased in red mudstone in the Wasatch Formation and lacustrine carbonate and sandstone beds intercalated with organic-rich dark mudstone in the lower Green River Formation. On 320 acre spacing, wells were completed by perforating target horizons and using light acid treatments to stimulate flow. Typically, 12 to 35 Wasatch and 10 to 20 Green River intervals, each 3 to 30 feet thick, were perforated in a section totaling 1800 to 3000 feet thick (Smouse, 1993). The reservoir targets have low porosity, averaging 10%, very low permeability, and required natural fractures for both storage and good deliverability. The wells produced a medium to light high-wax oil and large quantities of associated natural gas comingled from the many completed intervals. Solution gas drive was aided by the abnormally high initial formation pressures. Regardless of the number of zones perforated and acid treated in each well, production tests indicated that generally fewer than 10 beds actually produce (Montgomery and Morgan, 1998). The Cedar Rim field has the same naturally-fractured Wasatch and lower Green River reservoirs and general characteristics as the western Altamont field, but production is shallower and the GORs are

higher, up to 13,000 (Eckels, 1993). In the greater Altamont-Bluebell district, all wells drilled through the lower Green River Formation and into the overpressured interval were producers (Smouse, 1993). However, within a decade or two, the fields were in decline and had been abandoned by their initial operators.

Over the past decade, several mid-size independent petroleum companies, new players in the Uinta Basin, have rediscovered the Green River-Wasatch continuous oil play. They have entered the basin armed with new technologies, massive slick-water fracture stimulation and horizontal drilling. In the four years beginning 2010, the year this study was first proposed, there has been a boom in oil and associated gas development within and along the southern margins of the Altamont-

Bluebell fields (Fig. 5-4). Most, but certainly not all, of the new activity has been focused in the region of anomalous formation pressure in the range of 0.5 to 0.7 psi/ft. Activity has been most intense in two new fields, Lake Canyon, established in 2006, and North Myton Bench, formed in 2009. In this period (through September 2013), a total of 617 new wells have either gone into production (231 wells), been spudded (64 wells), or have been approved (322 wells). The result has been a dramatic increase in oil and associated natural gas production (Table 5-2). The greater Altamont-Bluebell fields have had a 154% increase in oil production. The North Myton Bench field has grown from no production in 2009 to over 2.1 million barrels in just four years. In just five years, there was more than a thousand-fold increase in the Lake Canyon field. In large measure, the increase in production has made

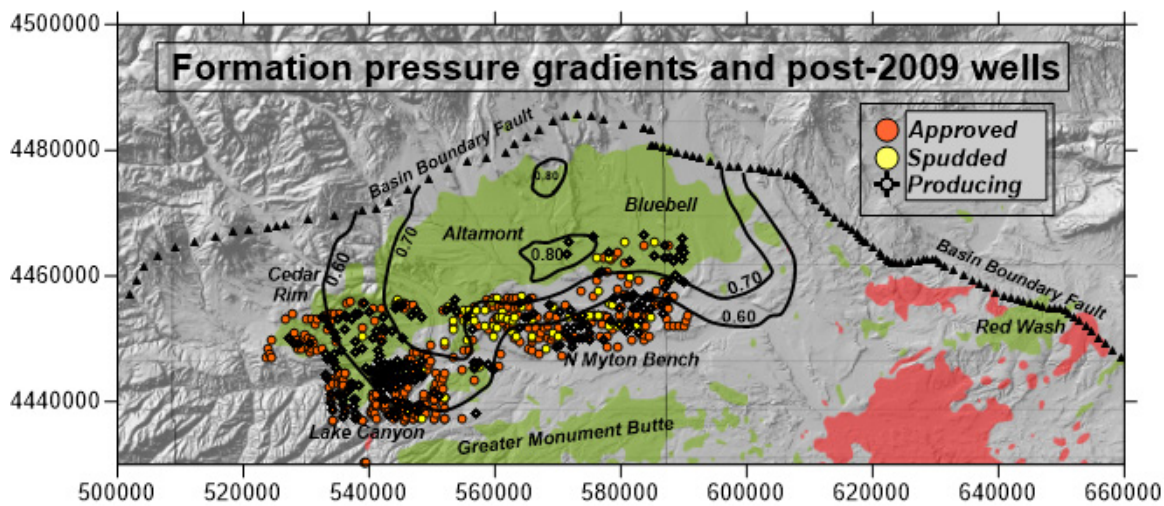


Figure 5-4: Distribution of wells that were brought into production, spudded or approved in the period 2010 through mid-2013 in 12 townships along the south and southwest margin of the overpressured greater Altamont-Bluebell field. The new wells shown are mainly in the North Myton Bench, the Lake Canyon, and the Blacktail Ridge portion of the Cedar Rim fields. The overpressure isopleths (psi/ft) are from Lucas and Drexler (1973) and the well locations and status as of June 2013 are from Utah DOGM. The geographic coordinates are meters in UTM NAD83, Zone 12.

Table 5-2: Contrasting annual oil production 2009 to 2013 for the group of fields within the region of elevated formation pressures (greater Altamont-Bluebell) and those to the south (greater Monument Butte) that produce from essentially the same general Green River–Wasatch reservoirs. The 2013 natural gas production as barrels-of-oil equivalent (BOe) show the relative contributions of gas in the two groups of fields. Data from Utah DOGM.

Field	2013	2009	%diff	Gas: 2013 BOe	O+G: 2013 BOe	%gas
Altamont	4,297,355	1,707,755	151.6	2,133,867	6,431,222	33.2
Bluebell	3,038,643	2,216,758	37.1	803,978	3,842,621	20.9
Cedar Rim	419,331	113,779	268.5	238,932	658,263	36.3
Lake Canyon	482,574	30,303	1492.5	311,277	793,851	39.2
N Myton Bench	2,101,854	0		450,896	2,552,750	17.7
Total	10,339,757	4,068,595	154.1	3,938,951	14,278,708	27.6
Monument Butte	5,078,350	4,647,015	9.3	1,365,650	6,444,000	21.2
Brundage Canyon	1,501,768	1,155,487	30	1,806,471	3,308,239	54.6
Antelope Creek	682,449	180,993	277.1	143,940	826,389	17.4
S Myton Bench	185,825	54,461	241.2	575,954	761,779	75.6
Total	7,448,392	6,037,956	23.4	3,892,015	11,340,407	34.3

possible by the expansion in the number of drill sites occupied due to progressive down-spacing from 320 acre to 160 acre and, more recently, to 80 acre. These fields also produce substantial quantities of natural gas. In 2013, on a barrels-of-oil equivalence (BOe), natural gas contributed over a quarter of the production from the greater Altamont-Bluebell fields and a third of the production from the greater Monument Butte fields (Table 5-2).

Fracture stimulation completions are being made in fewer, more carefully selected, intervals than were perforated in the older wells. Still, the new wells are being completed in many of the same multiple zones within the Green River and Wasatch Formations. For instance, the vertical Bar F 1-20-3-2 well (API 4301350009) in the North Myton Bench field was completed with six fracture stimulation stages, two in Wasatch sandstone intervals, two in the Uteland Butte limestone-sandstone, and two in the Castle Peak limestone-sandstone (source: DOGM well file). The geologic report for the Evans 1-4-3-3 well (API 4301350561), also in the North Myton Bench field, identifies multiple fractured “oil shale” oil shows on the order of many tens of feet thickness in the Middle and Lower Green River Members, shows in the Bar F Sandstone (15 ft of pay, 13% porosity) and Uteland Butte beds (19 ft of pay, 14% porosity) in the Lower Green River Member, and 65 ft of net pay (13% porosity) in Wasatch sandstones. The pay zones were identified from logs and resistivity values greater than 40 ohms. As in the past, the porous and brittle Uteland Butte carbonate-siliciclastic interval at the base of the Green River Formation is a favored reservoir target for both vertical and horizontal well completions (Vanden Berg and others, 2013).

Virtually all of the recent vertical wells are completed in both the lower Green River Formation, generally the Uteland Butte member and a few other relatively porous and/or brittle intervals, and the underlying Wasatch sandstones. The presence of overpressured reservoir targets appears to be a requisite for locating and designing the well. All wells are fracture stimulated, normally with multistage, large slickwater treatments, but after a year or so of natural flow, the wells must be put on artificial lift production of oil and associated natural gas from all intervals is comingled, making it impossible to associate production with specific completed intervals. It is observed that within one to three years, a well’s production rates drop off by an order of magnitude or more. The decline curves are hyperbolic, as would be expected of fractured, but otherwise tight, reservoir intervals. The decline curves for the recent, fracture-stimulated wells are similar to the older, pre-2000 wells, at least as far as can be observed in the shorter time of record (source: randomly selected DOGM records for groups of wells listed in Digital Appendix D). Production characteristics are similar by other measures, as well. For instance, the gas-oil ratios (GOR) and water-oil ratios (WOR) of the older and younger group of wells are indistinguishable (Fig. 5-5). The very recent horizontal wells may, in time, display different declines, but after two years of production, for instance, the 14-3-45 BTR well (API 4301350676) cited by Vanden Berg and others (2013) has seen an order of magnitude decrease in both oil and gas rates, similar to the recent vertical wells.

As more of the shale oil plays receive close scrutiny, it is becoming clear that no two are the same with regards to character of source rock or reservoir. What they all have in common,

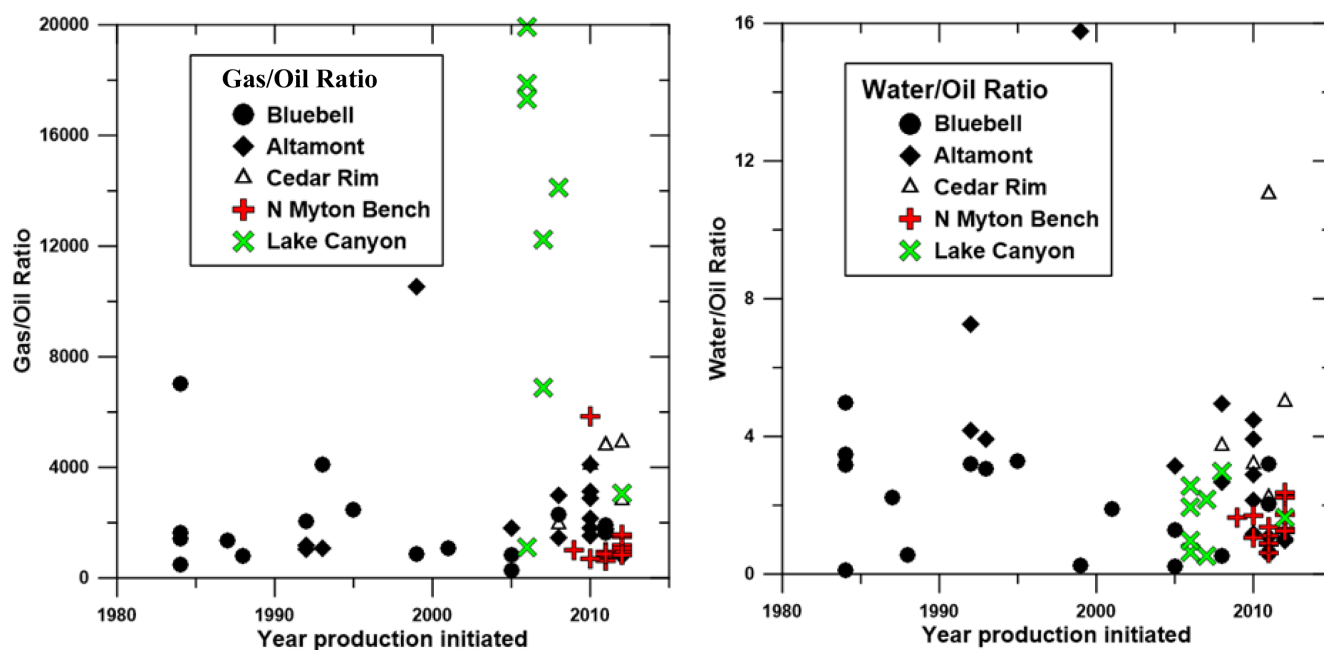


Figure 5-5: Gas/oil and water/oil ratios for representative production wells drilled over a 30-year period of time from 1984 to 2013. The cumulative ratios through mid-2013 are plotted against the year that production was initiated. The very high gas/oil ratios observed in the Lake Canyon field are also reflected in the very high portion of total production from this field that is natural gas (see Table 5-2). Data is from Utah DOGM; see Digital Appendix D for the data for specific wells.

however, is (1) an unusually organic-carbon-rich source rock capable of generating large volumes of oil, (2) interbedded or proximal reservoir intervals that, although tight, have sufficient porosity and/or natural fractures to be capable of hosting commercially significant volumes of the producible oil, and (3) inefficient carrier systems resulting in the oil generated remaining in proximity to the oil-generative source rock. The presence of anomalous formation pressures appears necessary to drive the oil from reservoir to well bore, even when fracture stimulated. These are “self-sourcing” petroleum systems only when viewed on a scale that encompasses the entire source rock formation and its immediately adjacent strata, or a significant portion thereof. And so it is with the Green River Formation, which has both an internal “self-sourcing” continuous oil play within the oil generative window and conventional oil accumulations on its periphery. Due to the lenticular character of the sandstone and carbonate beds in the Green River Formation and the underlying Wasatch Formation, some beds trap oil locally, while others carry the oil up-dip into traps at a distance from the oil generative window.

In the short-run, at least, the success of the newly rediscovered Green River continuous oil play may be due more to down-spacing to a higher density of wells than to the application of new well completion technologies, such as fracture stimulation and horizontal drilling. As has been observed in other “shale oil” plays with wells having similar hyperbolic declines, such as the Eagle Ford and Bakken, the pace of drilling activity must be maintained in order to support high overall field production. It remains to be seen if the application of the new technologies results in higher ultimate recoveries per well than has been observed in the first group of vertical wells drilled in the Altamont-Bluebell field over three decades ago. It could be that fracture stimulated horizontal wells are necessary to compensate for the lower anomalous formation pressures along the outer margins of the Green River shale oil play.

ACKNOWLEDGMENTS

This study received generous matching funds from the Utah Geological Survey’s *Characterization of Utah’s Hydrocarbon Reservoirs, Metals, and Industrial Minerals* – FY 2012 solicitation. Michael Vanden Berg was the Survey’s contract manager for the project.

Many persons aided the study with valuable advice and data: Jim Borer (Cimarex Energy), Marc Eckels (Wind River Resources), Dan Jarvie (Texas Christian University), Michael Lewan (U.S. Geological Survey), Tim Ruble (Weatherford), Doug Sprinkel (Utah Geological Survey), Michael Vanden Berg (Utah Geological Survey), and Stephen Wells (El Paso E&P).

Special gratitude is expressed to Dr. Jay Leonard, President of Platte River Associates for the temporary loan of licenses for BasinMod-1D and BasinView-3D to use for simulating

the thermal maturity of the Green River Formation. Access to these powerful analytical tools greatly enhanced the project. Nancy Hunter and Michelle Hayhurst, both with Platte River Resources, provided essential technical and logistic support during the basin modeling phase of the study.

REFERENCES

- Anders, D.E., and Gerrild, P.M., 1984, Hydrocarbon generation in lacustrine rocks of Tertiary age, Uinta Basin, Utah—Organic carbon, pyrolysis yield, and light hydrocarbons, *in* Woodward, J., Meissner, F.F., and Clayton, J.L., editors, Hydrocarbon Source Rocks of the Greater Rocky Mountain Region: Rocky Mountain Association of Geologists, p. 513–529.
- Anders, D.E., Palacas, J.G., and Johnson, R.C., 1992, Thermal maturity of rocks and hydrocarbon deposits, Uinta Basin, Utah, *in* Fouch, T.D., Nuccio, V.F., and Chidsey, T.C., Jr., editors, Hydrocarbon and Mineral Resources of the Uinta Basin, Utah and Colorado: Utah Geological Association 1992 Field Symposium, p. 53–76.
- Bergeneheier, L.P., and Vanden Berg, M.D., 2011, Core-based integrated sedimentologic, stratigraphic, and geochemical analysis of the oil shale bearing Green River Formation, Uinta Basin, Utah: U.S. Department of Energy National Energy Technology Laboratory, Document DE-FE0001243, p. 19.
- Berggren, W.A., and Prothero, D.R., 1992, Eocene-Oligocene climatic and biotic evolution—an overview, *in* Prothero, D.R., and Berggren, W.A., editors, Eocene-Oligocene Climatic and Biotic Evolution: Princeton University Press, p. 1–28.
- Bohacs, K.M., Carroll, A.R., and Neal, J.E., 2003, Lessons from large lake systems—thresholds, nonlinearity, and strange attractors, *in* Chan, M.A., and Archer, A.W., editors, Extreme Depositional Environments: Mega End Members in Geologic Time: Geological Society of America Special Paper 370, p. 75–90.
- Bredenhoeft, J.D., Wesley, J.B., and Fouch, T.D., 1994, Simulation of the origin of fluid pressure, fracture generation, and the movement of fluids in the Uinta basin, Utah: American Association of Petroleum Geologists Bulletin, v. 78, p. 1729–1747.
- Bryant, B., 2010, Geologic map of the east half of the Salt Lake City 1° x 2° quadrangle (Duchesne and Kings Peak 30' x 60' quadrangles), Duchesne, Summit, and Wasatch Counties, Utah, and Uinta County, Wyoming (1:125,000): Utah Geological Survey Miscellaneous Publication 10-1DM, 2 sheets.
- Carroll, A.R., and Bohacs, K.M., 2001, Lake-type controls on petroleum source rock potential in nonmarine basins: American Association of Petroleum Geologists Bulletin,

- v. 85, p. 1033–1053.
- Carroll, A.R., and Wartes, M.A., 2003, Organic carbon burial by large Permian lakes, northwest China, *in* Chan, M.A., and Archer, A.W., editors, *Extreme Depositional Environments: Mega End Members in Geologic Time*: Geological Society of America Special Paper 370, p. 91–104.
- Castle, J.W., 1990, Sedimentation in Eocene Lake Uinta (lower Green River Formation), northeastern Uinta Basin, Utah, *in* Katz, B.J., editor, *Lacustrine Basin Exploration—Case Studies and Modern Analogues*: American Association of Petroleum Geologists Memoir 50, p. 243–263.
- Chapman, D.S., Keoh, T.H., Bauer, M.S., and Picard, M.D., 1984, Heat flow in the Uinta Basin determined from bottom hole temperature (BHT) data: *Geophysics*, v. 49, p. 453–466.
- Dean, W.E., and Anders, D.E., 1991, Effects of source, depositional environment, and diagenesis on characteristics of organic matter in oil shale from the Green River Formation, Wyoming, Utah, and Colorado, *in* Tuttle, M.L., editor, *Geochemical, Biogeochemical, and Sedimentological Studies of the Green River Formation, Wyoming, Utah, and Colorado*: U. S. Geological Survey Bulletin 1973, p. F1–F16.
- Dubiel, R.F., 2003, Geology, depositional models, and oil and gas assessment of the Green River Total Petroleum System, Uinta-Piceance Province, eastern Utah and western Colorado, *Petroleum Systems and Geologic Assessment of Oil and Gas in the Uinta-Piceance Province, Utah and Colorado*: U.S. Geological Survey Digital Data Series DDS-69-B, Chapter 5, p. 1–41.
- Eckels, M.T., Cedar Rim, 1993, *in* Hill, B.G., and Bereskin, S.R., editors, *Oil and Gas Fields of Utah*: Utah Geological Association, Salt Lake City, Utah, unpaginated.
- England, W.A., 1994, Secondary migration and accumulation of hydrocarbons, *in* Magoon, L.B., and Dow, W.G., editors, *The Petroleum System—from Source to Trap*: American Association of Petroleum Geologists Memoir 60, p. 211–217.
- Fleet, A.J., Kelts, K.R., and Talbot, M.R., 1988, *Lacustrine Petroleum Source Rocks*: Geological Society of London Special Publication 40, 391 p.
- Fouch, T.D., Nuccio, V.F., Anders, D.E., Rice, D.D., Pitman, J.K., and Mast, R.F., 1994, Green River (!) petroleum system, Uinta Basin, Utah, U.S.A. *in* Magoon, L.B., and Dow, W.G., editors, *The Petroleum System—from Source to Trap*: American Association of Petroleum Geologists Memoir 60, p. 399–421.
- Fouch, T.D., Nuccio, V.F., Osmond, J.C., MacMillan, L., Cashion, W.B., and Wandrey, C.J., 1992, Oil and gas in uppermost Cretaceous and Tertiary rock, Uinta Basin, Utah, *in* Fouch, T.D., Nuccio, V.F., and Chidsey, T.C., Jr., editors, *Hydrocarbon and Mineral Resources of the Uinta Basin, Utah and Colorado*: Utah Geological Association 1992 Field Symposium, p. 9–47.
- Franczyk, K.J., Fouch, T.D., Johnson, R.C., Molenaar, C.M., and Cobban, W.A., 1992, Cretaceous and Tertiary paleogeographic reconstructions for the Uinta-Piceance basin study area, Colorado and Utah, *Evolution of Sedimentary Basins—Uinta and Piceance Basins*: U.S. Geological Survey Bulletin 1787, p. Q1–Q37.
- Hansen, W.R., 1986, Neogene tectonics and geomorphology of the eastern Uinta Mountains in Utah, Colorado, and Wyoming: U.S. Geological Survey Professional Paper 1356, 78 p.
- Jarvie, D.M., 2012, Shale resource systems for oil and gas: Part 2—Shale-oil resource systems, *in* Breyer, J.A., editor, *Shale reservoirs—Giant resources for the 21st century*: American Association of Petroleum Geologists Memoir 97, p. 89–119.
- Jarvie, D.M., Coskey, R.J., Johnson, M.S., and Leonard, J.E., 2011, The geology and geochemistry of the Parshall area, Mountrail County, North Dakota, *in* Robinson, J.W., LeFever, J.A., and Gaswirth, S.B., editors, *Bakken-Three Forks Petroleum System in the Williston Basin*: Rocky Mountain Association of Geologists, p. 229–281.
- Jin, H., and Sonnenberg, S.A., 2012, Source rock potential of the Bakken Shales in the Williston Basin, North Dakota and Montana: American Association of Petroleum Geologists Annual Convention and Exhibition, Long Beach, CA, April 22–25, 2012, www.searchanddiscovery.com/documents/2012/20156jin/nix_jin.pdf.
- Johnson, R.C., 2003, Northwest to southeast cross section of Cretaceous and Lower Tertiary rocks across the eastern part of the Uinta Basin, Utah, *Petroleum Systems and Geologic Assessment of Oil and Gas in the Uinta-Piceance Province, Utah and Colorado*: U. S. Geological Survey Digital Data Series DDS-69-B, Chapter 11, p. 1–6.
- Johnson, R.C., and Roberts, L.N.R., 2003, Depths to selected stratigraphic horizons in oil and gas wells for Upper Cretaceous and Lower Tertiary strata of the Uinta basin, Utah, *Petroleum Systems and Geologic Assessment of Oil and Gas in the Uinta-Piceance Province, Utah and Colorado*: U. S. Geological Survey Digital Data Series DDS-69-B, Chapter 13, p. 1–30.
- Katz, B.J., 1990, *Lacustrine Basin Exploration*: American Association of Petroleum Geologists Memoir 50, 340 p.
- Katz, B. J., 1995, The Green River Shale: an Eocene carbonate lacustrine source rock, *in* Katz, B.J., editor, *Petroleum Source Rocks*: Berlin, Springer Verlag, p. 309–324.
- Keighley, D.G., and Flint, S.S., 2008, Fluvial sandbody geometry and connectivity in the middle Green River Formation, Nine Mile Canyon, southwestern Uinta basin, *in* Longman, M.W., and Morgan, C.D., editors, *Hydrocarbon Systems and Production in the Uinta Basin, Utah*: Rocky Mountain Association of Geologists – Utah Geological Association Publication 37, p. 101–119.
- Keighley, D., Flint, S., Howell, J., Andersson, D., Collins, S., Moscariello, A., and Stone, G., 2002, Surface and subsur-

- face correlation of the Green River Formation in central Nine Mile Canyon, SW Uinta Basin, Carbon and Duchesne Counties, east-central Utah: Utah Geological Survey Miscellaneous Publication 02-1, unpaginated.
- Kelso, B.S., and Eherenzeller, J.L., 2008, Petroleum geology of the Brundage Canyon oil field, Southern Tertiary Oil Trend, Uinta basin, *in* Longman, M.W., and Morgan, C. D., editors, Hydrocarbon Systems and Production in the Uinta Basin, Utah: Rocky Mountain Association of Geologists – Utah Geological Association Publication 37, p. 283–302.
- Kowallis, B.J., Christiansen, E.H., Balls, E., Heizler, M.T., and Sprinkel, D.A., 2005, The Bishop Conglomerate Ash Beds, south flank of the Uinta Mountains, Utah—Are they pyroclastic fall beds from the Oligocene ignimbrites of western Utah and eastern Nevada?, *in* Dehler, C.M., Pederson, J.L., Sprinkel, D.A., and Kowallis, B.J., editors, Uinta Mountain Geology: Utah Geological Association Publication 33, p. 131–145.
- Law, B.E., and Spencer, C.W., 1998, Abnormal pressure in hydrocarbon environments, *in* Law, B.E., Ulmshek, G.F., and Slavin, V.I., editors, Abnormal Pressures in Hydrocarbon Environments: American Association of Petroleum Geologists Memoir 70, p. 1–11.
- Lewan, M.D., and Roy, S., 2010, Role of water in hydrocarbon generation from Type-I kerogen in Mahogany oil shale of the Green River Formation: Organic Geochemistry, v. 42, p. 31–41.
- Lillis, P.G., Warden, A., and King, J.D., 2003, Petroleum systems of the Uinta and Piceance basins—Geochemical characteristics of oil types, Petroleum Systems and Geologic Assessment of Oil and Gas in the Uinta-Piceance Province, Utah and Colorado: U. S. Geological Survey Digital Data Series DDS-69-B, Chapter 3, p. 1–25.
- Lucas, P.T., and Drexler, J.M., 1975, Altamont-Bluebell—A major fractured and overpressured stratigraphic trap, Uinta Basin, Utah, *in* Bolyard, D.W., editor, Symposium on Deep Drilling Frontiers in the Central Rocky Mountains: Rocky Mountain Association of Geologists, p. 265–273.
- Mann, U., 1994, An integrated approach to the study of primary petroleum migration, *in* Parnell, J., editor, Geofluids: Origin, Migration and Evolution of Fluids in Sedimentary Basins: Geological Society of London Special Publication 78, p. 233–260.
- Montgomery, S.L., and Morgan, C.D., 1998, Bluebell field, Uinta Basin—reservoir characterization for improved well completion and oil recovery: American Association of Petroleum Geologists Bulletin, v. 82, p. 1113–1132.
- Morgan, C.D., 2003, The Bluebell Oil Field, Uinta Basin, Duchesne and Uintah Counties, Utah: Characterization and Oil Well Demonstration: Utah Geological Survey Special Study 106, 95 p.
- Morgan, C.D., 2008, Greater Monument Butte oil field: Infill drilling results and potential CO₂ enhanced oil recovery, *in* Longman, M.W., and Morgan, C.D., editors, Hydrocarbon Systems and Production in the Uinta Basin, Utah: Rocky Mountain Association of Geologists – Utah Geological Association Publication 37, p. 303–318.
- Morgan, C.D., Chidsey, T.C., Jr., McClure, K.P., Bereskin, S.R., and Deo, M.D., 2003, Reservoir characterization of the Lower Green River Formation, Uinta Basin, Utah: Utah Geological Survey Open-File Report 411, 140 p.
- Murphey, P.C., Townsend, K.E.B., Friscia, A.R., and Evanoff, E., 2011, Paleontology and stratigraphy of middle Eocene rock units in the Bridger and Uinta Basins, Wyoming and Utah, *in* Lee, J., and Evans, J.P., editors, Geologic Field Trips to the Basin and Range, Rocky Mountains, Snake River Plain, and Terranes of the U.S. Cordillera: Geological Society of America Field Guide 21, p. 125–166.
- Nelson, P.H., 2002, Subsurface fluid pressures from drill-stem tests, Uinta basin, Utah: The Mountain Geologist, v. 39, p. 17–26.
- Nelson, P.H., 2003, Subsurface pressures from drill-stem tests, Uinta and Piceance Basins, Utah and Colorado, Petroleum Systems and Geologic Assessment of Oil and Gas in the Uinta-Piceance Province, Utah and Colorado: U.S. Geological Survey Digital Data Series DDS-69-B, Chapter 14, p. 1–32.
- Noble, R.A., Kaldo, J.G., and Atkinson, C.D., 1997, Oil saturation in shales—Applications in seal evaluation, *in* Surdam, R.C., editor, Seals, Traps, and the Petroleum System: American Association of Petroleum Geologists Memoir 67, p. 13–29.
- Nuccio, V.F., and Roberts, L.N.R., 2003, Thermal maturity and oil and gas generation history of petroleum systems in the Uinta-Piceance Province, Utah and Colorado, Petroleum Systems and Geologic Assessment of Oil and Gas in the Uinta-Piceance Province, Utah and Colorado: U. S. Geological Survey Digital Data Series DDS-69-B, Chapter 4, p. 1–35.
- Nuccio, V.F., Schmoker, J.W., and Fouch, T.D., 1992, Thermal maturity, porosity, and lithofacies relationships applied to gas generation and production in Cretaceous and Tertiary low-permeability (tight) sandstone, Uinta basin, Utah, *in* Fouch, T.D., Nuccio, V.F., and Chidsey, T.C., Jr., editors, Hydrocarbon and Mineral Resources of the Uinta Basin, Utah and Colorado: Utah Geological Association Guidebook 20, p. 77–93.
- Ogg, J.G., Ogg, G., and Gradstein, F.M., 2008, The Concise Geologic Time Scale: Cambridge University Press, 177 p.
- Pederson, J.L., and Hadder, K.W., 2005, Revisiting the classic conundrum of the Green River's integration through the Uinta uplift, *in* Dehler, C.M., Pederson, J.L., Sprinkel, D.A., and Kowallis, B.J., editors, Uinta Mountain Geology: Utah Geological Association Publication 33, p. 149–154.
- Pepper, A.S., 1991, Estimating the petroleum expulsion behavior of source rocks: a novel quantitative approach, *in*

- England, W.A., and Fleet, A.J., editors, Petroleum Migration: Special Publication of Geological Society London, v. 59, p. 9–31.
- Peters, K.E., and Cassa, M.R., 1994, Applied source rock geochemistry, *in* Magoon, L.B., and Dow, W.G., editors, The Petroleum System—from Source to Trap: American Association of Petroleum Geologists Memoir 60, p. 93–120.
- Picard, M.D., Thompson, W.D., and Williamson, C.R., 1973, Petrology, geochemistry and stratigraphy of Black Shale Facies of Green River Formation (Eocene), Uinta Basin, Utah: Utah Geological and Mineralogical Survey Bulletin 100, 52 p.
- Prothero, D.R., 1996, Magnetic stratigraphy and biostratigraphy of the middle Eocene Uinta Formation, Uinta Basin, Utah, *in* Prothero, D.R., and Emry, R.J., editors, The Terrestrial Eocene-Oligocene Transition in North America: Cambridge University Press, p. 3–24.
- Prothero, D.R., and Swisher, III, C.C., 1992, Magnetostratigraphy and geochronology of the terrestrial Eocene-Oligocene transition in North America, *in* Prothero, D.R., and Berggren, W.A., editors, Eocene-Oligocene Climatic and Biotic Evolution: Princeton University Press, p. 46–73.
- Remy, R.R., 1992, Stratigraphy of the Eocene part of the Green River Formation in the south-central part of the Uinta Basin, Utah: U.S. Geological Survey Bulletin 1787, p. BB1–BB25.
- Rice, D.D., Fouch, T.D., and Johnson, R.C., 1992, Influence of source rock type, thermal maturity, and migration of composition and distribution of natural gases, Uinta Basin, Utah, *in* Fouch, T.D., Nuccio, V.F., and Chidsey, T.C., Jr., editors, Hydrocarbon and Mineral Resources of the Uinta Basin, Utah and Colorado: Utah Geological Association 1992 Field Symposium, p. 95–109.
- Robinson, W.E., and Cook, G.L., 1975, Compositional variations of organic material from Green River oil shale—WOSCO EX-1 core (Utah): U.S. Bureau of Mines Report of Investigations 8017, 40 p.
- Rowley, P.D., Hansen, W.R., Tweto, O., and Carrara, P.E., 1985, Geologic map of the Vernal 1° x 2° quadrangle, Colorado, Utah, and Wyoming (1:250,000): U.S. Geological Survey.
- Ruble, T.E., Bakel, A.J., and Philp, R.P., 1994, Compound-specific isotopic variability in Uinta Basin native bitumens: paleoenvironmental implications: Organic Geochemistry, v. 21, p. 661–671.
- Ruble, T.E., Lewan, M.D., and Philp, R.P., 2001, New insights on the Green River petroleum system in the Uinta basin from hydrous pyrolysis experiments: American Association of Petroleum Geologists Bulletin, v. 85, p. 1333–1371.
- Ruble, T.E., and Philp, R.P., 1998, Stratigraphy, depositional environments and organic geochemistry of source-rocks in the Green River petroleum system, Uinta basin, Utah, *in* Pitman, J.K., and Carroll, A.R., editors, Modern and Ancient Lake Systems—New Problems and Perspectives: Utah Geological Association Guidebook 25, p. 289–328.
- Ryder, R.T., Fouch, T. D., and Elison, J. H., 1976, Early Tertiary sedimentation in the western Uinta Basin, Utah: Geological Society of America Bulletin, v. 87, p. 496–512.
- Schamel, S., 2005, Shale Gas Reservoirs of Utah: Survey of an Unexploited Potential Energy Resource: Utah Geological Survey Open-File Report 461, 114 p.
- Schamel, S., 2009, Shale gas potential of the Paradox Basin, Colorado and Utah, *in* Houston, W.S., Wray, L.L., and Moreland, P.G., editors, The Paradox Basin Revisited—New Developments in Petroleum Systems and Basin Analysis: Rocky Mountain Association of Geologists Special Publication, p. 568–603.
- Schamel, S., 2013, Unconventional oil resources of the Uinta Basin, Utah, *in* Hein, F.J., Leckie, D., Larter, S., and Suter, J.R., editors, Heavy-Oil and Oil-Sand Petroleum Systems in Alberta and Beyond: American Association of Petroleum Geologists Studies in Geology 64, p. 437–480.
- Smith, M.E., Carroll, A.R., and Mueller, E.R., 2008a, Elevated weathering rates in the Rocky Mountains during the Early Eocene Climatic Optimum: Nature Geoscience, p. 370–374.
- Smith, M.E., Carroll, A.R., and Singer, B.S., 2008b, Synoptic reconstruction of a major ancient lake system: Eocene Green River Formation, western United States: Geological Society of America Bulletin, v. 120, p. 54–84.
- Smouse, D., 1993, Altamont-Bluebell, *in* Hill, B.G., and Berekstein, S.R., editors, Oil and Gas Fields of Utah: Utah Geological Association, Salt Lake City, Utah, unpaginated.
- Sonnenberg, S.A., 2010, The Bakken petroleum system of the Williston Basin—a tight oil resource play: Hart Energy Shale Oil Webinar, March 2, 2010.
- Sonnenberg, S.A., 2011, The Niobrara petroleum system—a new resource play in the Rocky Mountain Region, *in* Estes-Jackson, J.E., and Anderson, D.S., editors, Revisiting and Revitalizing the Niobrara in the Central Rockies: Denver, Colorado, Rocky Mountain Association of Geologists, p. 13–32.
- Spencer, C.W., 1987, Hydrocarbon generation as a mechanism for overpressuring in Rocky Mountain region: American Association of Petroleum Geologists Bulletin, v. 71, no. 4, p. 368–388.
- Sprinkel, D.A., 2006, Interim geologic map of the Dutch John 30' x 60' quadrangle, Daggett and Uintah Counties, Utah, Moffat County, Colorado, and Sweetwater County, Wyoming (1:100,000): Utah Geological Survey Open-File Report 491DM, 3 Plates.
- Sprinkel, D.A., 2007, Interim geologic map of the Vernal 30' x 60' quadrangle, Uintah and Duchesne Counties, Utah, and Moffat and Rio Blanco Counties, Colorado

- (1:100,000): Utah Geological Survey Open-File Report 506DM, 3 Plates.
- Sprinkel, D.A., 2009, Interim geologic map of the Seep Ridge 30' x 60' quadrangle, Uintah, Duchesne, and Carbon Counties, Utah, and Rio Blanco and Garfield Counties, Colorado (1:100,000): Utah Geological Survey Open-File Report 549DM, 3 Plates.
- Sprinkel, D.A., Sharp, W., and Schamel, S., 2013, New insights into the timing of exhumation of the Uinta Basin and mountain-front retreat of the Uinta Mountains, Utah: 2013 American Association of Petroleum Geologists Rocky Mountain Section Meeting, Salt Lake City, Utah, 22–24 September, 2013.
- Stone, D.S., 1977, Tectonic history of the Uncompaghre uplift, in *Exploration Frontiers of the Central and Southern Rockies*: Denver, Rocky Mountain Association of Geologists Guidebook, p. 23–30.
- Swarbrick, R.E., Osborne, M.J., and Yardley, G.S., 2002, Comparison of overpressure magnitude resulting from the main generating mechanisms, in Huffman, A.R., and Bowers, G.L., editors, *Pressure Regimes in Sedimentary Basins and Their Prediction*: American Association of Petroleum Geologists Memoir 76, p. 1–12.
- Sweeney, J.J., 1988, Application of maturation indicators and oil reaction kinetics to put constraints on thermal history models for the Uinta Basin, Utah, U.S.A.: *Organic Geochemistry*, v. 13, p. 199–205.
- Thompson, W.D., 1971, Stratigraphy of black-shale facies of Green River Formation (Eocene), Uinta Basin, Utah: M.S. Thesis, University of Utah, 122 p.
- USGS Uinta-Piceance Assessment Team, 2003, Petroleum systems and geologic assessment of oil and gas in the Uinta-Piceance Province, Utah and Colorado: US Geological Survey Digital Data Series DDS-69-B.
- Vanden Berg, M.D., 2008, Basin-wide evaluation of the uppermost Green River Formation's oil-shale resource, Uinta Basin, Utah and Colorado: Utah Geological Survey Special Study 128, 19 p.
- Vanden Berg, M.D., Morgan, C.D., Chidsey, T.C, Jr., and Nielsen, P., 2013, The Uteland Butte Member of the Eocene Green River Formation—an emerging unconventional carbonate tight oil play in the Uinta Basin, Utah: American Association of Petroleum Geologists Annual Convention & Exhibition, May 19–22, 2013, Pittsburgh, PA.
- Waples, D.W., 1994, Maturity modeling: Thermal indicators, hydrocarbon generation, and oil cracking, in Magoon, L.B., and Dow, W.G., editors, *The Petroleum System—from Source to Trap*: American Association of Petroleum Geologists Memoir 60, p. 285–306.
- Weiss, M.P., Witkind, I.J., and Cashion, W.B., 2003, Geologic map of the Price 30' x 60' quadrangle, Carbon, Duchesne, Uintah, Utah, and Wasatch Counties, Utah (1:100,000): Utah Geological Survey Map 198DM.
- Wiggins, W.D., and Harris, P.M., 1994, Lithofacies, depositional cycles, and stratigraphy of the lower Green River Formation, southwestern Uinta Basin, Utah Notes for SEPM Core Workshop: Lacustrine Source-Rock Depositional Environments, American Association of Petroleum Geologists Annual Convention, Denver, June 11, 1994, SEPM, p. 105–141.